THE SYNTHESIS AND REACTIVITY OF VITAMIN E QUINONES

Nicholas W. Krueger

A thesis submitted to the Biotechnology program

in partial fulfillment of the requirements for the degree

of Master of Science

Brock University

St. Catharines, Ontario

August, 2017

Abstract

Vitamin E has been the subject of numerous studies over the last nine decades since its discovery. Still, the biological activity of vitamin E is not completely understood. Various studies suggest that the primary function of vitamin E is a fat-soluble antioxidant preventing lipid peroxidation in cellular membranes. The antioxidant efficiency across the vitamin E isomers have been shown to be similar *in vitro* in various organic solvents and aqueous lipid suspensions. Despite these results, significantly different biological effects have been observed in biological assays supplemented with the various tocols. Furthermore, the differences are more pronounced when comparing the biological effects of the α-tocols to non α-tocols. We hypothesized the different biological effects observed were correlated to differences in the chemical reactivity of the products of tocol oxidation: tocol quinones. Herein, an investigation of the adduct formation of tocol quinones with *N*-acetyl cysteine (NAC) is described.

The synthesis of the tocopheryl quinones is described via the two-electron oxidation of the parent tocols with ceric ammonium nitrate supported on silica. The synthesis of α-tocopherol quinone and α-tocotrienol quinone produced the target compounds in 80% yield. The oxidations of the other tocol isoforms yielded *para*-tocol quinones (29-45% yield) and *ortho*-tocol quinones (20-35% yield). The rate of reaction of the tocopheryl quinones with NAC was monitored by following the production of the tocopherol hydroquinone adduct by the increase in absorption at 308 nm over time in a 67% methanol/ 33% aqueous Tris/HCl buffer. The curves generated were fit to a one-phase exponential. The rate of reaction increased as the pH increased for the γ- and δ-tocopheryl quinone isoforms. There was no reactivity observed between the α-tocopheryl quinone isoforms and NAC. There was no significant difference in the reactivity between the tocopherol quinones and tocotrienol quinones with the same methylation pattern. At the most

physiologically relevant pH in our study (pH = 7.5), the δ-tocopheryl quinones ($k \approx 0.63$) reacted approximately 8 times faster than the γ-tocopheryl quinones ($k \approx 0.08$). The electrochemistry of the parent tocols was studied using cyclic voltammetry (CV). The formal redox potential increased slightly as the methylation on the chromanol ring decreased while no significant differences between the tocopherols and tocotrienols were established. The CV of all tocols showed two quasi-reversible one-electron oxidation processes; the first oxidation produced a radical cation, which quickly deprotonated to form a tocopheryl radical, which then undergoes a second oxidation to the corresponding phenoxonium cation. The redox activity of the tocopheryl quinones was also studied using CV. The quinones underwent a quasi-reversible two one-electron reduction process. The δ-tocopheryl quinones have the lowest formal redox potential which slightly increases as methylation increases, while there were no significant differences in the electrochemical behavior of the tocopheryl quinones and the tocotrienyl quinones with the same methylation. We have presented reaction rate differences in the reactivity of the tocol quinones which correlates to the differences in biological activity observed by others with respect to the methylation pattern on the chromanol ring, while no differences in the chemical reactivity of the tocopherol and tocotrienol quinones was observed. Still, this presents convincing evidence that the activity of the tocol quinones should be considered in biological assays.

Acknowledgements

I am using this opportunity to express my sincere appreciation to all those who have supported me throughout the duration of my studies. Foremost, I would like to thank my supervisor, Dr. Jeffrey Atkinson, for providing me with the opportunity to join his research team. I am forever grateful for the professional guidance, knowledge and support he has offered me over the course of the project. His personable and enthusiastic character is appreciated and made for a comfortable and effective learning environment.

I would also like to thank my laboratory supervisor, labmate and friend, Mikel Ghelfi, for the endless amounts of guidance, suggestions and constructive criticism he has given me over the course of the project. Mikel's dedication to science is impossible to ignore. His work ethic is remarkable and truly admired. I would also like to thank my other labmates and friends for their encouragements, helpful suggestions and discussions: Andrew Hildering, Dr. Candace Panagabko, Dr. Matilda Baptist, Dr. Parthajit Mukherjee and Kaylie Meehan. I enjoyed a lot of the time that was spent working together. I would like to thank Dr. Paul Zelisko and Dr. Doug Bruce for their valuable suggestions and time that were offered to me during the project. I would like to extend my expression of gratitude to Liqun Qiu and Razvan Simionescu for their help in the acquisition of spectral data. Special thanks are given to Nico Bonnano and Dr. Martin Lemaire for allowing me to use their cyclic voltammetry apparatus and their valuable help and insight with the operation of the apparatus and interpretation of the data.

Finally, I would like to thank my parents and brothers who have provided unconditional support throughout my degree. Your encouragement and guidance have made this possible.

Table of Contents

1. INTRODUCTION 1
1.1 The Vitamin E Family 1
1.2 Sources of Vitamin E 4
1.3 Vitamin E Absorption and Transport 5
1.4 Vitamin E as an Antioxidant 10
1.5 Biological differences among tocol isoforms 13
1.4 Tocol Quinones 31
1.5 Reactive Thiols in Cells 33
1.6 Project Overview 37
2. RESULTS AND DISCUSSION 39
2.1 Isolation of Vitamin E Congeners 39
2.2 Synthesis of Vitamin E Quinones 40
2.3 The Synthesis of Quinone Thiol Adducts 43
2.4 Tocol quinone reactivity with N-Acetyl Cysteine 50
2.3 Tocol and Tocol Quinone Redox Activity 66
3. SUMMARY AND FUTURE PERSPECTIVES 86
4. EXPERIMENTAL 89
4.1 General Methods 89
4.2 Preparation of Starting Materials 90
4.3 General Procedure for Synthesis of Quinones 95
4.4 General Procedure for Synthesis of Quinone Thiol Conjugates 104
4.5 Monitoring Reactivity of Quinones with Model Thiol 110
4.6 General procedure for Cyclic Voltammetry 112
5. REFERENCES 113

List of Figures

Figure 1: The structures of the members of the vitamin E family. 3

Figure 2: The biosynthesis of vitamin E.[19] 5

Figure 3: A schematic of the absorption and transport of vitamin E in humans.[21] 8

Figure 4: The pathway of hepatic metabolism of γ-tocopherol to its corresponding CEHC metabolite.[31] 9

Figure 5: Hydroxyl radicals generated by the Fenton reaction. [37] 10

Figure 6: The inhibition of lipid peroxidation by tocopherol in lipid membranes. 11

Figure 7: The inhibition of PC-OOH formation in PC liposomes by α-tocopherol using various concentrations of peroxynitrite 16

Figure 8: The reaction products of α- and γ-tocopherol in the presence of peroxynitrite. 17

Figure 9: The cell viability of a mouse macrophage cell line RAW 264.7 after incubation with different tocopherols 19

Figure 10: The effect of tocopherol isoforms on the levels of IL-8 in a IFNγ/PMA induced inflammatory and oxidative response conditions of a Caco-2 cell line 21

Figure 11: Tumor growth studies in a mouse A431 model (A) and a mouse B16-F10 model (B) after intravenous administration of transferrin-bearing vesicles entrapping α-T3 27

Figure 12: The viability of melanoma B16 cells 48 hours after the incubation with various tocols. 30

Figure 13: The hinge and latch model of the Nrf2:Keap1 pathway..... 36

Figure 12: The UV/Vis absorption spectral changes of α-tocopherol quinone with the addition of $NaBH_4$. 44

Figure 13: The structure of the p-benzohydroquinone mono-NAC adduct. 45

Figure 14: The UV/Vis absorption spectral changes of γ-tocopherol quinone NAC adduct with $NaBH_4$. 48

Figure 15: The setup used to exclude atmospheric oxygen using N_2 gas. 49

Figure 16: The titration of γ-tocopheryl quinone with NAC 51

Figure 17: The effect of solvent conditions on the rate of reactivity of γ-tocopherol quinone with NAC. 53

Figure 18: The reactivity of γ-tocopherol quinone with NAC (pH 8.5) in the presence of air.54

Figure 20: The rate of reactivity of tocol quinones with NAC at pH 8.5 64

Figure 21: The rate of reactivity of tocol quinones with NAC at pH 7.5 64

Figure 22: The rate of reactivity of tocol quinones with NAC at pH 6.5 65

Figure 23: The effect of pH on the rate of reactivity of γ-tocopherol quinone with NAC 65

Figure 24: The the rate of reactivity of γ-tocopheryl quinone and γ-tocotrienyl quinone with NAC. 66

Figure 25: The cyclic voltammogram of ferrocene at a scan rate of 100 mV/s. 71

Figure 26: Electrochemical oxidation mechanism of α-tocopherol in acetonitrile determined over a range of scan rates and water concentrations. 74

Figure 27: The cyclic voltammetry at 100 mV/s of α-tocopherol in dry CH_2Cl_2 and 300 mV/s of α-tocotrienol in dry CH_2Cl_2. 76

Figure 28: The cyclic voltammetry at 500 mV/s of γ-tocopherol in dry CH_2Cl_2 and 300 mV/s of γ-tocotrienol in dry CH_2Cl_2 76

Figure 29: The cyclic voltammetry at 300 mV/s of δ-tocopherol in dry CH_2Cl_2 and 500 mV/s of δ-tocotrienol in dry CH_2Cl_2 77

Figure 30: The cyclic voltammetry at 100 mV/s of α-tocopherol in dry CH_2Cl_2, 500 mV/s of γ-tocopherol in dry CH_2Cl_2, and 300 mV/s of δ-tocopherol in dry CH_2Cl_2. 77

Figure 31: The cyclic voltammetry at 300 mV/s of α-tocotrienol in dry CH_2Cl_2, 300 mV/s of γ-tocotrienol in dry CH_2Cl_2, and 500 mV/s of δ-tocotrienol in dry CH_2Cl_2. 78

Figure 32: The cyclic voltammetry at 300 mV/s of α-tocopheryl quinone in dry CH_2Cl_2, and 600 mV/s of α-tocotrienyl quinone in dry CH_2Cl_2 82

Figure 33: The cyclic voltammetry at 300 mV/s of γ-tocopheryl quinone in dry CH_2Cl_2, and 500 mV/s of γ-tocotrienol in dry CH_2Cl_2..... 82

Figure 34: The cyclic voltammetry at 300 mV/s of δ-tocopheryl quinone in dry CH_2Cl_2, and 300 mV/s of δ-tocotrienyl quinone in dry CH_2Cl_2..... 83

Figure 35: The cyclic voltammetry at 300 mV/s of α-tocopheryl quinone in dry CH_2Cl_2, 300 mV/s of γ-tocopheryl quinone in dry CH_2Cl_2, and 300 mV/s of δ-tocopheryl quinone in dry CH_2Cl_2..... 83

Figure 36: The cyclic voltammetry at 600 mV/s of α-tocotrienyl quinone in dry CH_2Cl_2, 500 mV/s of γ-tocotrienyl quinone in dry CH_2Cl_2, and 300 mV/s of δ-tocotrienyl quinonein dry CH_2Cl_2..... 84

List of Tables

Table 1: Comparison of ligand specificity of α-TTP for various tocopherol derivatives and the biological activity.[27] 7

Table 2: The antioxidant capabilities of the tocopherols in various media.[36] 14

Table 3: Concentration-dependent effects of dietary d-α-tocotrienol on cholesterol metabolism in broiler cockerels. Feeding period, 21 days, fast 2, refed 3; n = 9.[55] 24

Table 4: The effect of various tocols on the inhibition of cholesterol synthesis and HMGR activity in human HepG2 cells.[57] 25

Table 5: The efficacy of tocol isoforms on cancer cell viability. The control vesicles consist of tocol containing lipid vesicles not linked to transferrin.[60] 27

Table 6: Comparison of apoptotic properties of various tocols in two human breast cancer cell lines.[62] 29

Table 7: The extracted rate constant of the reaction γ-tocopherol quinone with NAC fit to a one-phase association curve. The buffer consists of 100 mM Tris/HCl aqueous buffer at pH 8.5. Two equivalents of NAC were used. 53

Table 8: The extracted rate constants of the reactions of tocol quinones with NAC fit to a one-phase association curve at three different pHs. 63

Table 9: The formal reduction potential of the tocopherols obtained by digital simulation of CV data[a] for the two one-electron oxidation processes of tocopherols to the phenoxonium cation.[91] 73

Table 10: The extracted data from the experimental CV of the tocols. Ferrocene was used as an external standard. 79

Table 11: The extracted data obtained from the cyclic voltammetry of the vitamin E quinones. 85

List of Schemes

Scheme 1: The protein arylation mechanism of non α-tocol quinones ……32

Scheme 2: General scheme for the synthesis of tocol quinones from their parent quinones……42

Scheme 3: The proposed mechanism of thiol addition to quinone derivatives…….43

Scheme 4: The proposed redox cycle of the vitamin E quinones…….…….79

Abbreviations

AAPH	2,2'-azobis-(2-amidinopropane) hydrochloride
ABCA1	ATP-binding cassette A1
AMVN	2,2’-Azobis(2,4-dimethylvaleronitrile)
ARE/EpRE	antioxidant/electrophilic response element
ATP	adenosine triphosphate
AVED	ataxia with vitamin E deficiency
CAN	ceric ammonium nitrate
CV	cyclic voltammetry
^{13}C-NMR	carbon nuclear magnetic resonance
Cul3	cullin3-based ubiquitin E3 ligase
cPLA$_2$	cytosolic phospholipase A_2
d	doublet
DNA	deoxyribonucleic acid
DLG	aspartic acid, leucine, glycine
EI	electron impact
eq.	equivalents
ETGE	glutamic acid, threonine, glycine, gluatmic acid
GC	gas chromatography
GSH	glutathione
GST	glutathione S-transferase
HDL	high density lipoprotein
HMG-CoA	3-hydroxy-3-methylglutaryl coenzyme A
^{1}H- NMR	proton nuclear magnetic resonance
IC50	concentration needed to inhibit the growth of the culture by 50%
IL-8	interleukin-8
Keap1	kelch-like ECH associated protein 1
LDL	low density lipoprotein
LDLR	LDL receptor protein
LPL	lipoprotein lipase
LRP	LDL receptor related protein

m	multiplet
MS	mass spectrometry
MTP	microsomal transfer protein
m/z	mass to charge ratio
NAC	N-acetyl cysteine
NADPH	reduced nicotinamide adenine dinucleotide phosphate
NQ01	NADPH: quinone reductase
Nrf2	NF-E2 related factor 2
o-	*ortho-*
p-	*para-*
PC	phosphatidyl choline
PG	pyrogallolsulfonphthalein
PLTP	plasma phospholipid transfer protein
PKC	protein kinase c
PUFA	polyunsaturated fatty acid
q	quartet
ROS	reactive oxygen species
SR-BI	scavenger receptor BI
s	singlet
t	triplet
TLC	thin-layer chromatography
UDP	uridine diphosphate
UGT	UDP-glucuronosyl transferase
UPR	unfolded protein response
UV/Vis	ultra-violet/visible light
VLDL	very low-density lipoprotein

The Synthesis and Reactivity of Vitamin E Quinones

1. INTRODUCTION

1.1 The Vitamin E Family

In 1922 Bishop and Evans studied the effect on rats of a minimalist diet consisting of purified protein, fat, carbohydrates, salts, vitamin A, vitamin B, and vitamin C.[1] Although female rats were able to grow, such animals were sterile. In as early as the second day of gestation, blood extravasations in the placentae were observed, increasing in extent until fetal resorption occurred. Interestingly, the sterility observed in these rats, as evidenced by fetal resorption, was reversed by the implementation of a natural food source such as green lettuce or dried alfalfa leaves. Thus, Bishop and Evans concluded that the natural food sources contain a dietary factor X, which restores fertility to the sterile rats when supplemented to a minimalist diet.[1] Shortly after, Barnett Sure identified dietary factor X as vitamin "E", inspired by the nomenclature utilized for the previously discovered vitamins A, B, C, and D.[2] This event launched an extensive period of studies in the late 1920s which proposed the biochemical function of vitamin E as a fat soluble anti-oxidant.[3–5] The vitamin was first isolated in 1935 by Evans and his research team from wheat germ oil as an oily concentrate. [6] To investigate the structure of the vitamin, Evans and his team sought to purify the oily vitamin E concentrate by creating a solid derivative. These attempts revealed three crystalline allophanates using cyanic acid.[6] One of the allophanates was void of biological activity while the other two had biological activity similar to that of the vitamin E concentrate. Combustion analysis of the allophanates revealed two structurally similar isomers of the vitamin: $C_{29}H_{50}O_2$ and $C_{28}H_{28}O_2$.[6] The $C_{29}H_{50}O_2$ isomer showed a slight increase in biological activity over the other isomer and was given the name: α-tocopherol.[6] The other isomer was given the name β-tocopherol.[7] The structure of α-

tocopherol was elucidated in 1938 by Fernholz upon elemental analysis of the thermal decomposition and oxidative decomposition of α-tocopherol, which also exposed four members of the vitamin E family including: α, β, γ and δ tocopherol.[8] A few decades later, four additional members of the tocol family were discovered in palm oil: α, β, γ and δ tocotrienol.[9] The structures of the members of the vitamin E family can be seen in **Figure 1**.

The importance of vitamin E was demonstrated early on in several studies using a vitamin E deficient diet which resulted in sterility in rats, lymphoblastoma in chicks, and muscular dystrophy in guinea pigs and rabbits.[1,10–12] The importance of vitamin E is established in human patients suffering from ataxia, infertility, and muscle atrophy in a genetic condition called ataxia with vitamin E deficiency (AVED).[13] Vitamin E deficiency has been shown to be the result of a genetic mutation in the gene coding for the plasma transport protein, α-tocopherol transfer protein (α-TTP). In a large cohort study of AVED patients, gait impairment was reported as the initial onset of symptoms in 93.4 % of subjects.[14] Head tremors, cerebellar ataxia, blindness, and dysarthria are also reported symptoms of vitamin E deficiency, while some patients may be wheel-chair bound by the age of 28.[14,15] Consequently, the complications observed in vitamin E deficient biological systems solidify its biological significance as an essential dietary factor.

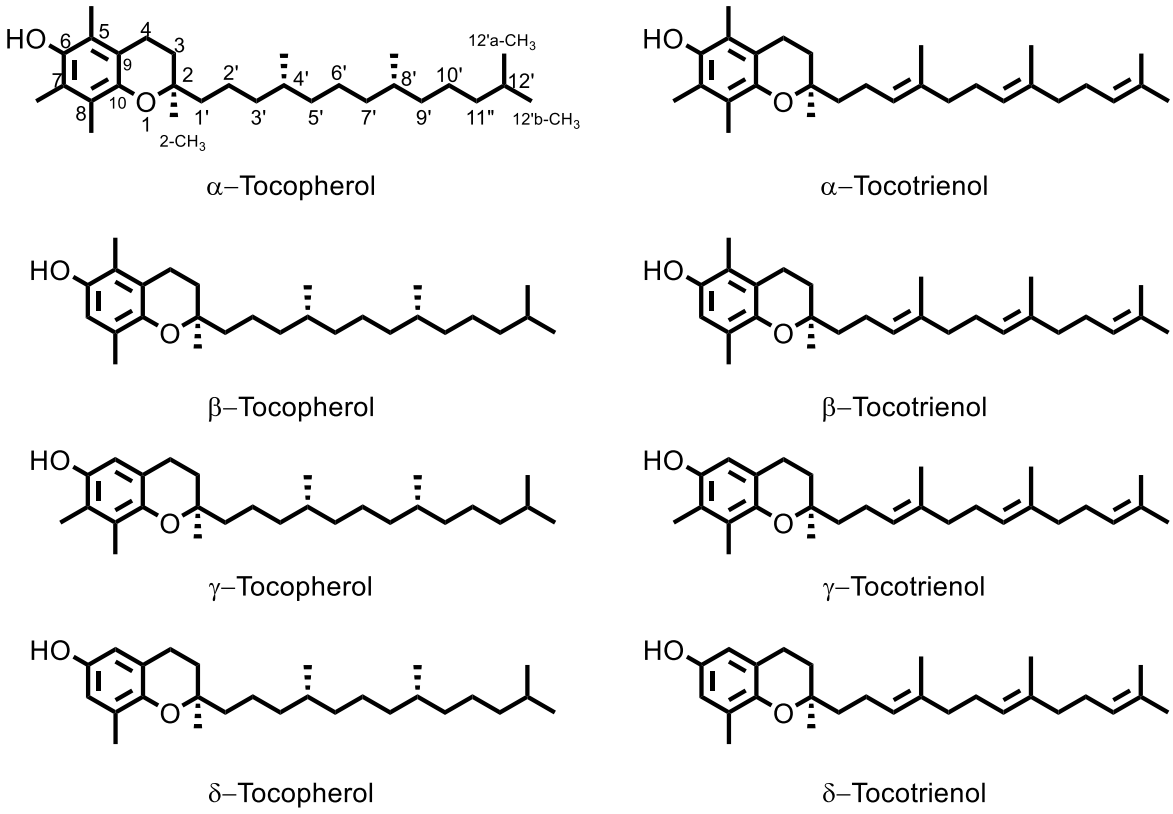

Figure 1: The structures of the members of the vitamin E family.

Tocols, also known as tocochromanols, are a class of compounds that contain a chroman-6-ol group with a isoprenoid side chain of sixteen carbon atoms. The degree and position of methylation on the chromanol head group is the differentiating factor between α-, β-, γ- and δ-tocol homologues, α being fully methylated. The three positions of unsaturation on the phytyl side chain (3', 7', 11') distinguish the tocotrienols from the fully saturated phytyl side chain of tocopherols.[9] All tocol homologues have a stereocenter at the 2-position of the chromanol ring in the *R*-configuration, while tocopherols have an additional two stereocenters at the 3' and 7' position of the hydrophobic side chain.[12] Natural sources of tocopherol exist as the *R, R, R*-configuration at the three stereocenters whereas the only stereocenter at the 2-position of the tocotrienols is also in the *R*-configuration and the double bonds are in the E geometry.[16] The

unsaturation of the phytyl side chain in tocotrienols is responsible for the loss of two additional stereocenters present in tocopherol.

1.2 Sources of Vitamin E

As mentioned previously, the importance of vitamin E is demonstrated in patients suffering from ataxia, infertility, muscle atrophy, and peripheral neuropathy due to vitamin E deficiency.[14] The lack of the ability of humans to synthesize vitamin E necessitates that it must be obtained from dietary sources. The largest sources of vitamin E in the human diet are leafy green vegetables, seeds, grains and fruits.[17] The different congeners of vitamin E are found in various amounts depending on the source, for instance, canola oil is rich in α-, γ, and δ tocopherol whereas palm oil is rich in α-tocopherol, α- and γ -tocotrienol.[18]

Tocochromanols are synthesized in the chloroplast of plant cells with specific stereochemistry.[19] Briefly, the synthesis of tocochromanols involves the addition of phytyl diphosphate (geranylgeranyl diphosphate for tocotrienols) to homogentisic acid depicted in **Figure 2**.[19] This complex goes through an enzymatic-assisted intramolecular cyclization by cyclase followed by methylation of the chromanol ring achieved by tocopherol methyl transferase enzyme using S-adenosylmethionine.[19] Tocopherols occur naturally in the *R,R,R*-configuration and naturally occurring tocotrienols have *R*-configuration stereochemistry at the 2-position of the chromanol ring.[20]

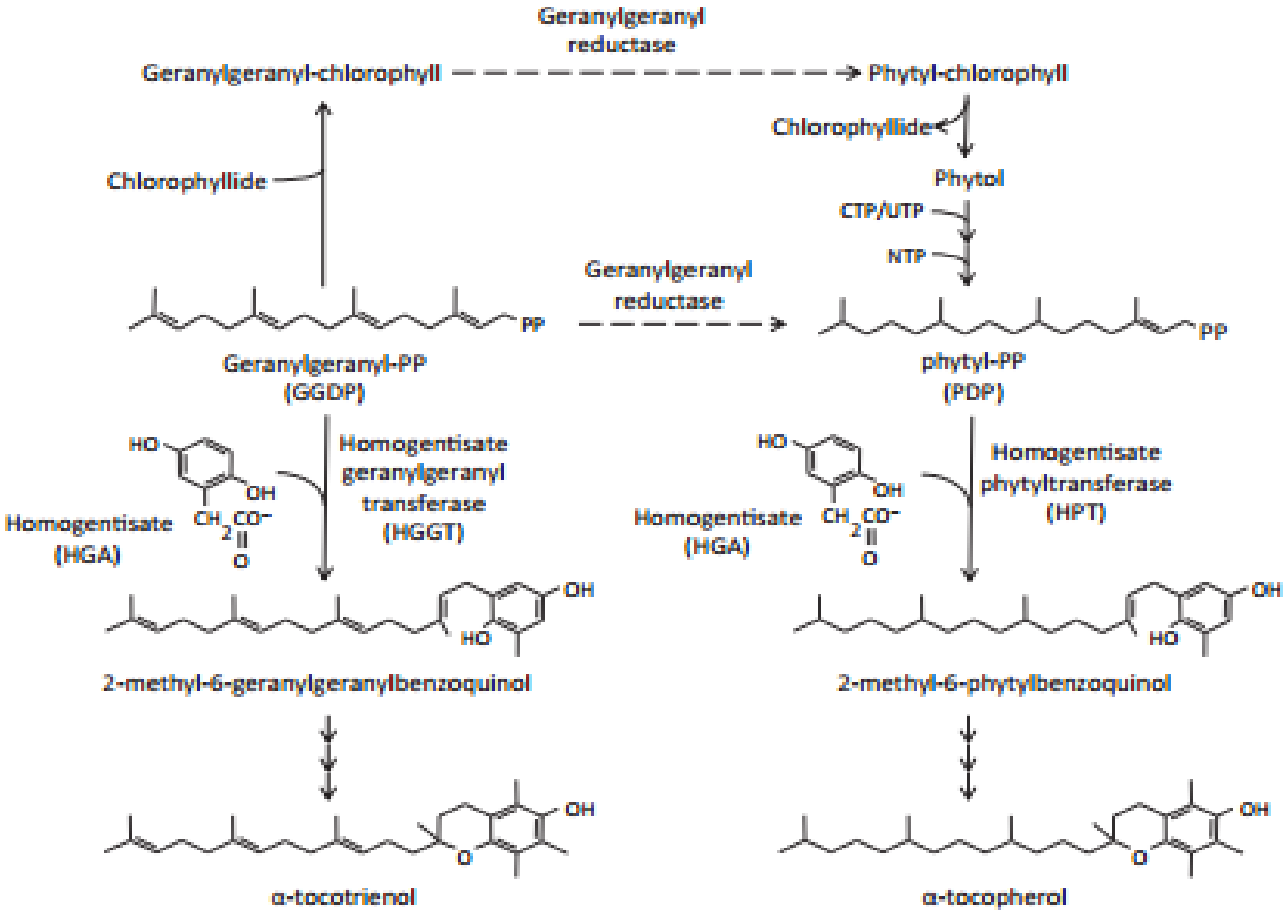

Figure 2: The biosynthesis of vitamin E. Taken with permission from Yang *et al*. [19]

1.3 Vitamin E Absorption and Transport

The hydrophobic nature of vitamin E presents a barrier for absorption and transport to tissues in the body. Fortunately, evolution has provided the necessary means to overcome this barrier using various proteins as seen in **Figure 3**. After the intake of dietary food, the fats and oils, including vitamin E, are solubilized into small micelles by bile acids in the duodenum. Initially, it was thought that the uptake of vitamin E by intestinal cells was a process entirely mediated by passive diffusion.[21] However, one study has demonstrated that the scavenger receptor class B type I (SR-BI) is also involved in the uptake of vitamin E by enterocytes.[22] Once

inside the enterocytes, vitamin E is packed into lipoprotein complexes called chylomicrons and re-secreted from the basal side of the intestinal cells into the lymph duct by microsomal triglyceride transfer protein (MTP).[21,23,24] Once in the bloodstream, the chylomicrons are enzymatically hydrolyzed to chylomicron remnants by lipoprotein lipase (LPL). As the bloodstream passes through the liver, hepatocytes take up the chylomicron remnants by the interaction between the apolipoprotein E segment of the remnant and the LDL receptor-related protein (LRP) of the hepatocyte.[21] Inside the cytosol of the hepatocytes, α-tocopherol transfer protein (α-TTP) is responsible for the retention of tocols. *In vitro* and *in vivo* studies have demonstrated that this protein binds with high selectivity to *R,R,R*-α-tocopherol compared to other isoforms of vitamin E as depicted in **Table 1**.[13,21,25,26] The dissociation constant, K_d, was significantly lower and the relative affinity was significantly greater for α-tocopherol with α-TTP compared to the other ligands tested *in vitro* using tritium labelled α-tocopherol competition assays indicating a greater selectivity towards α -tocopherol.[27] The high selectivity for α-tocopherol by α-TTP is demonstrated in humans by significantly higher levels of plasma α-tocopherol (~32 μM) compared to the other tocols which are present in concentrations lower than 2 μM.[28] The evolutionary advantage regarding the high selectivity towards α-tocopherol is unknown and of particular interest. Nonetheless, the tocols retained by the α-TTP in the hepatocytes are packed into very-low density lipoproteins (VLDL) and exported throughout the bloodstream. The phospholipid transfer protein (PLTP) has been shown to be associated with α-tocopherol transfer between VLDLs and other circulating lipoproteins such as high density lipoproteins (HDLs) and low density lipoproteins (LDLs).[29] The tissues absorb the vitamin E containing lipoproteins by various receptors such as low-density lipoprotein receptors (LDLR) and SR-BI or by the PLTP ligand exchange pathway.[21]

Table 1: Comparison of ligand specificity of α-TTP for various tocopherol derivatives and the biological activity. Table taken with permission from Panagabko *et al.* [27]

ligand	dissociation constant (nM)[a] α-TTP	relative affinity of TTP for α-tocopherol	rat-resorption gestation assays
α-tocopherol	25.0 ± 2.8	100	80
β-tocopherol	124 ± 4.7	38.1 ± 9.3	45
γ-tocopherol	266 ± 9	8.9 ± 0.6	13
δ-tocopherol	586 ± 75	1.6 ± 0.3	<0.4
SRR-α-tocopherol	545 ± 62	10.5±0.4	59 (d/l)
Trolox	1004 ± 126	9.1 ± 1.2	
α-tocopheryl acetate	1639 ± 89	1.7 ± 0.1	136
α-tocopheryl succinate	526 ± 54		
6-*O*-carboxymethyl-α-tocopherol	879 ± 65		
α-tocotrienol	214 ± 13	12.4 ± 2.3	13
α-tocopheryl quinone	814 ± 86		

[a] All data are expressed as the average ± SEM.

As seen in **Figure 3** vitamin E can also undergo an alternative absorption pathway in the absence of an exogenous lipid supply. It can be packed into high density lipoprotein (HDL) inside enterocytes and secreted into the lymph duct by the trans-membrane transporter ATP-Binding Cassette A-1 (ABCA1) protein.[21,23] The HDL containing vitamin E can be directly absorbed by peripheral tissues with the use of ABCA1 and plasma phospholipid transfer protein (PLTP).[21,23] Tocols reside in the phospholipid bilayers of the cell with the phenolic group directed towards the polar phosphate head groups of the membrane phospholipids.[30]

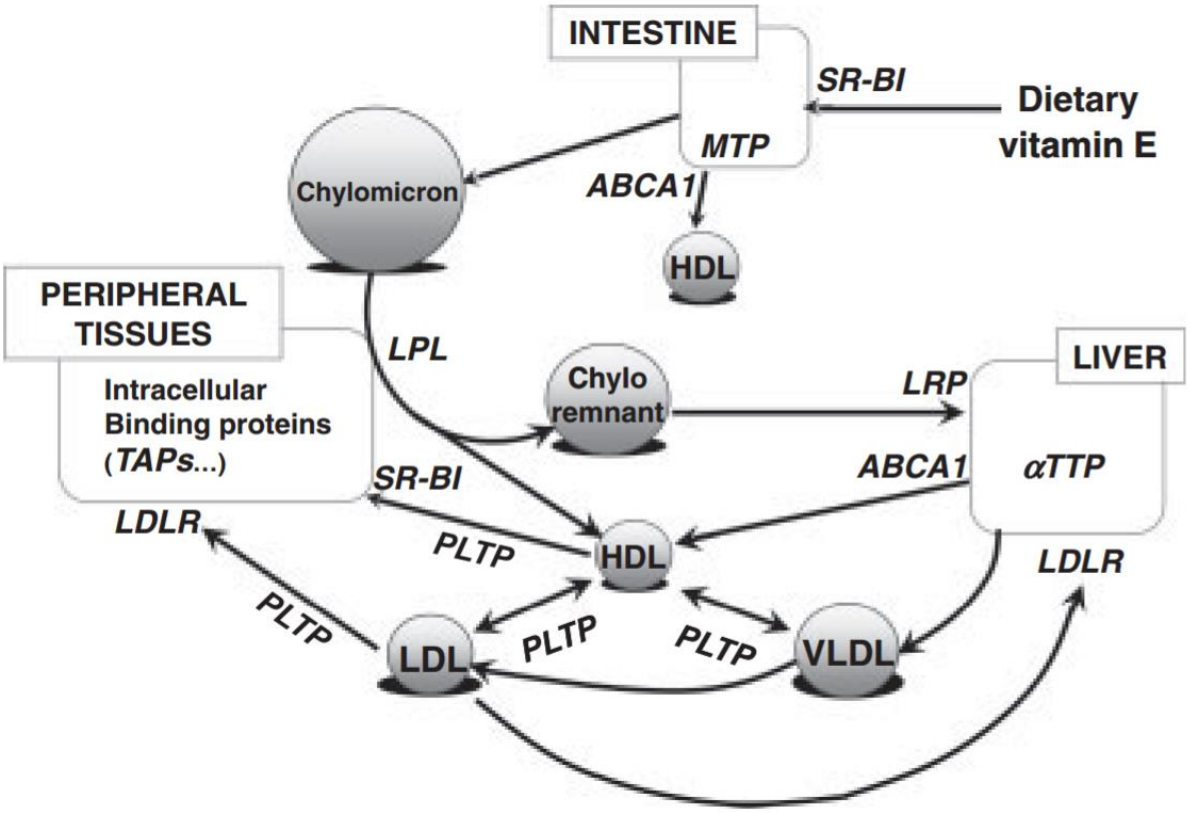

Figure 3: A schematic of the absorption and transport of vitamin E in humans.[21] See main text for details. α-TTP- α-tocopherol transfer protein, ABCA1- ATP-Binding Cassette A-1, HDL- high density lipoprotein, LDL- low-density lipoprotein, LDLR- low-density lipoprotein receptors, LPL- lipoprotein lipase, LRP- LDL receptor-related protein, MTP- microsomal triglyceride transfer protein, PLTP- plasma phospholipid transfer protein, SR-BI- scavenger receptor class B type I, TAPs VLDL- very-low density lipoprotein. Figure taken with permission from Lemaire-Ewing *et al*.[21]

Tocols that are not retained are either excreted into the bile or feces, or degraded and excreted in the urine.[21] The major tocol degradation products found in the urine are carboxyethyl hydroxychromans (CEHCs). These products are derived from enzymatic degradation in the liver achieved mainly by cytochrome P450 4F2 (CYP4F2) via a ω-hydroxylation pathway starting at one of the terminal methyl groups of the phytyl side chain.[31] The hydroxylation product is further oxidized to the corresponding carboxylic acid followed by a series of β-oxidations to yield the corresponding CEHC as seen in **Figure 4**.[31,32] In addition to the preferential retention of α-

tocopherol by α-TTP, it has been shown that the activity of the CYP4F2 enzyme is several fold greater towards non α-tocopherol isoforms of vitamin E.

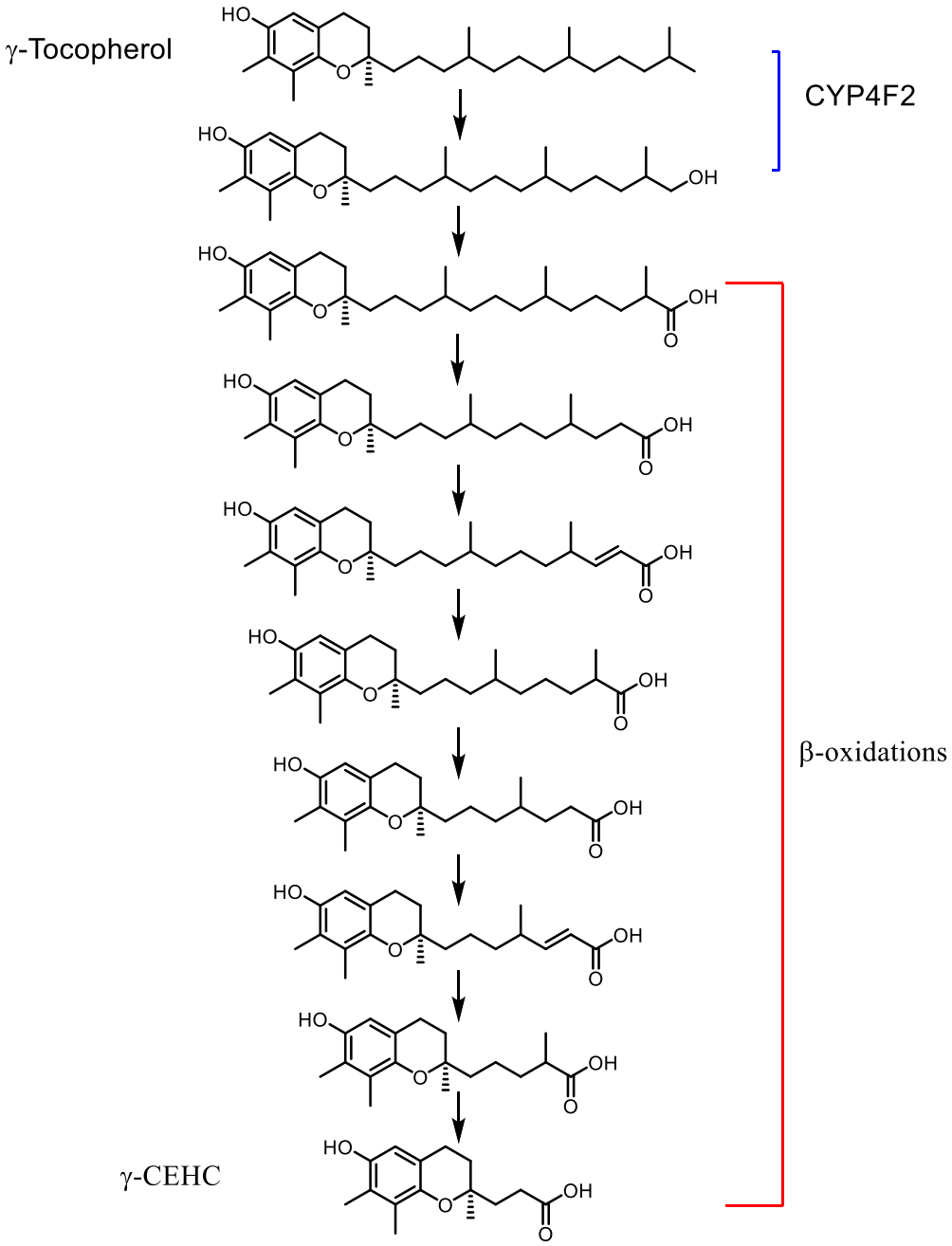

Figure 4: The pathway of hepatic metabolism of γ-tocopherol to its corresponding CEHC metabolite.[31]

1.4 Vitamin E as an Antioxidant

The aerobic nature of mammalian metabolism presents the cell with a potential for oxidative stress induced by a variety of free radicals derived from oxygen, also known as reactive oxygen species (ROS).[33] It is well known that the biological significance of vitamin E is to protect the cell from such oxidative stress.[34] Due to the location of vitamin E inside the cell (*i.e.* the phospholipid bilayer) vitamin E is exposed to a limited variety of ROS.[35] There are few reactive oxygen species that are capable of entering the lipid bilayer; the hydroxyl radical ($^{\bullet}OH$), protonated superoxide radical ($HOO^{\bullet}$), and peroxynitrites ($ONOO^{\bullet}$) being the most biologically significant ROS in the bilayer.[34,36] The hydroxyl radical can be generated by the reductive cleavage of hydrogen peroxide by iron(II). This is known as the Fenton reaction which is illustrated in **Figure 5**.[35] Inside the bilayer, ROS are capable of initiating lipid peroxidation which disrupts the integrity of the cellular membrane.

Figure 5: Hydroxyl radicals generated by the Fenton reaction. [35]

Lipid peroxidation is initiated when a free radical abstracts a hydrogen atom from a carbon center of a lipid.[33,35] The lipids most inclined to hydrogen abstraction are polyunsaturated fatty acids (PUFAs), particularly PUFAs with a 1,4-pentadiene group. These PUFAs contain two *bis*-allylic hydrogen atoms that are susceptible to hydrogen abstraction because the carbon-centered radical generated is resonance stabilized as seen in **Figure 6**. The carbon-centered free radical quickly reacts with molecular oxygen which produces a lipid peroxyl radical.[33,35]Lipid peroxyl radicals are capable of abstracting hydrogen atoms from other PUFAs in the bilayer, a process known as chain-reaction lipid peroxidation.[35] The progression of this process is

devastating as the integrity of cellular membranes would be compromised.[35] Fortunately, various *in vivo* and *in vitro* studies demonstrate the capacity of tocols to prevent lipid peroxidation by scavenging lipid peroxyl radicals.[34]

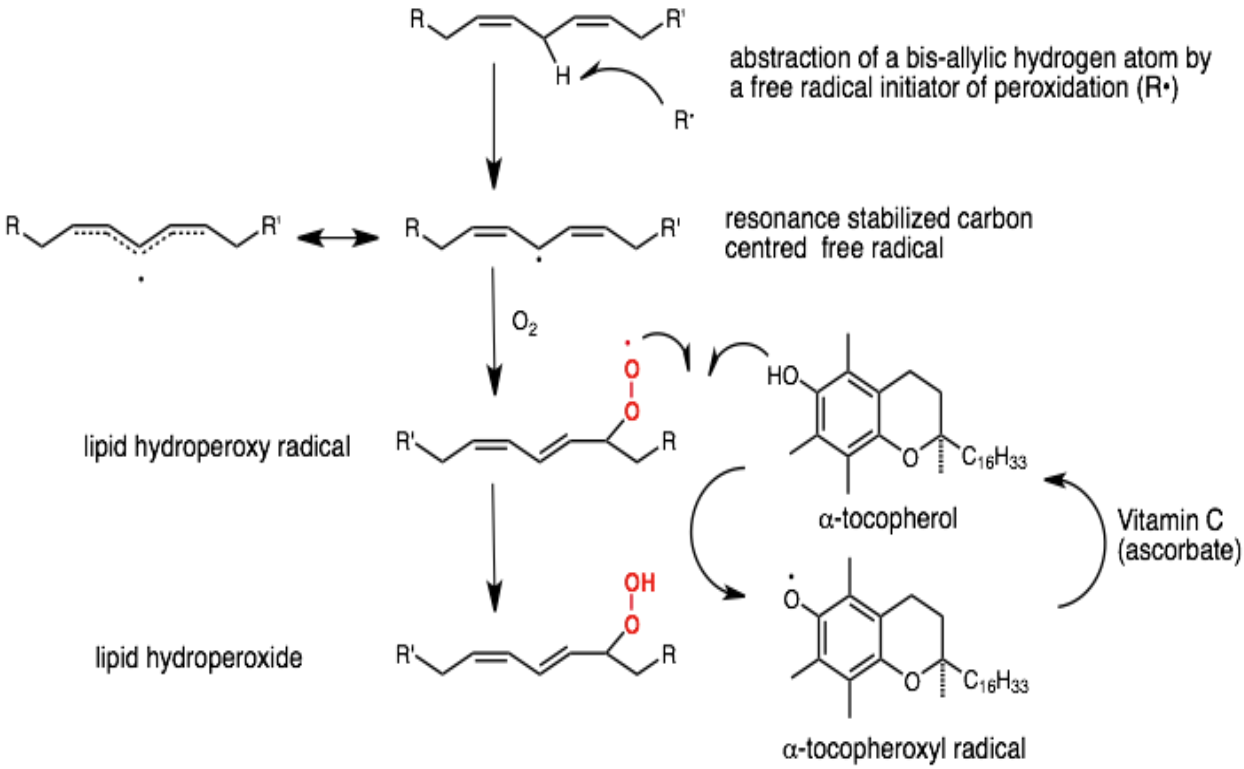

Figure 6: The inhibition of lipid peroxidation by tocopherol in lipid membranes.

The chemical properties and location in membranes of tocols make them ideal for preventing lipid peroxidation.[35] Carbon-6 on the chromanol ring of tocols contains a phenolic hydrogen which is prone to hydrogen atom abstraction by lipid peroxyl radicals. This terminates the lipid peroxidation chain reaction and the tocopheroxyl generated is resonance stabilized.[35] The lipid hydroperoxide generated can be reduced to an alcohol by enzymes such as glutathione:hydrogen-peroxide oxidoreductase (GPx-1) which uses glutathione as a reducing agent.[37]

The location of the tocols in the membrane is also important for this antioxidant mechanism. The chromanol headgroup of the tocopherols reside near the glycerol backbone of the phospholipid bilayer whereas the tail is buried into the hydrophobic core of the bilayer. The location of the chromanol headgroup near the lipid/aqueous interface enables it to intercept free-radicals found in the aqueous environment from reaching the unsaturated bonds of the hydrocarbon chains.[38] In addition, in the case where a lipid peroxide is generated, the acyl chain may diffuse towards the membrane surface owing to its increased hydrophilicity.[38] The height of α-tocopherol in the bilayer, measured by the distance from the center of the bilayer, can vary slightly depending on the lipid composition of the local environment.[38] The proximity of the tocopheroxyl radical to the aqueous membrane surface allows tocols to be recycled by water soluble reducing agents such as ascorbate.[35] Consequently, the ROS radicals are removed from the lipid membrane and lipid peroxidation is terminated.

Over the past few decades, the literature has been focused on the tocopherols capacity to be a lipid peroxidation chain-breaking antioxidant. This is achieved by generating the resonance stabilized tocopheroxyl radical which can be recycled by water-soluble reducing agents such as ascorbate.[35,39] The rate of reduction of the tocopheroxyl radical to the tocopherol is of course highly dependant on the concentration of the reducing agent. If the concentration of the reducing agents are low enough, the radical may undergo several competing reactions such as dimerization, addition reactions with other lipid peroxyl radicals or even a second-electron oxidation leading to the formation of a quinone.[39]

Some studies suggest that differences observed *in vivo* might be associated with properties not related to the antioxidant function of vitamin E.[40] It has been suggested that α-tocopherol might be involved in the inhibition of protein kinase c (PKC) by activation of protein phosphatase 2A, modulate the activity of cytosolic phospholipase A_2 ($cPLA_2$), stimulating the release of cytokines, and anti-inflammatory responses.[40] Such effects were not observed with a diet supplemented with β-tocopherol.[40] On the other hand, some researchers argue that the difference in biological effects are still related to the antioxidant function of α-tocopherol.[34] When bovine pulmonary artery endothelial cells were stimulated with peroxynitrite, an oxidative stress inducer, the activity of PKC and $cPLA_2$ also increased.[41] Therefore, if oxidative stress increases the activity of these enzymes, then it would be reasonable that an antioxidant such as α-tocopherol decreases their activity by reducing oxidative stress.[34] It is hypothesized that the biological effects observed are due to changes in oxidative stress or membrane properties (fluidity and packing errors).[34,42] The differences in biological activities between the vitamers may be explained by three reasons: the chromanol head of α-tocopherol sits higher in the membrane than the other vitamers, because the concentration of α-tocopherol is much higher than other tocols *in vivo*, or because the tocopherols may exhibit different antioxidant efficiencies in membranes.[34,42,43]

1.5 Biological differences among tocol isoforms

The antioxidant capabilities across the tocol family is well described *in vitro* in various solvents and lipid suspensions.[34,44–47] In one study, the antioxidant activity of the tocols were tested in a competition reaction against pyrogallolsulfonphthalein (PG) using 2,2'-azobis(2,4-dimethylvaleronitrile) (AMVN) as a radical initiator. The antioxidant activity of the tocols

decreased in the order of α- > γ- ≈ β- > δ-tocopherol, while no significant difference was observed between the tocopherols and tocotrienols within the respective chromanol substitution patterns.[47] Traber and Atkinson have reviewed the literature that described a similar rank order across the tocol family with respect to the hydrogen atom abstraction rate constants in various solvents as seen in **Table 2**.[34] Although these studies demonstrate the possibility to rank the antioxidant ability across the tocol family, the differences are minimal compared to the much more significant biological differences seen in the fetal resorption assay seen in **Table 2**.[34] The differences in the fetal resorption assay can be attributed to the preferential retention and distribution of α-tocopherol by the hepatic α-tocopherol transfer protein and higher metabolism of the other isomers by Cyp 4F2.[13,17,34] Nonetheless, the reason for preferential retention of α-tocopherol in animals over the other isoforms remains unknown.

Table 2: The antioxidant capabilities of the tocopherols in various media. Table taken with permission from Traber & Atkinson. [34]

Chemical assessments of the antioxidant abilities of tocopherols in organic solution and aqueous suspension of phospholipids

	Rates					Antioxidant efficiencies			Fetal resorption assay
	$k_a \times 10^{-3}$ M^{-1} s^{-1} [52]	$k_a \times 10^{-5}$ M^{-1} s^{-1} [55]	$k_5 \times 10^{-4}$ M^{-1} s^{-1} [51]	$k_1 \times 10^{-4}$ M^{-1} s^{-1} [50]	$k_1 \times 10^{-4}$ M^{-1} s^{-1} [50]	[53]	[53]	[54]	[56]
	EtOH	Triton micelle		IAS	LKEPR	0.10 M HDTBr	0.10 M SDS	0.5 M SDS	% of all rac α-tocopheryl acetate
						Conjugated dienes	Conjugated dienes	O_2 uptake	
α-Tocopherol	5.12	5.12	235±50	320	260	1770±90	1830±50	1000	80
β-Tocopherol	2.24	1.05	166±33	130		970±140	950±30	590	45
γ-Tocopherol	2.42	1.00	159±42	140	70	1020±40	980±60	590	13
δ-Tocopherol	1	0.149	65±13	44	33	530±30	570±50	240	<0.4
Tocol	0.56	0.0353							
PMC			214±81	380		2850±100	2880±120	4050	
Trolox				110		8300±360	1320±90	2970	

It would be attractive to answer this question by observing various effects *in vivo* in animal trials supplemented with different isoforms of vitamin E. However, the preferential absorption and distribution of α-tocopherol over the other isoforms presents a significant barrier. To overcome this issue, some studies sought to evaluate the difference in cell culture assays, some of which are discussed here.[44] Up to the 1990s, much of the research on vitamin E was dedicated to α-tocopherol because it is the most biologically active isoform of the vitamin.[44] In 1997, Christen *et al.* were curious as to why the supplementation of α-tocopherol failed to produce any protective effects on coronary heart disease in a large cohort of post-menopausal women,[48] or reduce the risk of lung cancer in a randomized, double-blind placebo controlled prevention trial in male smokers.[49,50] Their hypothesis was that supplementation of α-tocopherol lowers the concentrations of γ-tocopherol in plasma and other tissues. As such, the difference in the ability to inhibit peroxynitrite induced lipid peroxidation between α and γ-tocopherol in phosphatidylcholine (PC) liposomes from soybeans as well as in human LDL was examined. It was found that γ-tocopherol was significantly more efficient at preventing PC hydroperoxide (PC-OOH) formation compared to α-tocopherol as seen in **Figure 7A**. Furthermore, the rate and amount of of PC-OOH formation in PC liposomes treated with 1 mM 3-morpholinosydnonimine (SIN-1), a nitric oxide generator, was significantly reduced when comparing γ-tocopherol to α-tocopherol as seen in **Figure 7B**.[49] In contrast, it was found that α-tocopherol was slightly more efficient at inhibiting the formation of cholesteryl ester hydroperoxides (CE-OOH) in human LDL treated with 0.2 mM SIN-1. To rationalize these results, the mechanism of inhibition of peroxynitrite induced lipid peroxidation by the tocopherols was accomplished by characterizing the products of reaction with nitrous acid (HNO_2). Indeed, fundamentally different reactivities between α and γ-tocopherol were reported as seen in **Figure 8**: α-tocopherol underwent a two

electron oxidation to form α-tocopherol quinone whereas γ-tocopherol formed a 5-nitro-γ-tocopherol derivative in greater than 90% yield.[49] In the liposome experiments, α-tocopherol was oxidized almost quantitatively to α-tocopherol quinone (90%) and γ-tocopherol formed an *ortho*-γ-tocopherol quinone product called tocored (~25%), 5-nitro-γ-tocopherol derivative (50%) and 25% remained unreacted.[49] This study demonstrates the difference in electrophilic nature of the 5-position of γ-tocopherol compared to α-tocopherol. It is suggested that the supplementation with only α-tocopherol should be reconsidered because it suppresses the levels of γ-tocopherol *in vivo*.[49]

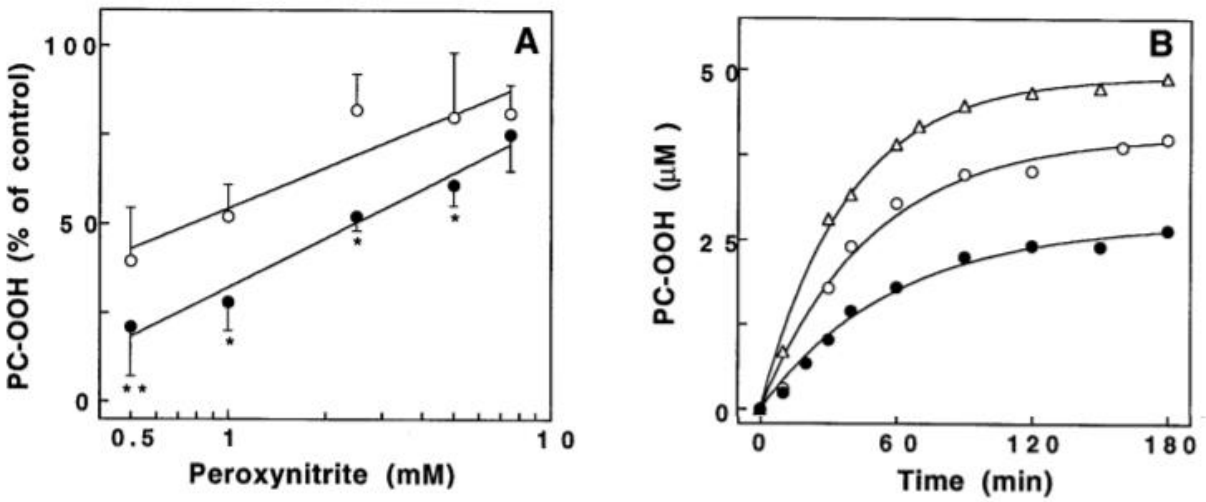

Figure 7: A) The inhibition of PC-OOH formation in PC liposomes by 0.1mM α-tocopherol (open circles) and γ-tocopherol (closed circles) using various concentrations of peroxynitrite. B) The effect of 20 μM α-tocopherol (open circles), γ-tocopherol (closed circles) and without tocopherols (open triangles) on the rate of PC-OOH formation in PC liposomes treated with 1mM 3-morpholinosyndonimine (SIN-1) to induce PC-OOH formation. Figure taken with permission from Christen *et al*. [49]

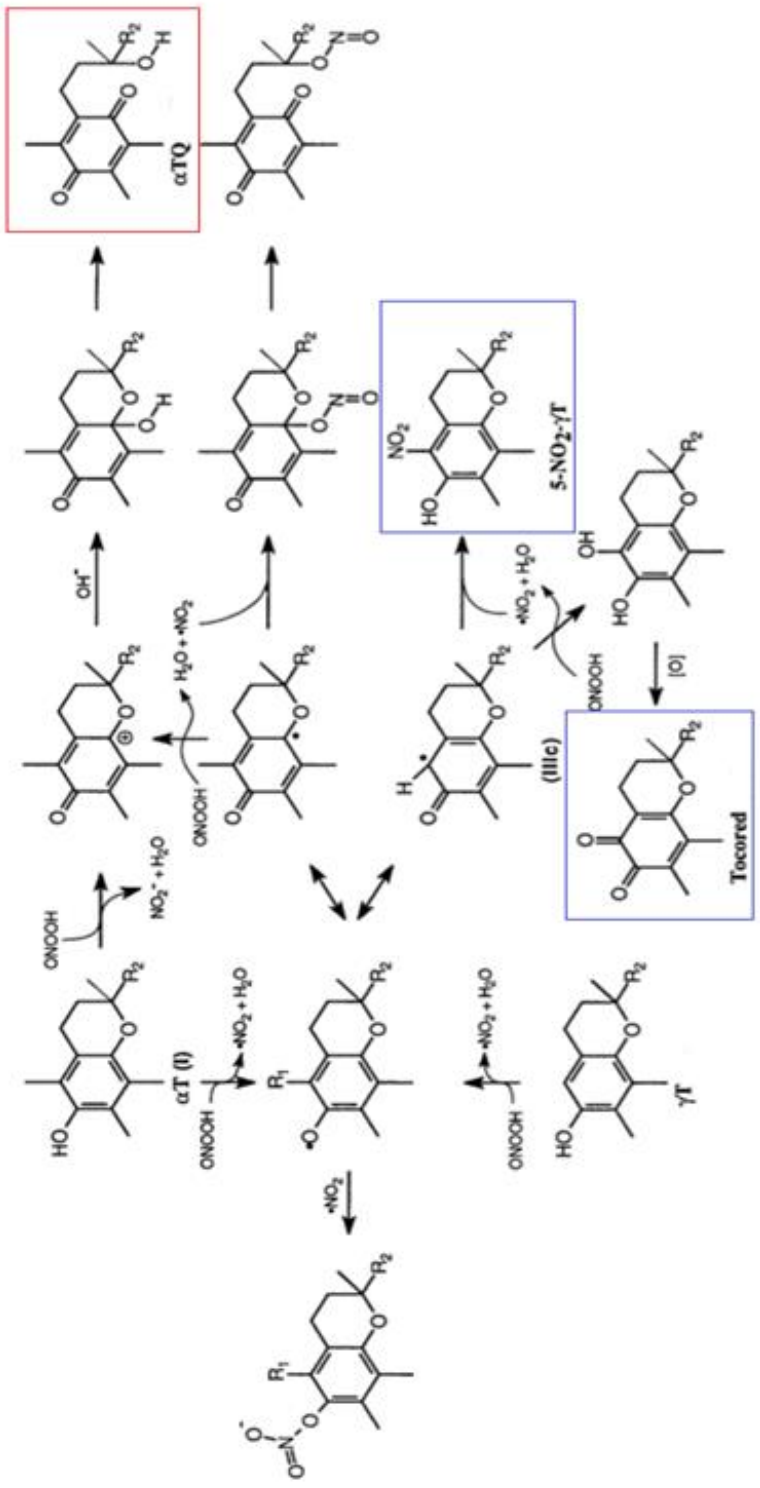

Figure 8: The reaction products of α and γ-tocopherol in the presence of peroxynitrite. The major product of α-tocopherol is highlighted in red and the major products of γ-tocopherol are highlighted in blue. Figure taken with permission from Christen *et al.*[49]

A few years later, McCormick and Parker were interested in the effects of supplementation of the different tocopherols (α, γ and δ) on the cell viability of a mouse macrophage tumour cell line, RAW 264.7.[51] Interestingly, drastic differences in cytotoxicity were observed between the tocopherol vitamers: δ-tocopherol being more cytotoxic than γ-tocopherol, whereas no cytotoxicity was observed with α-tocopherol as seen in **Figure 9**. The doses are within the physiological range of 30-60 μM for the concentration of α-tocopherol in human plasma.[51] Next, the effect of the different isoforms on cell viability in various cell lines was of interest. Of all the cell lines tested: primary mouse macrophages, human breast cancer cell line (MCF-7), mouse fibroblasts (NIH 3T3), human hepatocytes (HepG2) and bovine endothelial cell (endo), the HepG2 and the endo cells appeared resistant to the cytotoxic effects of γ and δ-tocopherol. The other cell lines followed the same rank order of cytotoxicity (i.e. δ > γ >> α) as the RAW 264.7 cell line. Interestingly, the HepG2 showed only a ~20% accumulation of tocopherols compared to the macrophage cell line owing to hepatic metabolism which may explain its resistance to cytotoxicity. Moreover, no significant difference in accumulation between the different tocopherols was observed in all cell lines, indicating that the cytotoxic properties of γ and δ-tocopherol are not a result of differences in cellular accumulation of the vitamers. By analysis of caspase-3 activity and DNA fragmentation in the RAW 264.7 cells incubated with various concentrations of δ-tocopherol, it was concluded that δ-tocopherol is associated with apoptosis, though the mechanism is not clear.[51] These results suggest that the degree of methylation on the chromanol ring may correlate to the cytotoxicity observed. Furthermore, it may explain the preferential retention of the less toxic α-tocopherol over the other isoforms of vitamin E.[51]

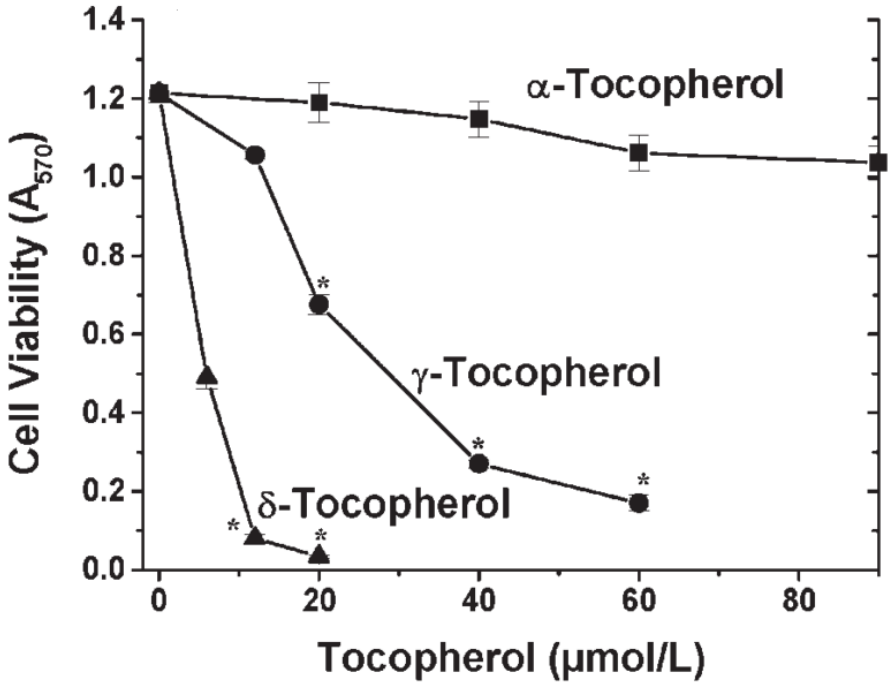

Figure 9: The cell viability of a mouse macrophage cell line RAW 264.7 after incubation with different tocopherols for 24 hours (n=4). Figure taken with permission from McCormick & Parker.[51]

More recently, Elisia and Kitts investigated the effect of α-,γ- and δ-tocopherol on interferon gamma/phorbol myristate acetate (IFNγ/PMA) induced pro-inflammatory oxidative conditions of Caco-2 cells.[52] More specifically, the study aimed to explore the effect of the different tocopherol isoforms on the inflammatory response and the oxidative stress-activated cell signaling pathways that involve the transcription factor complexes Nf-κB and Nrf-2. The inflammatory response was measured by levels of interleukin-8 (IL-8), a peptide secreted by macrophages during inflammatory responses. In theory, the higher the levels of IL-8, the less effective the tocopherol is at inhibiting the inflammatory response. As mentioned previously, Nf-κB is an oxidative stress-activated transcription factor responsible for the expression of cytokines, whereas Nrf- 2 is a transcription factor, activated under oxidative stress, that is responsible for the expression of various antioxidant enzymes. The experiments performed by

Elisia and Kitts used three concentrations of tocopherols: 1, 10 and 100 μM. No significant effects were observed at 1 and 10 μM in most of the experiments. Thus, most of the conclusions obtained from these experiments were extracted from the results at 100 μM. It was observed that IL-8 secretion was inhibited in decreasing order of γ>α>δ when cells were incubated with 100 μM tocopherols as seen in **Figure 10A**. However, at 10 μM, α-tocopherol showed no effect on IL-8 secretion whereas a ~40 % reduction in IL-8 secretion was observed in γ and δ-tocopherol. It would be interesting to measure the effect of tocopherol isoforms on IL-8 secretion at more physiologically relevant concentrations. The attenuation of the Nf-κB pathway was most prominent in α-tocopherol while no clear concentration dependant relationship was established with γ and δ-tocopherol (**Figure 10C**). In contrast, a significant difference in the activation of the Nrf-2 pathway was observed between the tocopherol isoforms as seen in **Figure 10B**. δ-Tocopherol had the greatest effect on the activation of the Nrf-2 pathway and showed significant activation even at 10 μM. γ-Tocopherol showed a significant effect on the activation of Nrf-2 at 100 μM, however no significant effect was observed with α-tocopherol at any concentration. These experiments suggest that tocopherol isoforms have distinct capabilities in modulating cell signaling pathways related to the oxidative status of the cell.[52] The authors proposed that the oxidation of tocopherols results in the formation of water soluble tocopherol derived radicals which may impart pro-oxidant activity in the cytosol. They suggested that the differences may be attributed to the polarity of the isoforms; δ-tocopherol is the most polar isoform, therefore, the pro-oxidant δ-tocopherol derived radicals would be more partitioned in the cytoplasm.[52] More

insight into the distinct mechanisms of Nf-κB and Nrf-2 activation by tocopherol isoforms is warranted.

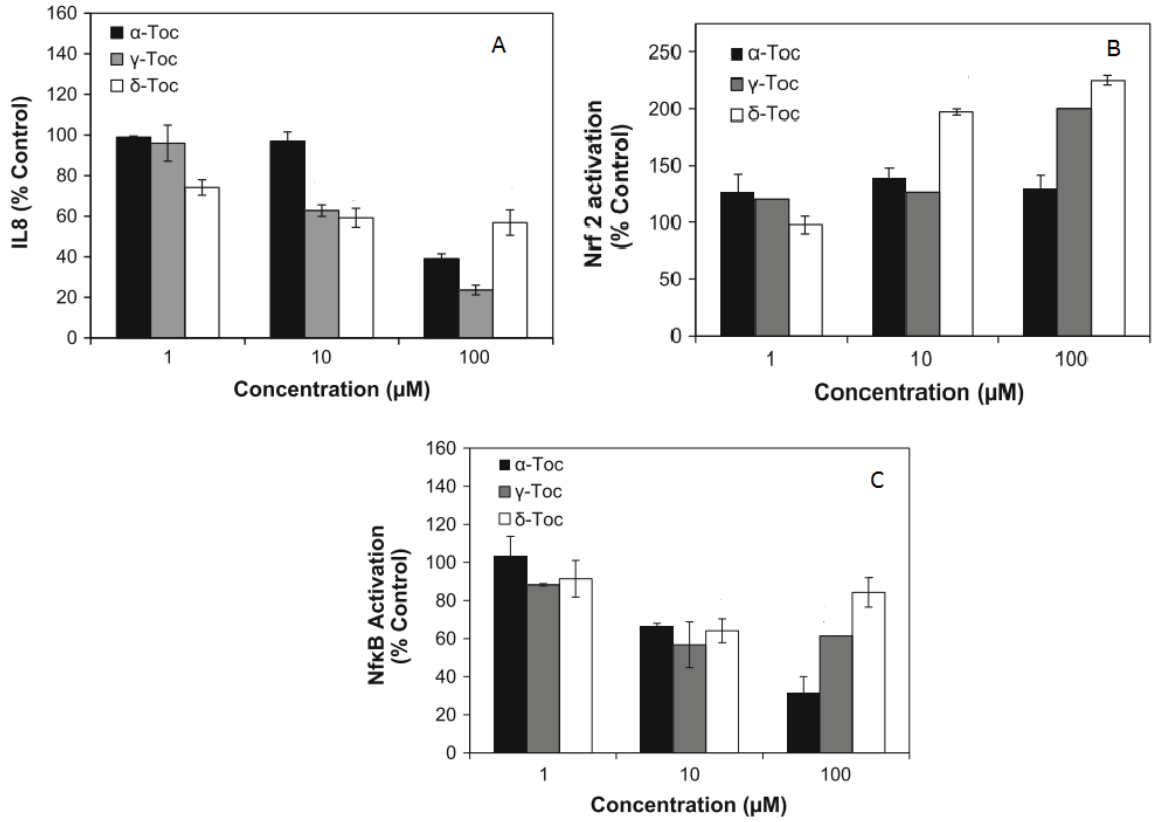

Figure 10: A) The effect of tocopherol isoforms on the levels of IL-8 in a IFNγ/PMA induced inflammatory and oxidative response conditions of a Caco-2 cell line compared to a control. B) The effect of tocopherol isoforms on the Nrf-2 activation in a IFNγ/PMA induced inflammatory and oxidative response conditions of a Caco-2 cell line compared to a control C) The effect of tocopherol isoforms on the Nf-κB activation in a IFNγ/PMA induced inflammatory and oxidative response conditions of a Caco-2 cell line compared to a control. In all cases, the values refer to the percentage of differences between a negative and positive control: the negative control being Caco-2 cells without IFNγ/PMA and tocopherols, the positive control being Caco-2 cells incubated with IFNγ/PMA but without tocopherols. Figure adapted from Elisia & Kitts.[52]

The previously mentioned studies demonstrate the differences between the tocopherol isoforms, however, the effects of the tocotrienols were neglected. Unfortunately, most of the literature on vitamin E is performed with α-tocopherol. Equally concerning is that, the majority

of the research on tocotrienols is performed using a tocotrienol rich fraction (TRF) derived from palm oil which contains a mixture of tocopherols and tocotrienols.[44] Thus, the effects observed can not be attributed to a specific tocol isoform in these studies using unpurified TRF. Nonetheless, some studies have suggested that tocotrienols may exhibit increased anti-cancer, anticholesterolemic, anti-inflammatory, cardioprotective and neuroprotective properties compared to tocopherols.[44] To focus in on the difference between tocotrienols and tocopherols, it would be wise to compare the tocopherol and tocotrienols having the same methylation pattern, given the different effects observed between the tocopherol isoforms. That is, α-tocopherol should be compared to α-tocotrienol, γ-tocopherol compared to γ-tocotrienol, and so on.

There are few reports in the literature examining different biological effects between α-tocopherol and α-tocotrienol. As mentioned previously, it is difficult to study the effects *in vivo* due to the preferential retention of α-tocopherol by α-TTP. Nonetheless, in the 1980s, Qureshi *et al.* noticed that populations that consumed diets rich in cereal grains had a lower incidence of cardiovascular disease owing to lower levels of cholesterol.[53] They demonstrated that barley was the most effective cereal grain in lowering blood cholesterol levels in animal trials out of the cereal grains tested.[53] Furthermore, they had demonstrated that the lower levels of cholesterol was the result of a suppressive action on the 3-hydroxy-3-methylglutaryl coenzyme A (HMG-CoA) reductase enzyme.[53] HMG-CoA reductase is the rate-limiting enzyme in the mevalonate pathway of the biosynthesis of isoprenoids including cholesterol.[53] The sequential extraction of barley flour using petroleum ether yielded a fraction with HMG-CoA reductase inhibitory properties. The isolation of the components of the petroleum ether soluble fraction yielded 10 compounds, two of which (compounds I and II) demonstrated HMG-CoA reductase inhibitory properties. Compound I was characterized as α-tocotrienol by mass spectrometry and no

comment on the identify of compound II was offered. The dietary administration of α-tocotrienol to broiler cockerels for 21 days showed a concentration dependant inhibition on the activity of HMG-CoA reductase in the hepatocytes as seen in **Table 3**.[53] This study may demonstrate potential benefits of tocotrienols over tocopherols because the rank of grains in the order of their increasing effect on the suppression of cholesterol biosynthesis as measured by the cholesterol concentrations in chicks was: corn (100% or 139 ± 7 mg/100 mL in plasma, 100% or 318 ± 17 mg/100 g in liver), wheat (76%, 80%), rye (75%, 79%), oats (68%, 75%), and barley (55%, 65%). The tocol concentrations in these cereal grains (mg/kg) are: corn (23.6), wheat (35.0), rye (44.6), oats (17.8), and barley (30.5); it would be expected that the rank order for cholesterol inhibition correlates to the total tocol concentration. However, it is interesting because an increase in tocol contents do not correlate with the observed suppression of cholesterol concentrations. On the other hand, the tocotrienols as per cent of tocols are: corn (15%), wheat (61%), rye (62%), oats (71%) and barley (81%).[53,54] This measure (tocotrienols as percent of total tocols) reflects more closely the cholesterol-suppressive pattern of these grains than does the measure of the quantity of tocols. The inhibitory mechanism of α-tocotrienol on HMG-CoA reductase may be similar to that of squalene or ubiquinone-9 which all share an isoprenoid chain but no specific mechanism of inhibition was offered.[53] The authors suggested that the inhibition of the mevalonate pathway from one of the multiple end products (squalene, vitamin K, cholesterol, etc.) will decrease not only its own production, but also that of the products of the other branches. Therefore, it is plausible that the isoprenoid chain of the tocotrienol mimics the isoprenoids of the mevalonate pathway and inhibits their production through an end product inhibition.[53]

Table 3: Concentration-dependent effects of dietary *d*-α-tocotrienol on cholesterol metabolism in broiler cockerels. Feeding period, 21 days, fast 2, refed 3; n = 9. Table taken with permission from Qureshi *et al*.[53]

d-α-Tocotrienol	HMG-CoA reductase[a]	Cholesterol 7α-hydroxylase[b]	Fatty acid synthetase[c]	Serum cholesterol (mg/100 ml)		
				Total	HDL	LDL
ppm						
0	198 ± 15[d]	0.45 ± 0.03[d]	168 ± 20[d]	161 ± 13[d]	54 ± 5[d]	81 ± 7[d]
2.5	172 ± 12[d,e] (87)[g]	0.45 ± 0.02[d] (93)[g]	190 ± 12[d] (118)[g]	152 ± 10[d] (94)[g]	54 ± 6[d] (100)[g]	73 ± 5[d] (90)[g]
5.0	161 ± 12[e] (81)	0.39 ± 0.03[d] (87)	202 ± 10[e] (120)	144 ± 8[d] (89)	51 ± 4[d] (94)	60 ± 4[e] (74)
10.0	144 ± 9[e,f] (73)	0.37 ± 0.02[e] (82)	210 ± 15[e,f] (125)	125 ± 7[e] (78)	52 ± 5[d] (96)	54 ± 4[e] (67)
15.0	135 ± 8[f] (68)	0.38 ± 0.03[e] (84)	218 ± 17[e,f] (130)	122 ± 6[e] (76)	50 ± 6[d] (93)	52 ± 5[e] (64)
20.0	130 ± 6[f] (66)	0.35 ± 0.02[e] (78)	235 ± 18[f] (140)	105 ± 8[f] (65)	48 ± 5[d] (89)	38 ± 5[f] (47)

[a] pmol of mevalonic acid synthesized per min/mg of microsomal protein.
[b] pmol of ^{14}C-labeled cholesterol into ^{14}C-labeled 7α-hydroxycholesterol per min/mg of microsomal protein.
[c] nmol of NADPH oxidized per min/mg of cytosolic protein.
[d-f] Values not sharing a common superscript letter are different at $p < 0.01$.
[g] Percentage of control activity.

A few years later, Pearce *et al.* set out to extend the original findings of Qureshi *et al.* by examining the effects of synthetic α-tocotrienol on a cholesterol biosynthesis assay in primary rat hepatocytes.[55] In their investigations, the synthetic *d,l*- α-tocotrienol was substantially less active (17% inhibition of cholesterol biosynthesis at 210 μg/mL) in primary rat hepatocytes compared to tocotrienol fraction isolated from barley flour (31% at 138 μg/mL) even while factoring in the racemic mixture of the synthetic α-tocotrienol.[55] Around the same time, the researchers received a tocotrienol rich fraction (TRF) from palm oil. The TRF was subjected to flash chromatography and HPLC which identified the following components: *d*-α-tocopherol (26%), *d*-α-tocotrienol (18%), *d*-γ-tocotrienol (27%), and *d*-δ-tocotrienol (7%). The isolated tocols were assayed *in vitro* in human hepatoma HepG2 cells as seen in **Table 4**.[55] The cholesterol synthesis assay was measured by the amount of ^{14}C-acetate incorporated into cholesterol after incubation. As seen in **Table 4**, only 3 ± 1 % inhibition of cholesterol synthesis was observed in cells incubated with γ-tocopherol. Remarkably, the natural *d*-tocotrienols demonstrated at least a 32 ± 4 % inhibition as seen with α-tocotrienol. The effects are even more pronounced with *d*-γ-tocotrienol and *d*-δ-tocotrienol which showed 78 ± 3 % and 77 ± 4 % inhibition respectively. The little activity observed with γ-tocopherol highlighted the importance of the unsaturated phytyl chain of

tocotrienols in the inhibition of cholesterol synthesis. The inhibition of cholesterol synthesis by tocotrienols can be attributed to a reduction in the activity of HMG-CoA reductase as seen in **Table 4**.[55] The authors speculated that the mechanism of inhibition appears to involve the down-regulation of HMG-CoA reductase and not direct inhibition because the addition of γ-tocotrienol to an isolated microsomal HMG-CoA reductase fraction from HepG2 cells did not influence its activity.[55] Furthermore, the tocotrienols were shown to inhibit the incorporation of ^{14}C labeled acetate but not mevalonate into sterol which suggests a suppressive action on the HMG-CoA reductase enzyme.[55] The mechanism of inhibition was further investigated by Parker *et al.* of the same group a year later.[56] Using immunoblot protein quantification and mRNA quantification by slot-blot hybridization, the researchers determined that the mechanism of inhibition by tocotrienols involves a post-transcriptional process controlling the rate of degradation of the HMG-CoA reductase enzyme.[56] The mechanism of action for controlling the rate of degradation remains unclear.

Table 4: The effect of various tocols on the inhibition of cholesterol synthesis and HMGR activity in human HepG2 cells. Table taken with permission from Pearce *et al.*[55]

	% inhibition			
compound, 10 μM	*n*	[^{14}C]-Ac	*n*	HMGR
d-γ-tocopherol	2	3 ± 1	2	0
d-α-tocotrienol	2	32 ± 4	2	15 ± 1
d,l-α-tocotrienol	3	21 ± 10	2	19 ± 3
d-γ-tocotrienol	4	78 ± 3	4	64 ± 3
d,l-γ-tocotrienol	9	71 ± 4	9	62 ± 5
d-δ-tocotrienol	3	77 ± 3	3	65 ± 2
d,l-tocotrienol	4	63 ± 5	3	56 ± 8
23	2	38 ± 2	–	–
32	2	19 ± 4	–	–

[a] Cholesterol synthesis inhibition and HMGCoA reductase suppression were assayed in HepG2 cells incubated for 4 h with the compounds indicated at 10 μM. Values represent mean percent inhibition vs controls receiving DMSO vehicle; *n* = number of repeated experiments, each assayed in duplicate.

Inspired by previous reports which suggested promising anti-tumour activity exhibited by tocotrienols, Fu *et al.* sought to overcome the limited bioavailability barrier by using a novel drug transport system.[57] The authors recognized the need for iron in tumor cell growth, which is carried to cells by the transferrin protein. They demonstrated that an intravenous injection of a lipid vesicle containing a tocotrienol rich fraction (TRF) linked to a transferrin protein could be efficiently delivered and exhibit anti-tumor activity in mice. The shortcoming of these studies was that the TRF contains a mixture of tocopherols and tocotrienols so the extent of activity from each vitamer could not be examined. Recently, the same group aimed to investigate the effect of the individual tocols loaded in a transferrin linked lipid vesicles delivery system on two cancer cell lines: B16-F10 murine melanoma and A431human epidermoid carcinoma. As seen in **Table 5,** α-tocopherol and α-tocotrienol loaded transferrin vesicles exhibited the slightly greater effects on cell viability in the B16-F10 cell line expressed by the lowest IC_{50} values. The IC_{50} is the concentration required to inhibit the growth of the cell population by 50%. It is interesting that the α-tocotrienol loaded transferrin vesicle exhibited a significantly greater effect on A431 cell viability compared to the other isoforms. Because the α-tocotrienol loaded delivery system exhibited the greatest anti-cancer cell growth activity in both cell lines tested, the researchers determined the α-tocotrienol loaded delivery system *in vivo* in female immuno-deficient BALB/c mice implanted with A431 or B16-F10-luc-G5 cancer cells in exponential growth. The effects of the other tocol loaded vesicles were not assayed *in vivo.* As seen in **Figure 11**, significant tumour growth attenuation was achieved in both cancer types using the α-tocotrienol loaded delivery system compared to the controls.[58] The authors provide no insight into the mechanism of increased anti-cancer properties of α-tocotrienol which warrants future investigation.[58] In another study, α-tocotrienol was shown to exhibit inhibitory effects on human Tenon fibroblasts, a cell

responsible for scarring following eye surgery, at concentrations of 50 µM by as much as 40%, whereas no inhibitory effects were observed with α-tocopherol in concentrations as high as 100 µM.[59]

Table 5: The efficacy of tocol isoforms on cancer cell viability. The control vesicles consist of tocol containing lipid vesicles not linked to transferrin. Table taken with permission from Karim *et al*.[58]

Compound	IC_{50} (µg/mL) (mean ± S.E.M.)		
	Tf-vesicles	Control vesicles	Free drug
B16F10 cells			
α-T3	1.07 ± 0.07	1.23 ± 0.19	50.48 ± 0.12
γ-T3	2.27 ± 0.39	2.97 ± 0.16	>20
δ-T3	1.29 ± 0.11	1.39 ± 0.20	>20
α-Toc	1.06 ± 0.18	1.71 ± 0.25	>20
A431 cells			
α-T3	0.57 ± 0.26	0.99 ± 0.06	>20
γ-T3	1.01 ± 0.15	1.33 ± 0.09	>20
δ-T3	1.73 ± 0.52	2.94 ± 0.14	14.73 ± 0.20
α-Toc	1.13 ± 0.17	1.70 ± 0.48	>20

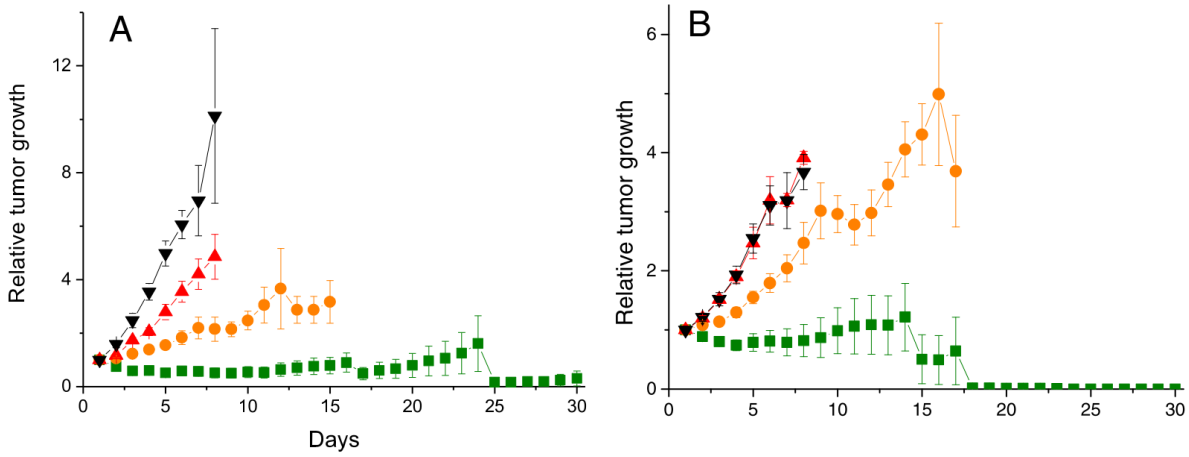

Figure 11: Tumor growth studies in a mouse A431 model (A) and a mouse B16-F10 model (B) after intravenous administration of transferrin-bearing vesicles entrapping α-tocotrienol, α-T3 (10 µg/injection) (green). Controls: lipid vesicles entrapping α-T3 (orange), free α-T3 solution (red), untreated tumors (black). Figure taken with permission from Karim *et al*.[58]

In 2000, Yu *et al.* investigated the apoptosis-inducing properties of tocols in estrogen-responsive MCF7 and estrogen-nonresponsive MDA-MB-435 human breast cancer cell lines.[60] After 3 days of incubation with the tocols, the cells were stained with 4,6-diamidino-2-phenylindole (DAPI) which selectively stains A-T rich regions of DNA to allow visualization of the chromatin structure by fluorescence microscopy. Cells with clearly condensed chromatin or exhibiting nuclei fragmentation were scored as apoptotic. The number of apoptotic versus non-apoptotic cells were counted to report an EC_{50} value, the concentration (in μg/ml) of the compound needed to induce apoptotic morphology in 50% of the cells.[60] As seen in **Table 6**, only the δ-tocopherol isoform showed any apoptotic properties amongst the tocopherol family. In contrast, the tocotrienols were significantly more effective at inducing apoptotic properties in the MCF7 cell line in the decreasing order: δ-tocotrienol > α-tocotrienol ≈ γ-tocotrienol > δ-tocopherol. In the MDA-MB-435 cell line, the same rank order is achieved except α-tocotrienol is less effective, and comparable to the properties of δ-tocopherol. Interestingly, the α-tocopherol succinate derivative demonstrated significant pro-apoptotic properties with an EC_{50} of 7 ± 1.0 μg/mL, whereas no significant apoptotic stimulation was observed with α-tocopherol or its acetate derivative. The cellular and molecular events responsible for the apoptotic properties observed by the tocols were not established in this study, however the authors postulate various reasons related to increased expression of different proteins involved in apoptosis.[60] Unfortunately, the molecular mechanism of increased expression of these proteins by tocols is not known.[60,61]

Table 6: Comparison of apoptotic properties of various tocols in two human breast cancer cell lines. Table taken with permission from from Yu *et al*.[60]

	EC_{50}, μg/ml test reagents[a,b]	
	MCF7 cells	MDA-MB-435 cells
Tocopherol Derivatives		
RRR-α-tocopheryl succinate	7 ± 1.0	8 ± 1.0
RRR-α-tocopheryl acetate	>200	>200
Tocopherols		
RRR-α-tocopherol	>200	>200
RRR-β-tocopherol	>200	>200
RRR-γ-tocopherol	>200	>200
RRR-δ-tocopherol	97 ± 5.0	145 ± 33
Tocotrienols		
α-tocotrienol	14 ± 2.0	176 ± 23
β-tocotrienol[c]	NT	NT
γ-tocotrienol	15 ± 2.0	28 ± 2.6
δ-tocotrienol	7 ± 0.8	13 ± 3.5

a: Values are means ± SE of 4 separate dose-response curves. EC_{50}, effective concentration for 50% response, i.e., concentration of test agent that induces 50% of cells to undergo morphologically detectable apoptosis, as visualized by 4,6-diamidino-2-phenylindole staining, after 3 days of treatment.

b: Compounds with EC_{50} values >200 were ineffective as inducers of apoptosis within the range of their solubility, i.e., 1–200 μg/ml; therefore, EC_{50} values were not established but are known to be >200 μg/ml.

c: β-Tocotrienol was not available for testing. NT, not tested.

In another study, researchers observed the cytotoxicity of different isoprenoids on a culture of murine B16 (F10) melanoma cells.[62] The cells were incubated for 24 hours prior to the introduction of the various tocols. They reported the cytotoxicity as an IC50 value: the concentration needed to inhibit the growth of the culture by 50%. α-Tocotrienol had a much higher IC50 value (110 μmol/L) than γ- tocotrienol (20 μmol/L) and δ-tocotrienol (10 μmol/L) as

seen in **Figure 12**.[62] Importantly, no cytotoxicity was observed with cells incubated with α-tocopherol.

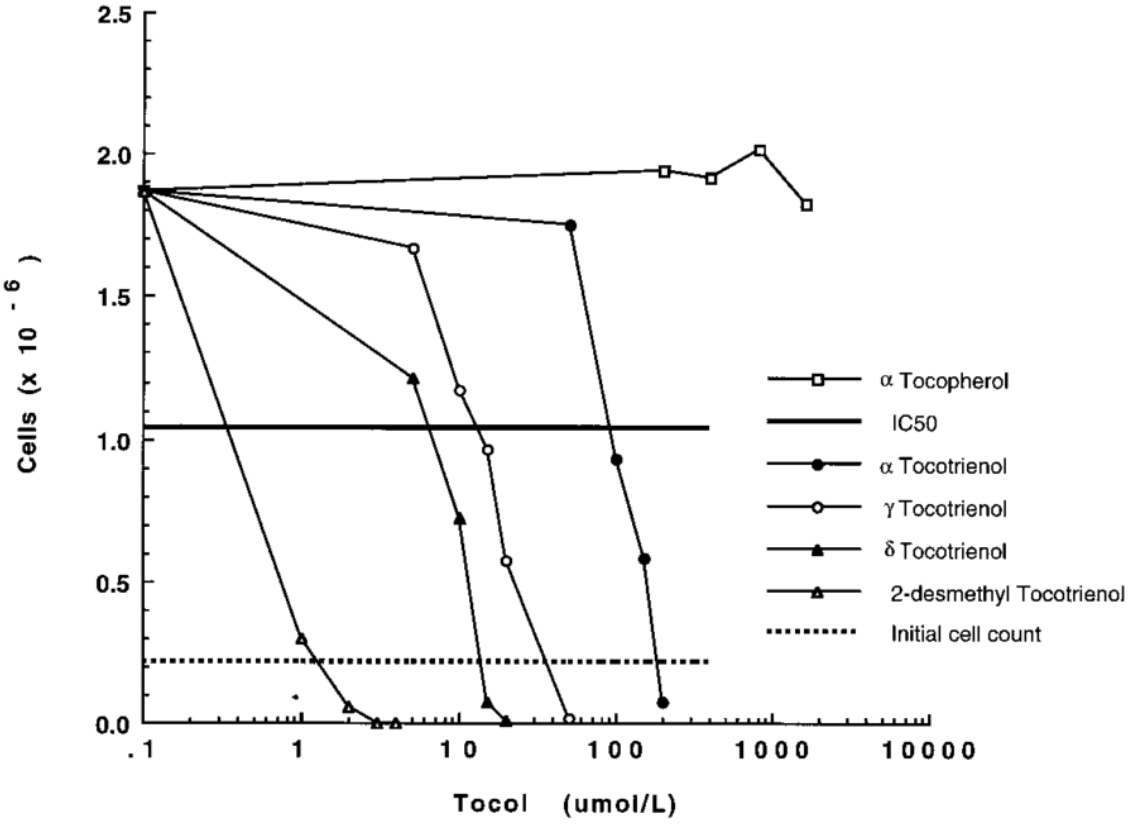

Figure 12: The viability of melanoma B16 cells 48 hours after the incubation with various tocols. Figure taken with permission from He *et al*.[62]

In summary, the antioxidant activities across the isoforms of the vitamin E family are very similar. However, drastic differences have been observed in measures of biological activity using cell culture assays. McCormick and Parker show that in a RAW 264.7 macrophage cell line, δ-tocopherol exhibited greater cytotoxicity than γ-tocopherol whereas α-tocopherol was not cytotoxic.[51] Elisia and Kitts have demonstrated that α-tocopherol may be involved in the mitigation of Nf-κB pathway in a Caco-2 cell line whereas γ and δ-tocopherol showed little effect. Furthermore, they demonstrated that δ-tocopherol had much greater effect on the

activation of the Nrf-2 cell signaling pathway compared to γ-tocopherol, while α-tocopherol showed no significant activity on this pathway.[52] In addition, various studies described above have shown biological properties unique to the tocotrienols. It would seem unreasonable to appoint such drastic biological differences to rather minor differences in antioxidant activity. The *in vivo* preference for α-tocopherol may then rest on the potential cytotoxic activity of the other tocols. That being said, low concentrations of the other tocols may be required to maintain a certain balance of cell signalling within the cell. Cornwell *et al.* have demonstrated the potential for biological differences arising from the formation of tocopherol derived oxidative products: vitamin E quinones. [63–65] The formation of quinones *in vivo* is the result of a one electron oxidation of the parent tocols to produce the radical cation, the subsequent loss of a proton and then a second electron oxidation produces the phenoxonium cation that reacts with water and thus the formation of the quinone in a mechanism like the one seen earlier in **Figure 8**.

1.4 Tocol Quinones

The difference in biological effects observed between the tocopherols may in fact be imparted by distinct biochemical properties between the tocol derived quinones.[63–65] The non α-tocols are oxidized to electrophilic arylating quinones which can form adducts with free thiol groups of proteins by a Michael addition mechanism. In contrast, the fully substituted chromanol ring of α-tocol quinone is not susceptible to Michael addition.[63–65] Indeed, Cornwell's group has reported the synthesis of glutathione adducts with γ and δ-tocopherol quinone, but not with α-tocopherol quinone.[63,66] Furthermore, they suggested that δ-tocopherol quinone should be more reactive towards nucleophiles than γ-tocopherol quinone because the lack of an electron donating methyl group makes it more electrophilic. This may be responsible for the differences observed between γ- and δ-tocopherol in cell culture assays where they can be oxidized to the

corresponding quinones, and the rate of reactivity with cellular thiol nucleophiles may correlate to the cytotoxicity observed. However, there is no chemical evidence to prove such rates of reactivity, thus it would be interesting to investigate this matter. Nonetheless, further evidence for the difference between arylating tocols and non-arylating tocols was revealed when smooth muscle cells and human acute lymphoblastic leukemia cells were treated with α-tocopherol quinone and γ-tocopherol quinone. Almost no effect was observed in both cell cultures treated with α-tocopherol quinone.[66] Contrarily, cytotoxicity was prominent in both cell cultures treated with γ -tocopherol quinone.[66] The mechanism for non α-tocol quinone arylation is illustrated in **Scheme 1.** Arylating tocol quinones are suggested to be involved in a variety of cell signalling pathways through protein arylation at reactive cysteine residues.[63–66] We suggest that the difference in biological activity observed between the tocols reflects the rate of reactivity of the tocol quinones with thiols.

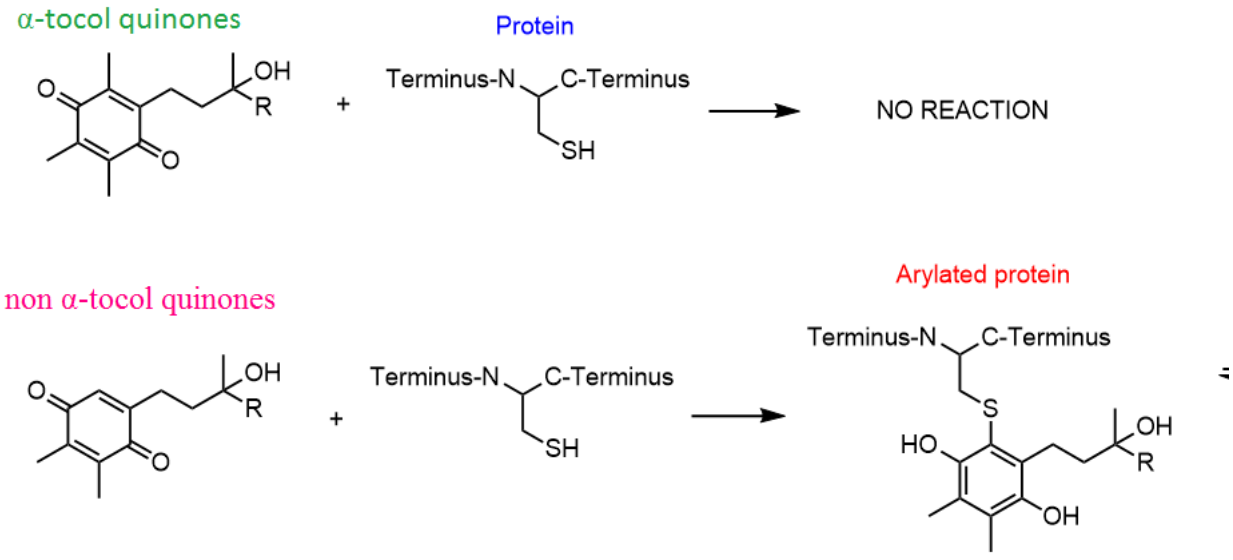

Scheme 1: The protein arylation mechanism of non α-tocol quinones

1.5 Reactive Thiols in Cells

It has been argued that the origin of the eukaryotic cell is marked by the acquisition of the mitochondrion through the endocytosis of bacteria from the archaea.[67] The bacterial endosymbiont has been postulated to be the origin of mitochondria by analysis of genomic studies. Almost all eukaryotic cells possess mitochondria which are responsible for ATP production by oxidative phosphorylation. Through millions of years of evolution, mitochondria have retained a similar core genome responsible for oxidative phosphorylation but have lost most of the other original bacterial genes which have been replaced by nuclear DNA.[67] The evolutionary advantage of this adaptation is that the cell can possess thousands of mitochondria to produce much more energy at a fraction of the total cost.[67] The oxidative phosphorylation pathway involves the two electron oxidation of the reduced form of nicotinamide adenine dinucleotide (NADH) or flavin adenine dinucleotide ($FADH_2$) to an electron acceptor complex which is passed through a series of redox active complexes to ultimately reduce molecular oxygen to water.[68] The energy gained from the electron transport chain is used to pump protons against its concentration gradient from the inside of the inner mitochondrial membrane to the intermembrane space. Consequently, a pH gradient is generated as well as a voltage gradient, collectively known as an electrochemical gradient.[68] The enzyme, ATP synthetase can use the energy from this gradient to synthesize ATP from ADP by allowing the protons to flow down the concentration gradient back to the inside of the cell. The overall process is generally very efficient, however, the electrons may leak to partially reduce oxygen or other organic substrates such as ubiquinone or flavin to generate radicals known as reactive oxygen species like superoxide.[68,69] As a result of electron leakage, reactive oxygen species rise, ATP synthesis decreases and a signal cascade ensues to either protect the cell or induce apoptosis by the release

of cytochrome c.[67] The mitochondria may reduce electron leakage by increasing the expression of the protein complexes involved in oxidative phosphorylation through redox sensitive transcription factors.[67] While the complete redox sensitive mechanisms for reducing electron leakage are not completely understood, the redox sensitivity may arise from reactive thiols in the mitochondrial proteome. For example, it has recently been revealed that the uncoupling protein-1 (UCP-1), a protein in the mitochondria of brown fat adipose tissue, is a redox sensitive protein regulated by the S-sulfenylation of a key cysteine residue.[70] The current efforts of the Weerapana group are focused on identifying reactive cysteine residues in the mitochondrial proteome.[71] Future investigation may reveal the implication of arylating tocol quinones as redox sensitive control in some of the mitochondrial proteins.

The implication of the arylating tocol quinones may not be limited to mitochondrial proteins. The excess formation of reactive oxygen species and electrophiles in eukaryotes may have profound biological effects such as the formation of DNA adducts, mutagenicity and membrane damage. These effects are known causes of cancer, cardiovascular complications, acute and chronic inflammation and neurodegenerative diseases.[72] It is imperative for the human body to effectively manage these compounds to survive, grow, and develop.[72] The Nrf2:Keap1 pathway is considered the most important cellular response to protect the cell from oxidative and electrophilic stress.[72,73] The expression of various enzymes which are responsible for the elimination of oxidants and electrophiles include: NADPH:quinone oxidoreductase 1 (NQ01), UDP glucuronosyltransferase (UGT) and glutathione S-transferase (GSH) all of which are regulated by the antioxidant/electrophile response element (ARE/EpRE) involved in the Nrf2:Keap1 pathway.[72,73]

NF-E2 related factor 2 (Nrf2) is a protein that binds to the ARE/EpRE region of DNA and promotes expression of the antioxidant/electrophilic stress response enzymes. Under normal unstressed conditions, two of these proteins are bound to a Kelch-like ECH associated protein 1 (Keap1) – Cullin3-based ubiquitin E3 ligase (Cul3) homodimer.[72–74] The association of Nrf2 and the Keap1/Cul3 homodimer inhibits Nrf2 as a *trans*-acting promoter. Under conditions of electrophilic stress, the association between Keap1:Nrf2 is inhibited and Nrf2 synthesized *de novo* can promote enzyme expression.[72–74]

The Nrf2 protein has six domains (Neh 1-6) each associated with a different property to achieve its overall function.[73,74] The Neh1 domain is associated with binding to small Maf proteins and binding to the ARE recognition site. Neh 4 and 5 are related to a trans-activation function by recruiting co-activator proteins. Neh 6 functions as a recognition site for degradation by proteasomes in the cytosol. Neh 3 represents the C-terminus of the protein. Neh2 is associated with binding to the Keap1 homodimer. It contains an ETGE and DLG Keap1 binding motif. Under normal conditions, the ETGE motif binds to one monomer and the DLG motif binds to the other. Thus, two Nrf2 proteins can be bound per Keap1 homodimer. The ETGE and DLG binding motifs are separated by seven lysine residues susceptible to ubiquitination by Cul3. Ubiquitination tags the protein complex for degradation by proteasomes in the cytosol. Therefore, the function of Nrf2 as an enzyme expression promoter is inhibited.[72–74]

Keap1 is a protein rich in reactive thiol groups that are susceptible to adduct formation with electrophiles. Cysteine 273 and cysteine 288 are exposed on the surface of Keap1 making them particularly susceptible to electrophiles.[72–74] Electrophile adduct formation with these cysteine residues brings a conformational change in the structure of the Keap1-Cul3 homodimer. The DLG binding motif of Nrf2 has much weaker binding interactions with Keap1 than the

ETGE binding motif. Consequently, only the DLG binding motif dissociates from the Keap1 complex. This is known as the hinge and latch model demonstrated in **Figure 11**.[73] As a result, Cul3 activity is decreased and newly synthesized Nrf2 can activate the antioxidant/electrophilic response element enzymes.[72–74]

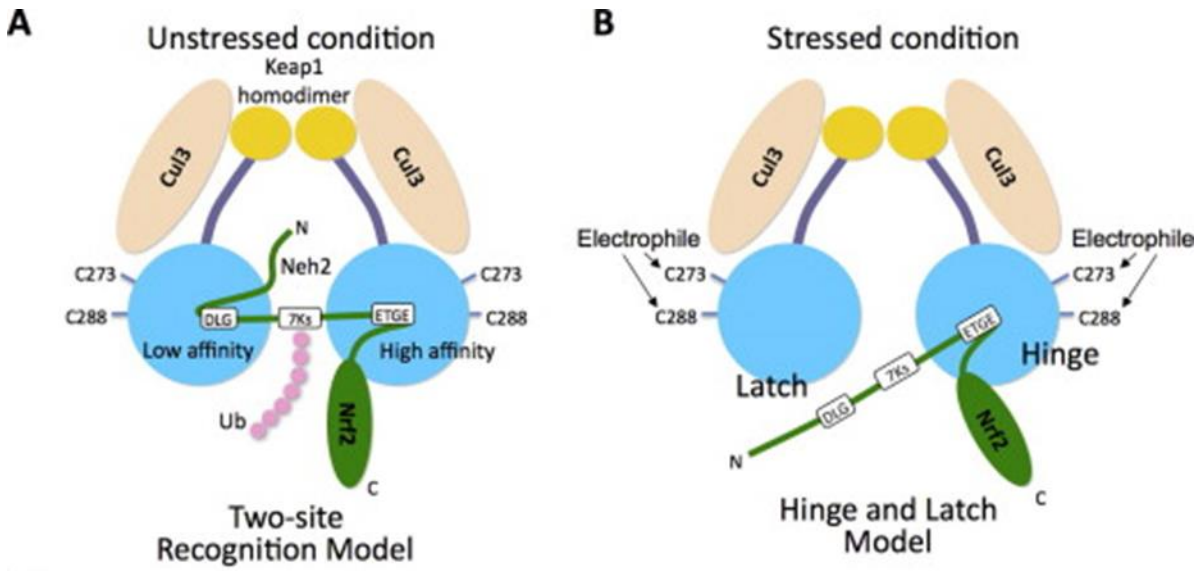

Figure 13: The hinge and latch model of the Nrf2:Keap1 pathway. Figure taken with permission from Urono & Motohasi.[73]

The endoplasmic reticulum is a highly membranous structure in the cell responsible for the synthesis of proteins, lipids and cholesterol.[75] It is suggested that the concentration dependent cytotoxicity observed in cultured cells treated with arylating quinones may be due to an endoplasmic reticulum stress response also known as the unfolded protein response (UPR).[65] The arylating tocol quinones may form adducts with free thiol groups of proteins being synthesized, in turn disrupting disulfide bond formation and proper folding. This would encourage endoplasmic stress and activate the UPR. The UPR slows down protein production, degrades misfolded proteins and increases activation of proteins involved in protein folding in an attempt

to remain viable.[76] If these attempts do not alleviate endoplasmic reticulum stress, the UPR induces apoptosis.[63–65,76]

In summary, the cell contains many different thiols which may be involved in cell signalling pathways upon modification. The role of arylating tocol quinones in these pathways is of current interest. The rate of reactivity of the tocol quinones with thiols as well as the cellular localization and concentration of the quinones may explain the biological differences observed between the isoforms of vitamin E.

1.6 Project Overview

To fully understand the role of the tocol quinones in cell signalling pathways, the reactivity of such species with model thiols needs to be established. The literature on tocol quinones is limited; Cornwell's group has demonstrated the capability for GSH arylation *in vitro* by γ-tocopherol quinone but not α-tocopherol quinone. In addition, the cytotoxicity of the tocol quinones in various cell cultures has been assessed and the general trend in order of decreasing cytotoxicity is as follows: δ> γ>α.[51] We propose that the cytotoxicity observed between the tocol quinones and differences in biological activity observed between the tocopherols is a function of the reactivity of the quinones towards thiols. We hypothesize a higher reactivity of δ-tocopherol quinone with thiols compared to γ-tocopherol quinone owing to the lack of electron donating methyl group in δ-tocopheryl quinone making it more electrophilic as well as less steric hindrance. While it might be reasonable to assume similar reactivities with the tocotrienol quinone, the formation of Michael adducts with thiols in the tocotrienol family is still unknown. There is no chemical justification for an increased rated of tocotrienol quinones, however, given some of the different biological effects exhibited by the tocotrienols such as the anti-cancer

properties mentioned earlier, it may be possible the tocotrienols quinones exhibit increased rate of reactivity with thiols.

This thesis will focus on the synthesis and reactivity of all tocochromanol quinones. The synthesis and reactivity of β-tocohromanol quinones is omitted owing to the similar structure and reactivity with γ and the limited biological relevance due to its scarcity in nature.[19] Tocol quinones will be synthesized from the oxidation of parent congeners. The rate of reactivity of the tocol quinones with a model thiol like N-acetyl cysteine will be performed using UV/Vis spectroscopy.

2. RESULTS AND DISCUSSION

2.1 Isolation of Vitamin E Congeners

The synthesis of vitamin E quinones was performed by the oxidation of the parent tocols. This required pure samples of each vitamer. Silica column chromatography was the general technique used for separation. A vegetable oil suspension rich in tocopherols (obtained from Archer Daniels Midland Co.) was used to isolate pure samples of α-, γ- and δ-tocopherol. The components of the oil suspension are eluted in order of increasing polarity. The first fractions eluted from the column contain undesired non-polar lipids, mostly triglycerides, and carotenoids. α-Tocopherol eluted next followed by γ-tocopherol and lastly δ-tocopherol. There is a very slight R_f difference between the tocopherols, thus, multiple columns were required for full separation. The best separation was achieved using a 99:1 hexane to ethyl acetate mixture. A slow stepwise increase in ethyl acetate concentration increased the rate of elution, however, this came at the expense of decreased resolution. The crude oil contains approximately 40 % by weight γ-tocopherol and ~15 % δ-tocopherol. The yield of α-tocopherol was not evaluated because it was left as impure fractions with non-polar lipids and/or carotenoids. α-Tocopherol was obtained by a much simpler method consisting of the hydrolysis of commercially available α-tocopherol acetate using potassium hydroxide in methanol.[77]

A palm kernel oil suspension rich in tocotrienols obtained from Carotech Sdn Bhd. called TOCOMIN® was used to isolate pure samples of α-, γ- and δ-tocotrienol. The order of elution of the components of this oil suspension was as follows: non-polar lipids and/or carotenoids, α-tocopherol, α-tocotrienol, γ-tocopherol, γ-tocotrienol, δ-tocopherol, δ-tocotrienol followed by some other unidentified oils. The degree of separation between these compounds is extremely minute, therefore, multiple turns of column chromatography are required using a 99:1 hexane to

ethyl acetate ratio, and should not exceed 9:1 hexane to ethyl acetate. The use of pressure to increase elution rate should be avoided as this results in greatly decreased resolution and almost no separation of the chief components. The sample oil should be dissolved in as little hexane as possible (~1-2 mL for 0.5 g of oil), the height of the sample upon loading should be minimized and the height of the silica in the column should be maximized for optimal separation. Typically, to achieve a good separation, 100 g of silica was used for 0.5 g of oil suspension in a column with an internal diameter of 24 mm and 40 cm in length. Approximately 2 g of each α-, γ-, δ-tocotrienol were obtained from a 25 g oil suspension. The mass yield percentage was not obtained due to incomplete separation in various fractions, which were stored for future purification.

2.2 Synthesis of Vitamin E Quinones

The general oxidative strategy employed for the synthesis of tocol quinones *in vitro* is shown in **Scheme 2**. The use of transition metals complexes of high oxidation potential presents a potentially useful tool for the oxidation of parent tocols to their respective quinones. The successful oxidation of α- and γ-tocopherol to their respective quinones by $FeCl_3$ has been reported.[63–65] The synthesis of δ-tocopherol has been reported using $AgNO_3$ as an oxidizing agent to prevent overoxidation.[63] In 2014, we had successfully synthesized α-tocopherol quinone using $FeCl_3$ in a ~50% yield (unpublished result). This same method was attempted using γ-tocopherol but this failed to produce γ-tocopherol quinone, however this was not extensively investigated. We sought more efficient means of preparation of the quinones. It has been reported that various oxygenated aromatics like phenols, hydroquinones, methoxyphenols, and dimethoxybenzenes could be oxidized to the corresponding quinone using a silica-supported oxidation with ceric ammonium nitrate (CAN, $(NH_4)_2Ce(NO_3)_6$) in good yields.[78] Typically, the

reagent is used in aqueous acetonitrile, but the silica-supported method increases reaction rates and yields, eliminates the wastewater contaminated with cerium, and a simple filtration removes excess reagents and by-products.[78] A variety of 4-methoxyphenols derivatives were reported to be converted to the corresponding quinone in yields of 87% or higher.[78] Cerium (IV) lanthanide complexes are efficient oxidants owing to a high redox potential of ~1.61 V.[79] Cerium (IV) is generally prepared as ceric ammonium nitrate salt because it is relatively non-toxic, easy to handle and stable.[79] Upon oxidation of electron-rich aromatics, cerium (IV) is reduced to cerium (III) in a one electron transfer, therefore, two equivalents of CAN are required for the complete two electron oxidation of tocopherols to the quinones.

4-Methoxyphenols represent a good model system for tocols. A second attempt at the oxidation of γ-tocopherol was performed using the solid-supported ceric ammonium nitrate method. The reaction was monitored by TLC and showed that after 15 minutes starting material had disappeared and two products had been produced. The reaction was performed multiple times. The products were separated by silica column chromatography. The first product to elute off the column was identified as *ortho*-γ-tocopherol quinone also known as tocored.[49] This product was isolated in a ~25% yield and the common name (tocored) given to this compound reflects its bright red oily appearance. The second product to elute off the column was a bright yellow oil identified as *para*-γ-tocopherol quinone. The product was isolated in a ~50% yield. The last 25% was left at the top of the column but was not isolated. This silica-supported CAN oxidation of parent tocols presents a simple synthesis of tocol quinones. Accordingly, the same procedure was repeated for the other tocol isoforms and similar results were obtained. The α-tocopherol and α-tocotrienol isoforms yielded only one product identified as the corresponding *para*-α-tocopheryl and *para*-α-tocotrienyl quinones in ~80% yield. It should be noted that no

degradation had been observed in the *para*-tocol quinones stored as an oil in the fridge at 4°C after ~20 months. However, the *ortho*-tocopheryl quinones seem far less stable and may form dimers or degradation products upon storage in the same conditions. This effect is more apparent in the *ortho*-δ-tocopheryl quinones.

Methods aimed towards the selective synthesis of the *ortho*- or *para*-quinone were not explored in this investigation. In this procedure, tocols dissolved in DCM were added to a slurry of CAN loaded silica stirring in DCM at room temperature. This procedure offers several parameters that can be altered and may produce different ratios of *ortho*- to *para*-quinones. Firstly, the order of addition can be changed. By adding the tocols to the slurry of CAN, there is a great excess of CAN initially, which impacts the ratio of *ortho*- to *para*-quinones. Adding the slurry of CAN loaded silica slowly to a solution of tocopherol would avoid the large excess of CAN initially in the original procedure. Secondly, the effects of solvent polarity on the ratio of *ortho*- to *para*-quinones can be explored. Thirdly, the ratio of CAN to silica can be changed which would have similar implications to the order of addition described above. In addition to providing a solid support for CAN, silica is also slightly acidic, so the amount of silica may also have an impact on the reaction yields. Lastly, the effect of temperature on the product ratio can also be explored. Failing these attempts, Saladino *et al.* have reported the efficient synthesis of quinones from parent tocopherols using a methyltrioxorhenium hydrogen peroxide (MTO/H_2O_2) catalytic system. Additionally, they have reported the ability to obtain different ratios of *ortho*- to *para*-quinones based on different polymer supported MTO/H_2O_2 catalysts.[80] The use of this catalyst was not explored in this investigation.

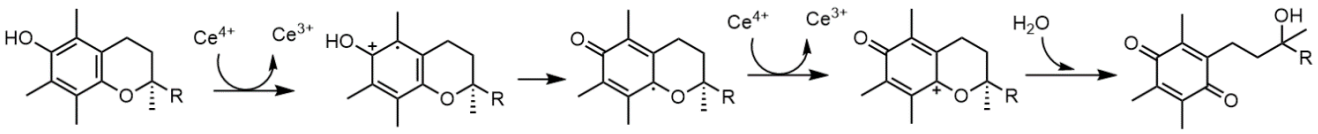

Scheme 2: General scheme for the synthesis of tocol quinones from their parent quinones

2.3 The Synthesis of Quinone Thiol Adducts

The main goal of this project was to measure the rate of reactivity of the tocol quinones with a model thiol such as *N*-acetyl cysteine (NAC) using UV/Vis absorption spectroscopy. The initial attempts to monitor the reaction of γ-tocopherol quinone with NAC seen in **Scheme 3** were performed in ethanol. There were no changes in absorption spectra observed after 8 hours upon the addition of a solution of NAC dissolved in ethanol to a solution of γ-tocopheryl quinone dissolved in ethanol. The lack of changes observed in the absorption spectra could indicate one of two things: either there was no reaction occurring, or the product has the same absorption spectrum as the starting material.

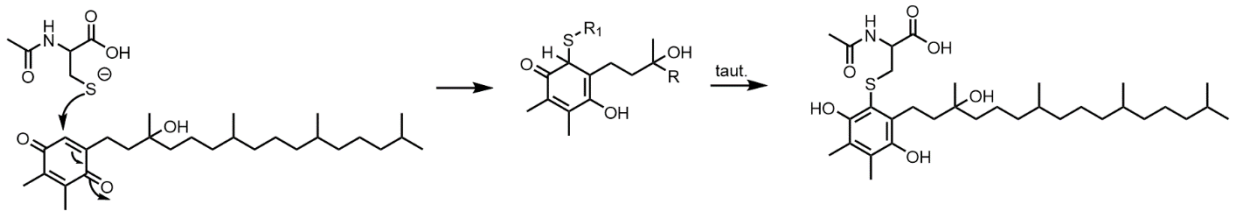

Scheme 3: The proposed mechanism of thiol addition to quinone derivatives.

At first, we proposed that the UV/Vis spectrum of α-tocopheryl hydroquinone may be a good model of the γ-tocopheryl hydroquinone NAC conjugate. The synthesis of α-tocopherol hydroquinone was attempted using excess $NaBH_4$ in a solution of methanol. Interestingly, the

yellow solution became clear but reverted to the yellow color within two minutes. It was hypothesized that $NaBH_4$ efficiently reduced the quinone to the hydroquinone which was then readily oxidized back to the quinone by atmospheric oxygen. To confirm this hypothesis, the reduction of α-tocopheryl quinone with $NaBH_4$ was monitored by UV/Vis absorption. The absorption spectra seen in **Figure 12** show the changes in absorption spectra upon the reduction of α-tocopheryl quinone with $NaBH_4$. After three hours, the UV/Vis absorption spectrum reverted to that of the original α-tocopheryl quinone, suggesting a re-oxidation by oxygen had occurred. As such, the α-tocopheryl hydroquinone product could not be isolated.

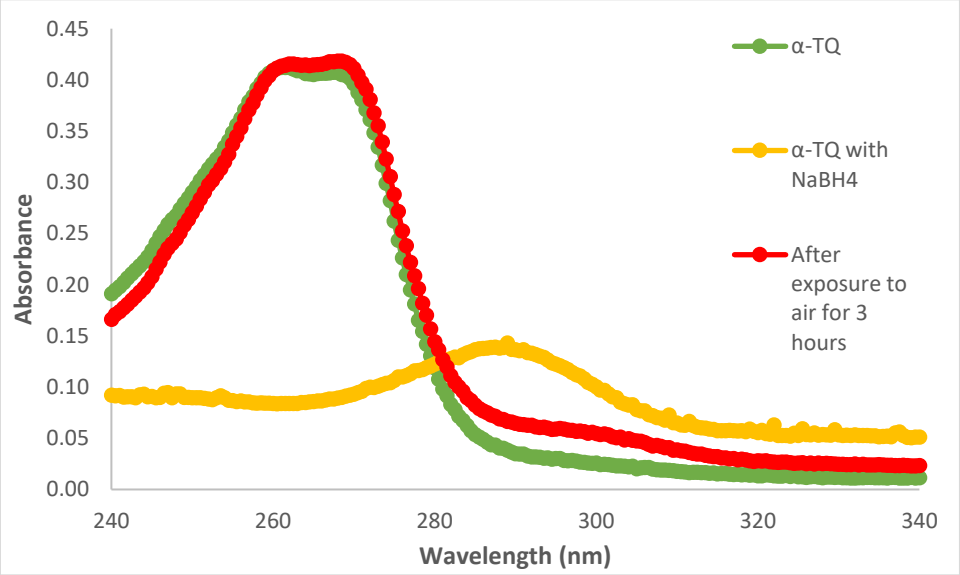

Figure 12: The UV/Vis absorption spectral changes of α-tocopherol quinone with the addition of $NaBH_4$.

It became apparent that a synthetic standard of the γ-tocopheryl hydroquinone NAC adduct was required to identify the UV/Vis absorption spectrum properties. The reaction of γ-tocopheryl quinone with NAC was attempted in ethanol in a round bottom flask while monitoring by TLC using a 4:1 hexane to ethyl acetate ratio. After stirring for twelve hours at room temperature, most of the starting material appeared to remain unreacted, although a spot on

the baseline was visible. It was assumed that no reaction had occurred and the spot on the baseline was an oxidized degradation product. This was a surprising result given the successful synthesis of γ- and δ-tocopheryl hydroquinone glutathione adducts previously reported.[63,64] To validate the unsuccessful synthesis of the γ-tocopheryl hydroquinone NAC adduct observed in our laboratory, the reaction was attempted using the same conditions we previously tried but with a theoretically more reactive quinone: *p*-benzoquinone. The benzoquinone is expected to be more reactive owing to its lack of electron donating groups and lack of steric hindrance. The full conversion of benzoquinone starting material to the NAC-adduct was observed by TLC to be complete after twelve hours, and only one spot was observed on the baseline using a 4:1 hexane to ethyl acetate ratio. A solvent ratio of 9:1:0.1 (ACN:MeOH:HOAc) was required to resolve the spot on the TLC sheet, which showed only one spot with a R_f of about 0.1. The product was isolated by column chromatography using the same 9:1:0.1 (ACN:MeOH:HOAc) solvent ratio and was identified as a *p*-benzohydroquinone mono-NAC adduct by ^{1}H NMR and electron ionization mass spectrometry (MS/EI) (**Figure 13)**.

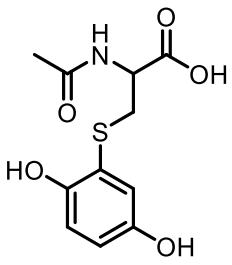

Figure 13: The structure of the *p*-benzohydroquinone mono-NAC adduct.

While the reaction yielded the desired quinone-thiol conjugate, the reaction rate was too sluggish (~24 hours) to monitor rates of reaction within an ideal timeline (minutes). To improve the rate of reaction, the reaction was performed under more basic conditions to promote the formation of the more nucleophilic thiolate. The pK_a of the side chain thiol of L-cysteine is

around 8.7,[81] therefore NAC was dissolved in a Tris/HCl buffer at pH 8.5 to increase the percent ionization (~50%). This was added to a solution of benzoquinone dissolved in methanol. A change in color from yellow to orange happened almost immediately and the starting material was consumed in less than five minutes as demonstrated by TLC. The product from this reaction was identified as the same adduct obtained previously in methanol and in similar yields (~75%), however the rate of reaction was drastically improved. Next, the successful synthesis of a 2,3,5-trimethylhydroquinone NAC adduct was achieved using these solvent conditions. Consequently, the methanol and Tris/HCl buffer solvent system appeared to be a good option for the synthesis of the γ-tocopheryl hydroquinone NAC adduct.

Accordingly, the reaction of γ-tocopherol quinone with NAC was re-evaluated using the methanol and Tris/HCl buffer (pH 8.5) solvent system. A change in color of the solution from yellow to orange occurred after 15 minutes. The complete conversion of the γ-tocopherol quinone was demonstrated by TLC (hex/EtOAC 4:1) and only one spot on the baseline was visible. This spot was isolated as one product using the 9:1:0.1 (ACN:MeOH:HOAc) solvent system. The product was hypothesized to be the desired γ-tocopheryl hydroquinone NAC adduct obtained in a 75% yield after isolation. The adduct was characterized by ^{1}H NMR, ^{13}C NMR, IR, UV/Vis absorption spectroscopy and electrospray ionization mass spectrometry (ESI-MS). The ^{1}H NMR and ESI-MS spectra were consistent with the predicted spectra for γ-tocopherol hydroquinone NAC adduct. However, the peaks at 184.12 ppm and 182.97 ppm in the ^{13}C NMR, and the lack of $\nu(OH)_{(s)}$ between ~3600-3100 cm^{-1} in the IR spectrum, were indicative of a quinone species. Furthermore, the UV/Vis absorption spectrum of this compound showed two peaks (λ_{max} = 267 nm, ε = ~2,200 M^{-1}•cm^{-1}, λ_{max} = 307 nm, ε = ~1,700 M^{-1}•cm^{-1}), which resembles the spectrum of a quinone. Khalife and Lupidi have previously monitored the reaction

of thymoquinone with glutathione (GSH) by UV/Vis spectroscopy. The absorbance for the original thymoquinone showed an absorbance maxima at 257 nm and an absorbance maxima at 303 nm for the thymohydroquinone GSH adduct.[82] Therefore, we hypothesized that the γ-tocopheryl hydroquinone NAC adduct was actually oxidized to a γ-tocopheryl quinone NAC adduct in the presence of oxygen. To test this hypothesis, $NaBH_4$ was added to a solution of the γ-tocopheryl quinone NAC adduct dissolved in ethanol. Similarly to the synthesis of α-tocopherol hydroquinone, the yellowish-orange solution turned clear then reverted to the yellowish-orange solution in the presence of air. The change in color was monitored by UV/Vis spectroscopy. The absorption spectrum of the starting material showed two peaks (λ_{max} = 267 nm, ε = ~2,200 M^{-1}•cm^{-1}, λ_{max} = 307 nm, ε = ~1,700 M^{-1}•cm^{-1}). Upon the addition of $NaBH_4$ the peak at 267 disappeared and the peak at 307 was increased (307 nm, ε = ~2,400 M^{-1}•cm^{-1}). After exposure to air for three hours the spectrum reverted to that of the original spectrum as seen in **Figure 14**. Consequently, the reactions of tocol quinones with NAC should be monitored in the absence of air. To overcome this obstacle, we secured the UV/Vis spectrophotometer in a two-hand zipper lock Aldrich® Atmosbag with a nitrogen inlet and vacuum outlet that allowed for the exclusion of oxygen. The apparatus is depicted in **Figure 15**.

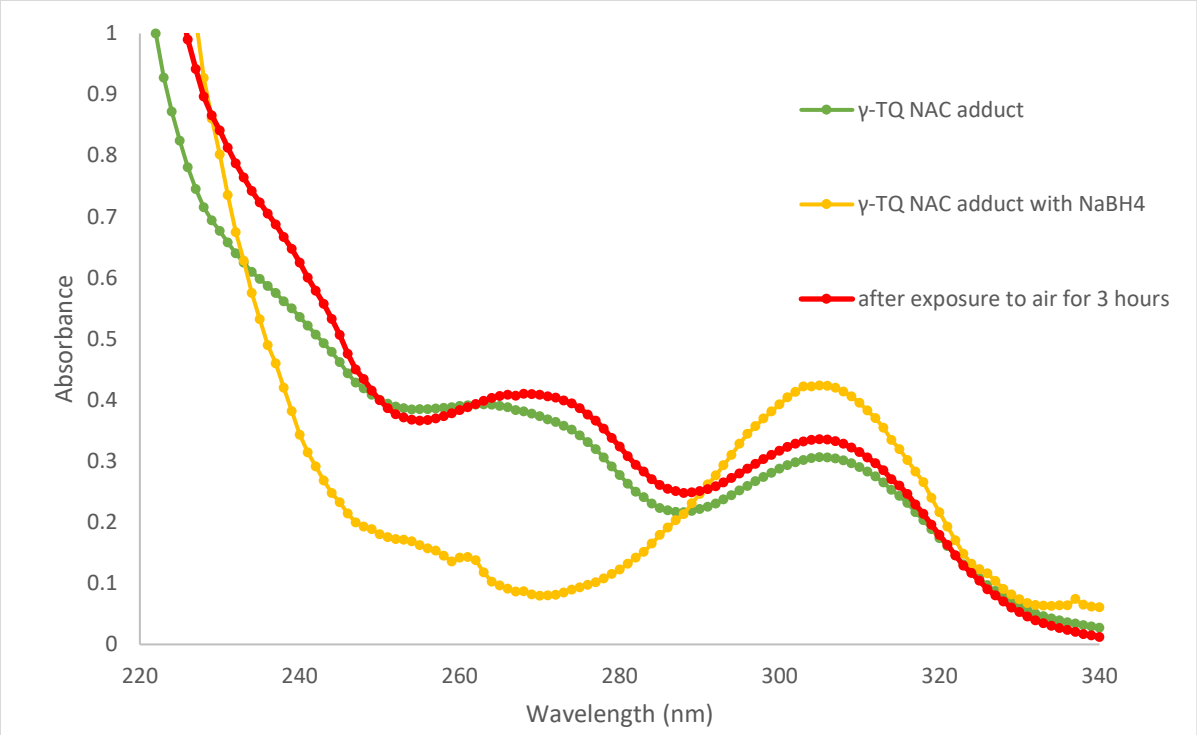

Figure 14: The UV/Vis absorption spectral changes of γ-tocopherol quinone NAC adduct (0.17 mM in MeOH) with $NaBH_4$.

Figure 15: The apparatus used to exclude atmospheric oxygen to monitor the of the rates of reaction of the tocopheryl quinones with NAC by UV/Vis spectroscopy. The UV/Vis spectrophotometer is inside the bag with the necessary reagents for the reaction and the bag was filled with N_2 gas.

2.4 Tocol quinone reactivity with *N*-Acetyl Cysteine

2.3.1 Stoichiometry of the reaction

The rate of reaction of tocol quinones with NAC was monitored by following the increase in absorption at 308 nm from the formation of the tocol hydroquinone-NAC adduct. It has previously been reported that the reaction of a naphthoquinone derivatives in the absence of oxygen proceeds through a reaction mechanism with the overall stoichiometry of two quinones for each thiol.[83] This was demonstrated by titrating the quinone with increasing equivalents of thiols which showed a maximum absorbance after the addition of 0.5 equivalents of thiol. The authors reported that the rate limiting step is the addition of the thiolate anion to the quinone. The resulting hydroquinone adduct is oxidized to a naphthoquinone adduct via a fast two electron comproportionation reaction reducing another equivalent of starting naphthoquinone to the naphthohydroquinone. The naphthohydroquinone is no longer reactive towards thiols, therefore two equivalents of naphthoquinone are consumed for each thiol.[83]

Therefore, we investigated the stoichiometry of reaction of γ-tocopheryl quinone with NAC using a similar method reported above. The absorbance at 308 nm was recorded following the sequential addition of twenty aliquots consisting of 0.1 mol equivalents of NAC. It can be seen in **Figure 16** that the maximum absorbance occurred at around one equivalent of NAC. There is a slight increase in absorbance observed after one equivalent of thiol. This is a product of residual quinone in solution which is slowly reacting when additional thiol is added. This limitation may be avoided by allowing longer times between additions of thiols. Nonetheless, this would indicate a one-to-one ratio of thiol to γ-tocopherol quinone in the formation of the γ-tocopheryl hydroquinone adduct. This suggested that the comproportionation reaction previously reported with naphthoquinone GSH adducts does not occur in our system. The rate of

comproportionation is directly influenced by the electron density in the aromatic moiety of the hydroquinone, that is, the rate of comproportionation is increased as electron density decreases.[84] The increased electron density of tocopheryl quinones compared to naphthoquinones may explain the failure to observe comproportionation in our system. In a previous study, the effect of electron density on a quinone/hydroquinone system on the rates of comproportionation was explored.[85] The rates of comproportionation drastically decreased as electron withdrawing groups were added and drastically increased as electron donating groups were added.[85]

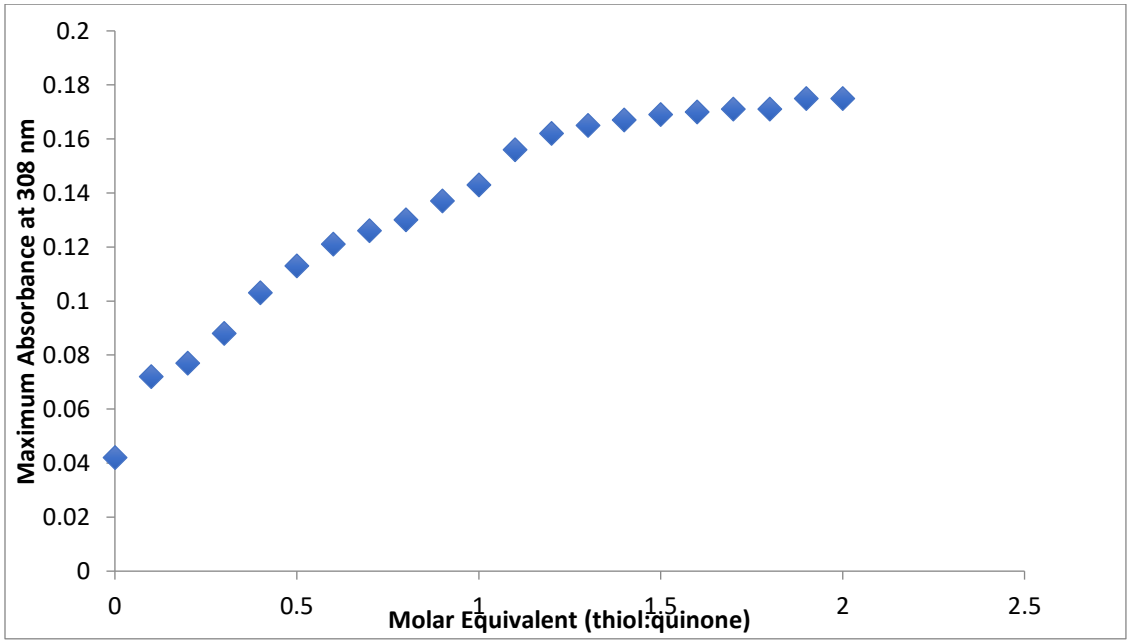

Figure 16: The titration of γ-tocopheryl quinone with NAC in a solvent system of 67% methanol/33% Tris buffer (pH8.5) by following the maximum absorbance at 308 after the addition of each aliquot. Concentrations after mixing were 74 μM γ-tocopheryl quinone, with NAC in the range of (0-147 μM). The reaction was monitored with a spectrophotometer that had been placed inside a N_2-purged glove bag.

2.3.2 Effect of solvent system on the rate of reaction

The first attempts at monitoring the rate of reactivity of γ-tocopherol quinone with NAC were done in a solvent system of 67% methanol/33% Tris buffer (pH 8.5) simply because it was

an easy solvent system and ratio to work with experimentally. Methanol was an attractive solvent for the organic solvent because it most closely resembles the properties of water in terms of its polarity and hydrogen bonding capabilities out of the most commonly used organic solvents. Its lower boiling point compared to ethanol was also an attractive feature since the quinone sample solutions were first evaporated prior to placing in the glove bag. The 67% methanol to 33 % Tris buffer was also easiest to manipulate in a 3-mL cuvette, however, the effect of the solvent system on the rate of reaction was of interest. The rates of reaction were recorded by following the increase in absorbance at 308 nm over time as seen in **Figure 17**. The effect of the solvent system on the rate constants (*k*) from curves fit to a one-phase exponential using Prism software are shown in **Table 7**. It was clear that the more aqueous the solvent-system was, the greater the rate constant was for the addition of NAC to the quinone. Furthermore, the rate of reaction was much slower at 67% iso-propanol compared to 67 % methanol. This would suggest that an increase in solvent polarity corresponds with an increased reaction rate. However, a certain concentration of organic solvent is required for the reaction to occur as demonstrated by the absence of reactivity observed in the reaction with 10% methanol. The organic solvent is required for the solubility of the quinones. The rate of reaction was fastest at 50% methanol, although a much greater error was observed and the fit to the one-phase association curve was less than optimal with an R^2 value of 0.3693. Together, these data suggest that the 67% methanol/33% aqueous buffer is an ideal solvent to assess and compare the reactivity of the other tocol quinones with NAC.

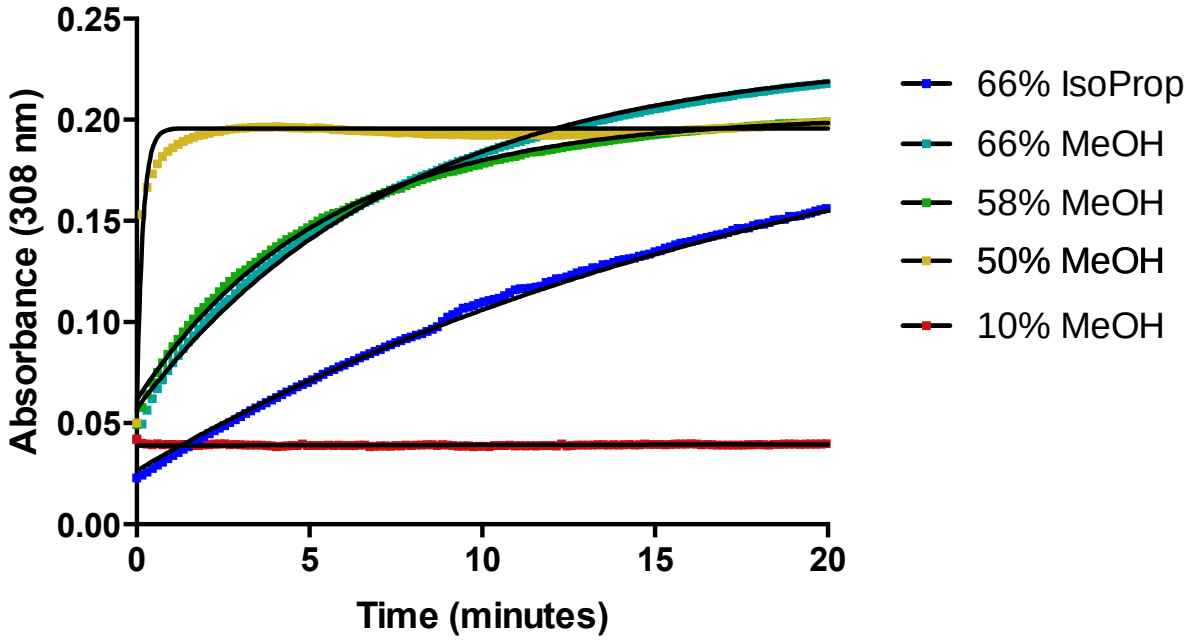

Figure 17: The effect of solvent conditions on the rate of reactivity of γ-tocopherol quinone (0.074 mM) with two equivalents of NAC using 100 mM Tris/HCl at pH 8.5 as the aqueous buffer.

Table 7: The extracted rate constant of the reaction of γ-tocopherol quinone with NAC fit to a one-phase association curve. The buffer consisted of 100 mM Tris/HCl aqueous buffer at pH 8.5. Two equivalents of NAC were used.

Solvent conditions	k	Std. Err.	R^2
67% MeOH/33% buffer	0.1301	± 0.0009	0.9981
58% MeOH/42 % buffer	0.185	± 0.002	0.9975
50% MeOH/50% buffer	3.1	± 0.4	0.3693
10% MeOH/90% buffer	-	-	-
67% Iso-Propanol/33% buffer	0.0480	± 0.0002	0.9993

2.3.3 The effect of oxygen on the reactivity

To measure the rate of reaction of the tocol quinones with NAC the reactions were performed under nitrogen atmosphere to prevent the oxidation of the hydroquinone adduct to a quinone adduct. The importance of excluding oxygen was demonstrated in a reaction with γ-tocopherol quinone and NAC in the presence of air. The absorbance was recorded at 308 nm over time which is depicted in **Figure 18**. The absorbance increased steadily in absorbance for the first few minutes indicating the formation of the γ-tocopheryl hydroquinone-NAC adduct. However, at around ten minutes, a steady decrease in absorbance is observed. The oxidation of the hydroquinone adducts to quinone adducts by oxygen is responsible for this effect. As such, the importance of excluding oxygen from the reaction conditions was established.

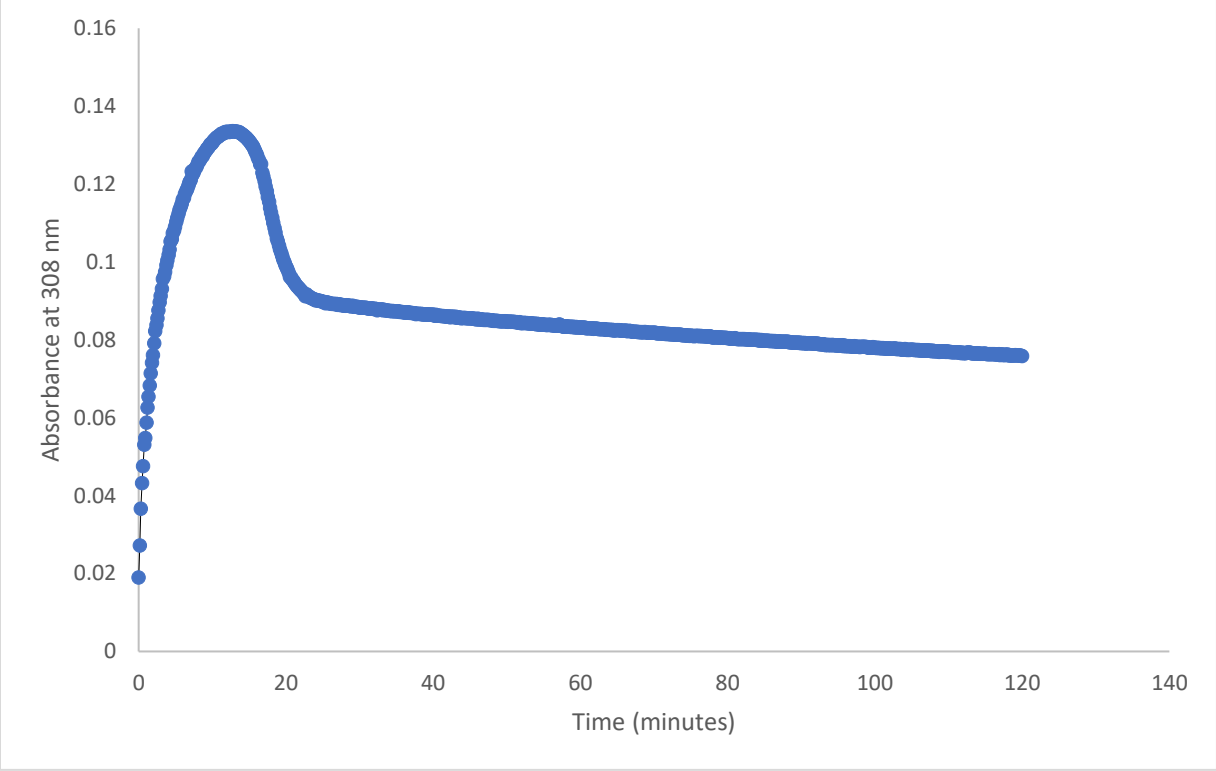

Figure 18: The reactivity of γ-tocopherol quinone (74 µM) with NAC (148 µM) at 67% MeOH/33% Tris HCl (pH 8.5) in the presence of air.

2.3.4 The rate of reactivity of tocol quinones with NAC

Figures 19 (A-L) shows the change in absorption spectra over time of the various tocol quinones after the addition of N-acetyl cysteine. The changes in the absorption spectra for γ-tocopherol quinone are almost identical to the changes observed in the spectra of the γ-tocotrienol quinone. As seen in **Figure 19 (A-F)** (γ-T and γ-T3 at pH 8.5, 7.5 and 6.5), the addition of NAC resulted in a progressive decrease in the absorbance at 260 nm and a progressive increase in the absorbance at 307 nm. The decrease in the absorbance at 260 nm is a result of the loss of tocol quinone which is being converted to the NAC-hydroquinone adduct. Consequently, the increase in the absorbance peak at 307 nm is a result of the formation of the NAC hydroquinone adduct. There are two points where the absorbance does not change over time, these are known as isosbestic points and they occurred at 241 nm and 281 nm; this suggests that the quinones were being converted to a single product. It should be noted that the initial absorption spectra at 0 minutes does not pass directly through the isosbestic points because the spectra were recorded prior to the 1 mL addition of NAC in aqueous buffer. The changes in absorption spectra of δ-tocopherol quinone are almost identical to the changes observed in δ-tocotrienol quinone after the addition of NAC. As seen in **Figure 19 (G-L)** (δ-T and δ-T3 at pH 8.5, 7.5 and 6.5), the addition of NAC resulted in a progressive decrease in the absorbance at 257 nm and a progressive increase in the absorption at 303 nm as a result of the conversion of the tocol quinone to the NAC hydroquinone adduct. There are two isosbestic points at 239 nm and 279 nm suggesting the conversion of the quinones to one single product.

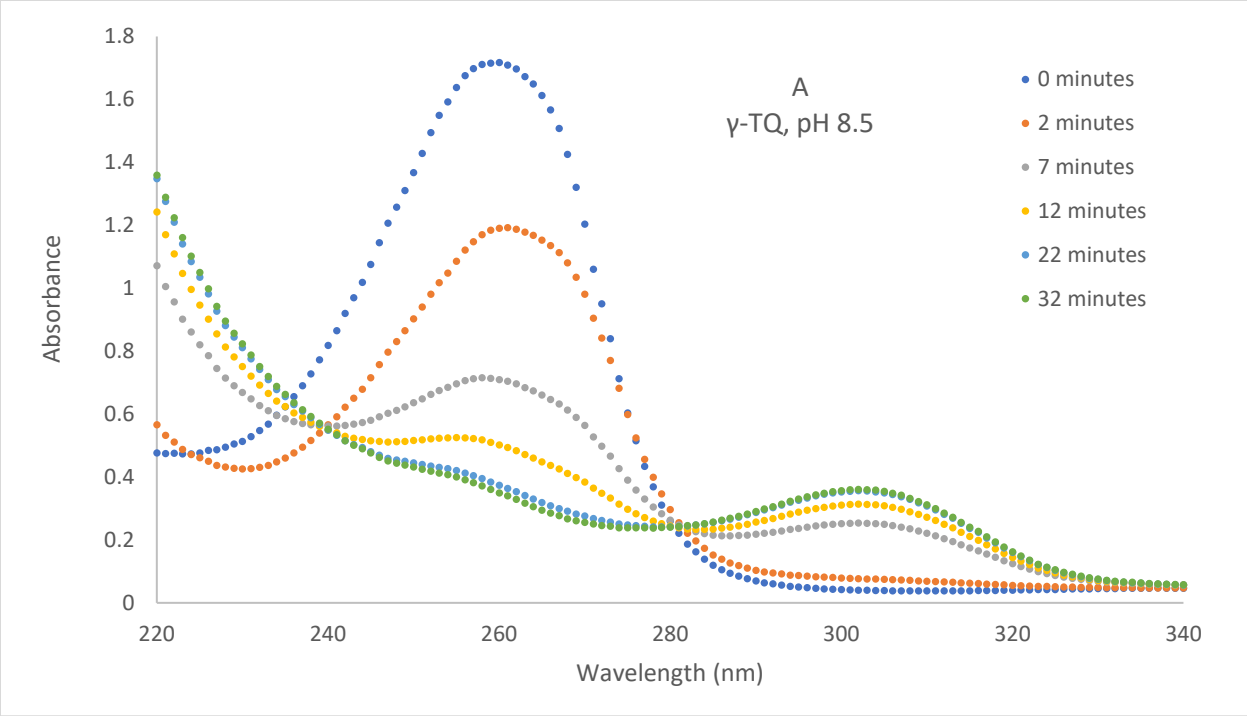
A
γ-TQ, pH 8.5
Absorbance
Wavelength (nm)
0 minutes
2 minutes
7 minutes
12 minutes
22 minutes
32 minutes

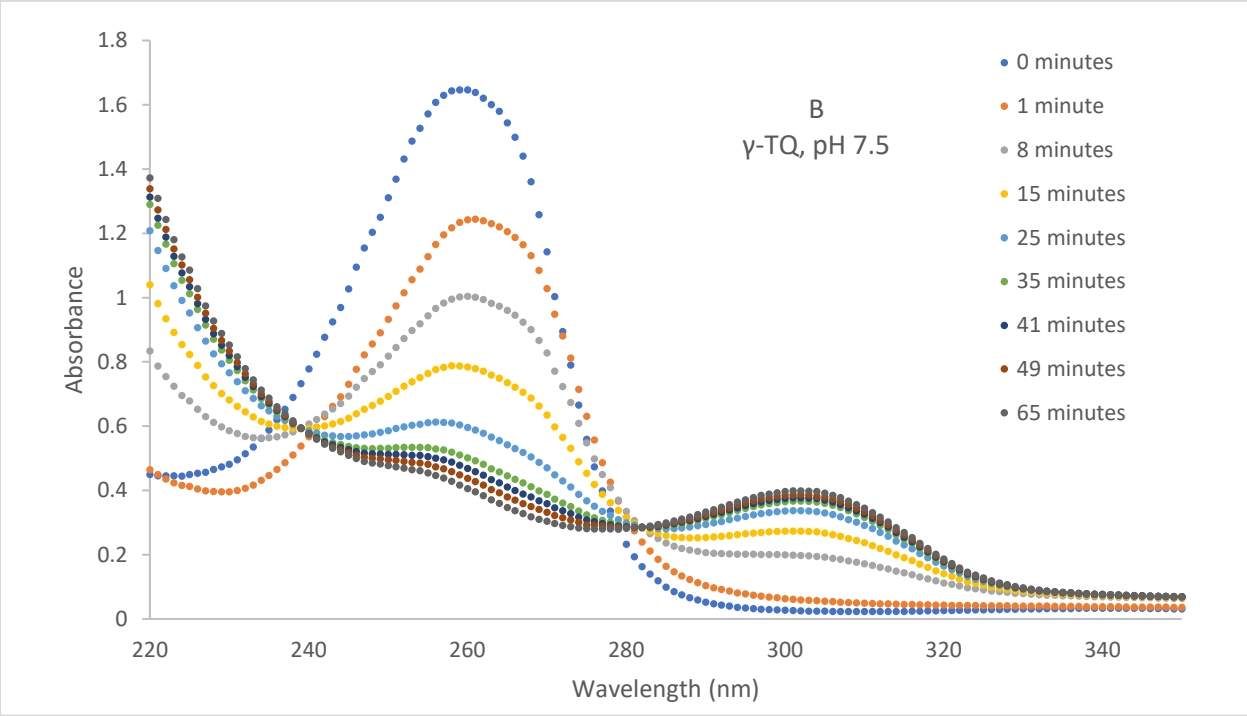
B
γ-TQ, pH 7.5
Absorbance
Wavelength (nm)
0 minutes
1 minute
8 minutes
15 minutes
25 minutes
35 minutes
41 minutes
49 minutes
65 minutes

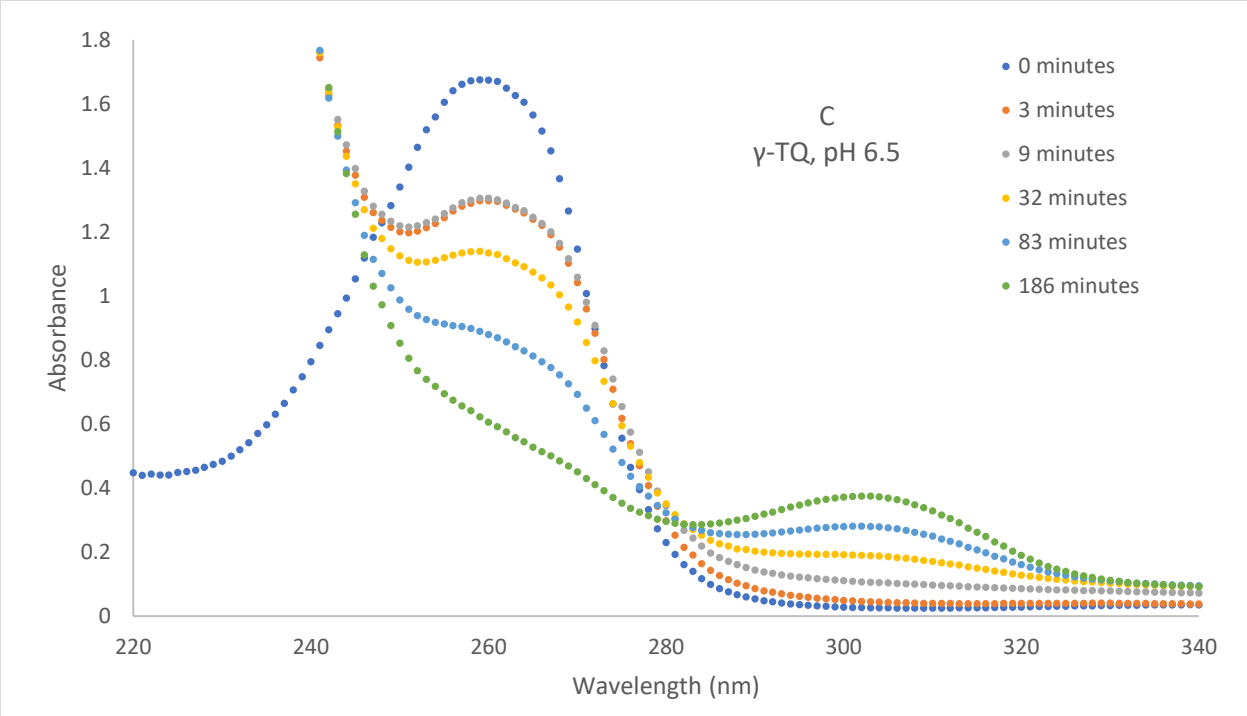
C
γ-TQ, pH 6.5
0 minutes
3 minutes
9 minutes
32 minutes
83 minutes
186 minutes
Absorbance
Wavelength (nm)
1.8
1.6
1.4
1.2
1
0.8
0.6
0.4
0.2
0
220
240
260
280
300
320
340

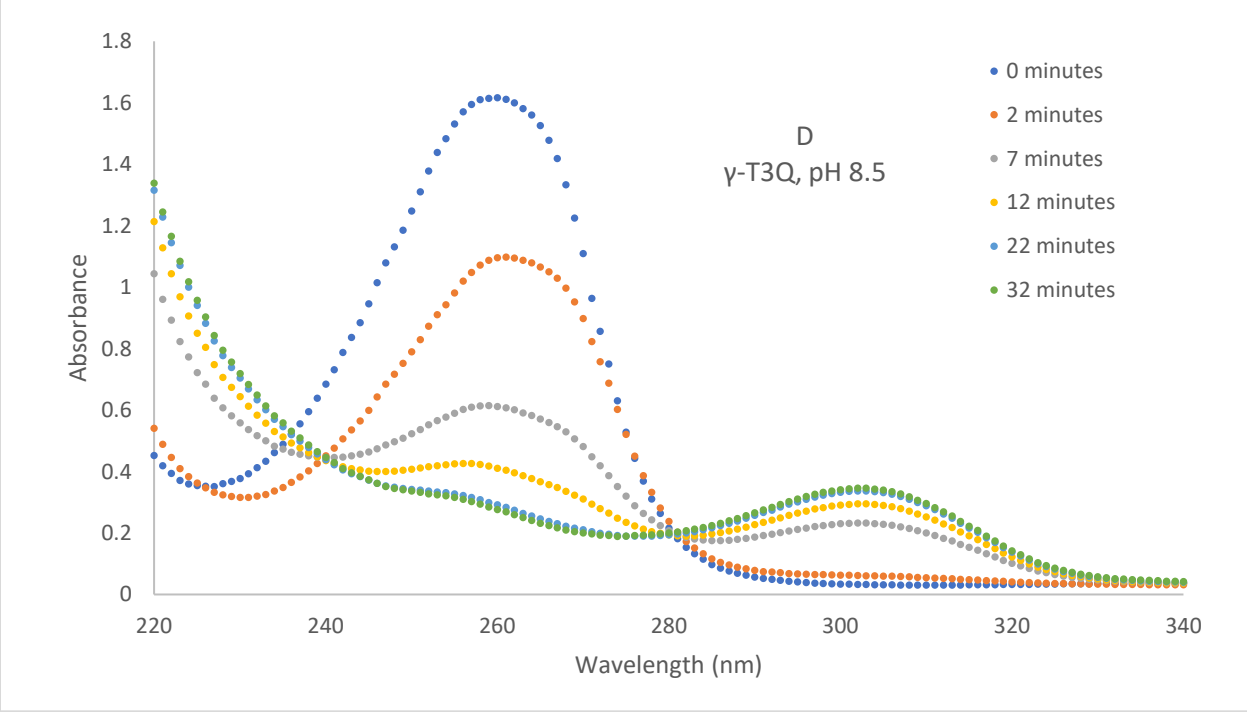
D
γ-T3Q, pH 8.5
0 minutes
2 minutes
7 minutes
12 minutes
22 minutes
32 minutes
Absorbance
Wavelength (nm)
1.8
1.6
1.4
1.2
1
0.8
0.6
0.4
0.2
0
220
240
260
280
300
320
340

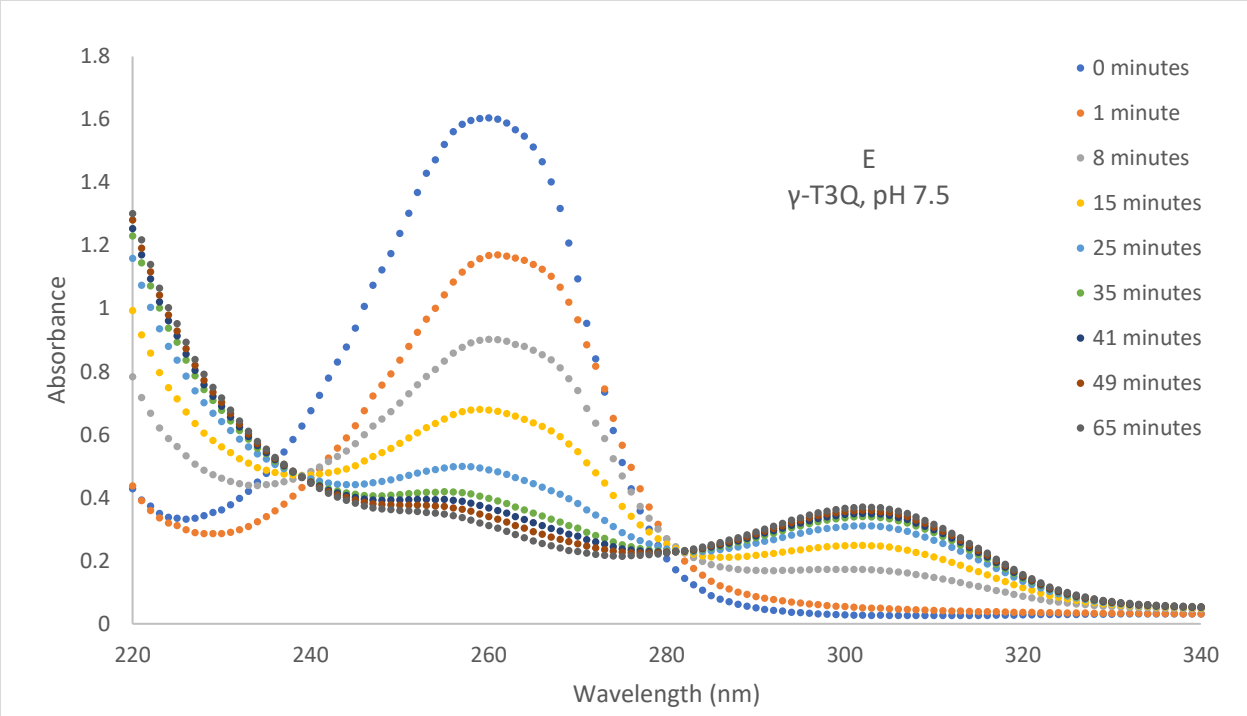
E
γ-T3Q, pH 7.5
Absorbance
Wavelength (nm)
0 minutes
1 minute
8 minutes
15 minutes
25 minutes
35 minutes
41 minutes
49 minutes
65 minutes

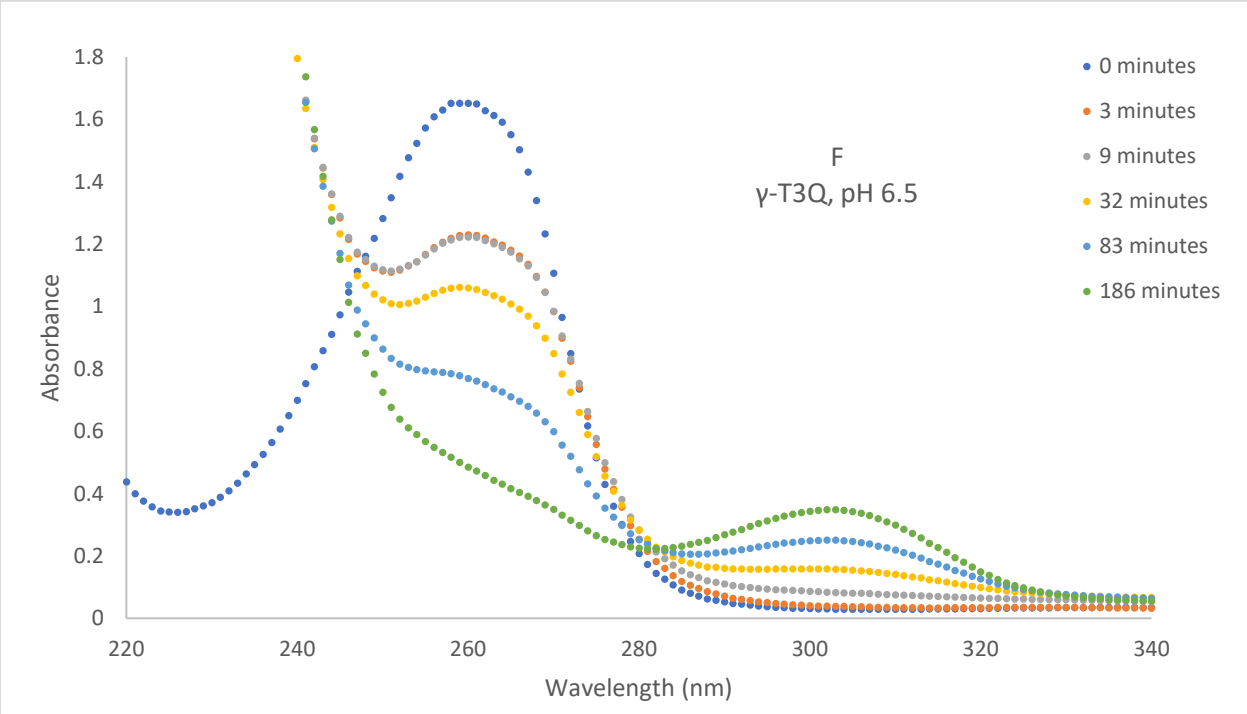
F
γ-T3Q, pH 6.5
Absorbance
Wavelength (nm)
0 minutes
3 minutes
9 minutes
32 minutes
83 minutes
186 minutes

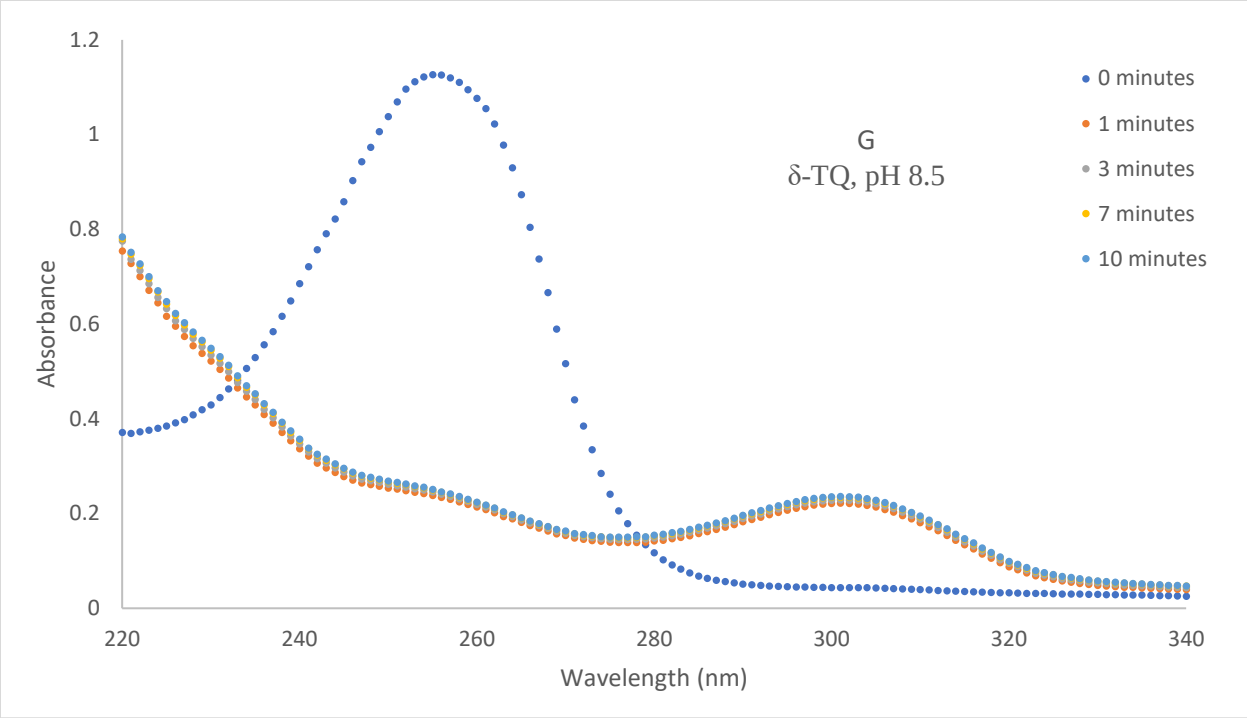
G
δ-TQ, pH 8.5
0 minutes
1 minutes
3 minutes
7 minutes
10 minutes
Absorbance
Wavelength (nm)
1.2
1
0.8
0.6
0.4
0.2
0
220
240
260
280
300
320
340

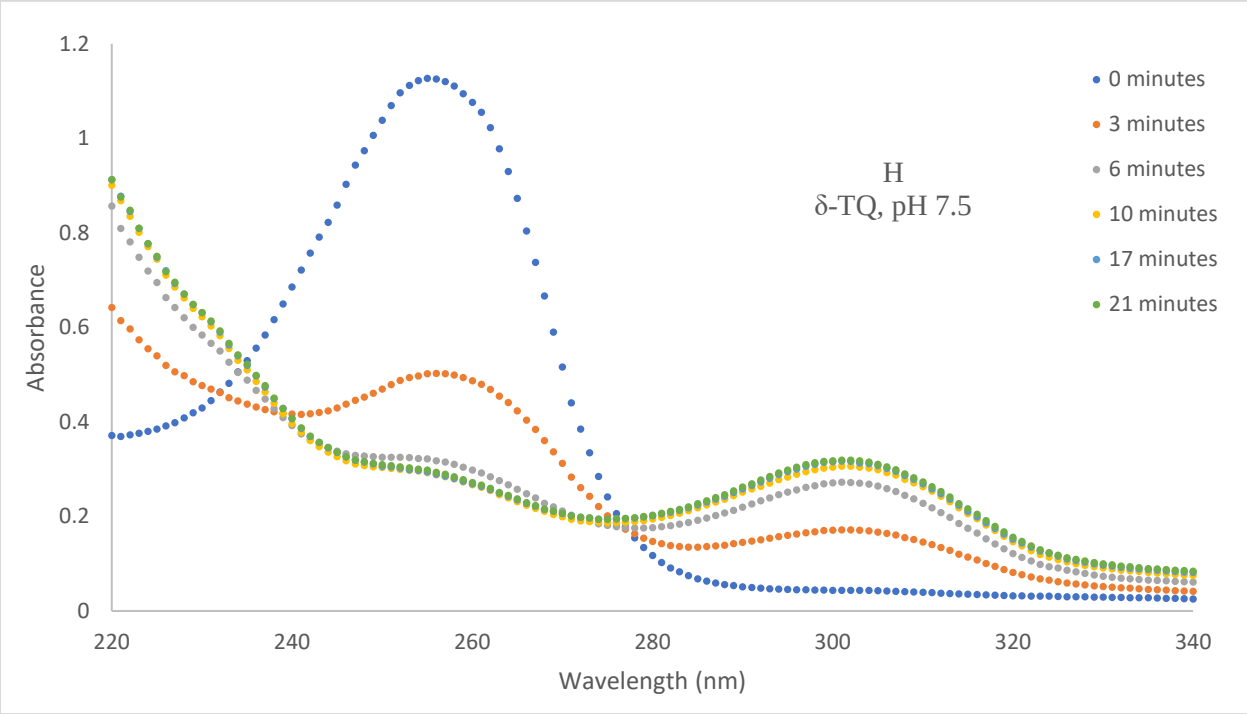
H
δ-TQ, pH 7.5
0 minutes
3 minutes
6 minutes
10 minutes
17 minutes
21 minutes
Absorbance
Wavelength (nm)
1.2
1
0.8
0.6
0.4
0.2
0
220
240
260
280
300
320
340

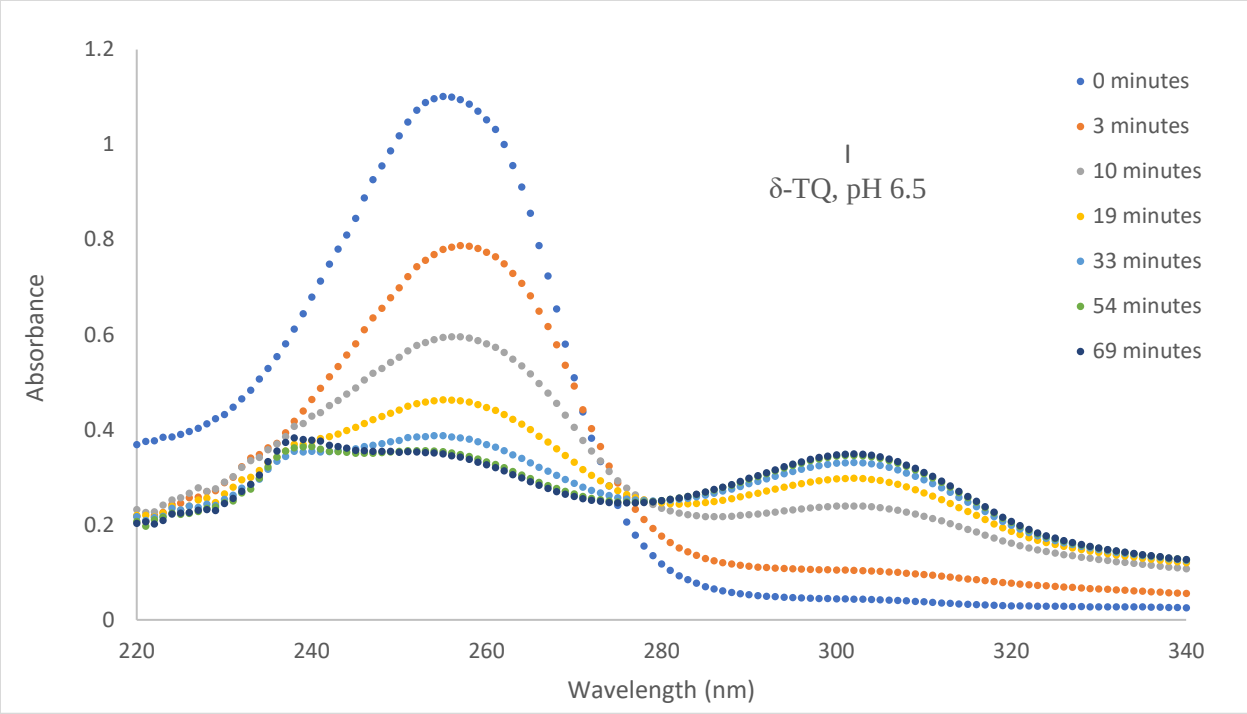
I
δ-TQ, pH 6.5
Absorbance
Wavelength (nm)
0 minutes
3 minutes
10 minutes
19 minutes
33 minutes
54 minutes
69 minutes
1.2
1
0.8
0.6
0.4
0.2
0
220
240
260
280
300
320
340

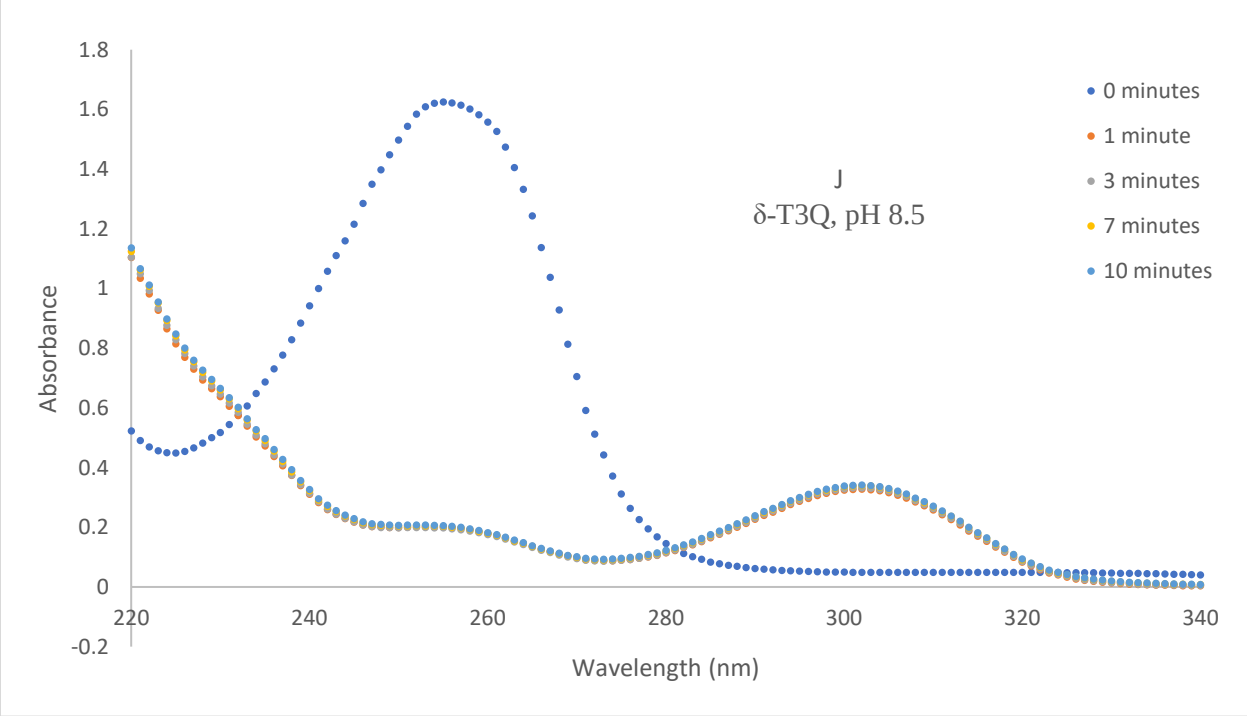
J
δ-T3Q, pH 8.5
Absorbance
Wavelength (nm)
0 minutes
1 minute
3 minutes
7 minutes
10 minutes
1.8
1.6
1.4
1.2
1
0.8
0.6
0.4
0.2
0
-0.2
220
240
260
280
300
320
340

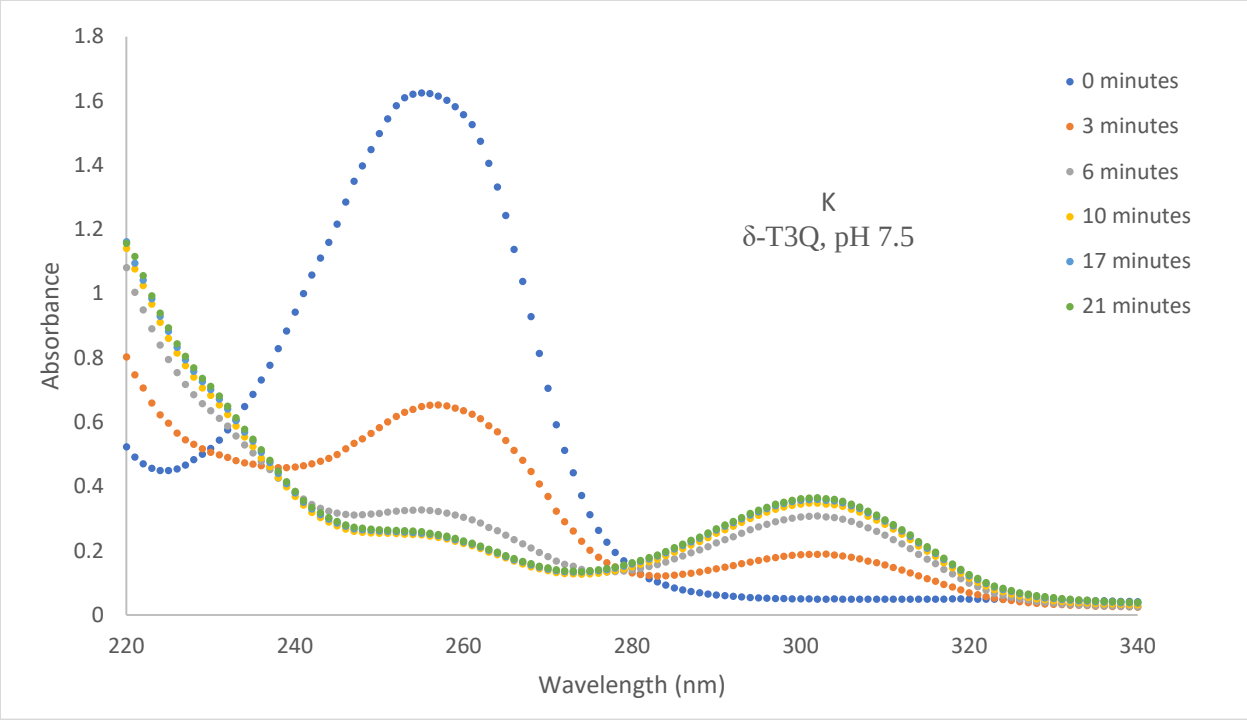

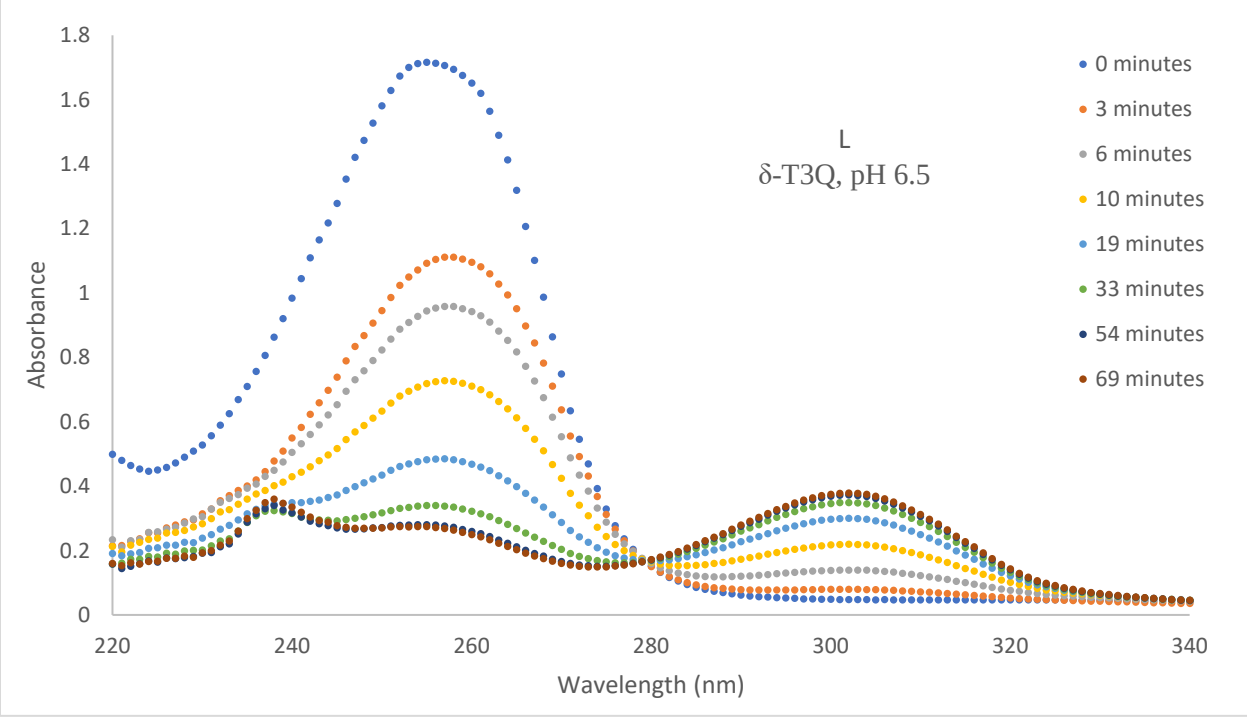

Figure 19 (A-L): The change in absorption spectra over time of the various tocol quinones (74 µM) after the addition of 4 eq. of N-acetyl cysteine in a solvent system of 67% MeOH/ 33% aqueous buffer at the pH stated.

The rates of reactivity of the various tocol quinones with NAC were recorded by following over time the formation of tocol hydroquinone NAC adduct which has a maximum absorbance at 308 nm. The reactions were performed under nitrogen atmosphere in 67% methanol/ 33% aqueous buffer. The rates of reactivity were assessed for each quinone at three different pHs: 8.5. 7.5 and 6.5. The average of three trials for each quinone was fit to a single exponential curve is shown in **Figures 20-22**. The curves were fit to both a one- and two-exponential equation. The single exponential equation was $Y=Y_0 + (Y_{max}-Y_0)\ (1-e^{(-kx)})$ and $Y = Y_{max1}(1 - e^{-k_1 x}) + Y_{max2}(1 - e^{-k_2 x})$ for the double exponential from the software GraphPad Prism where Y is the absorbance values, "plateau" is the same as Ymax, and x is time in minutes. The fit for both curves were excellent but we have no chemical reason to justify a double exponential which would be required if there were two simultaneous rates, one fast and one slow. The extracted rate constants (*k*) from single exponential fits of the data can be seen in **Table 8**. As expected, the rate constants increased as the pH increased for all the non α-tocol quinones which is also depicted in **Figure 23**. This is a result of the enhanced nucleophilicity of a thiolate anion compared to the neutral thiol. In addition, a significant difference in the rate of reactivity was observed; the rate of reactivity decreases from δ > γ>>>α (α = 0). The rate of reactivity was significantly faster for the δ-tocol quinones than for the γ-tocol quinones whereas the α-tocol quinones did not react. This agrees with our original hypothesis that the rate of reactivity of the quinones with NAC is a function of the substitution pattern on the chromanol ring. However, in contrast to our original hypothesis, there does not appear to be a significant difference between the reactivity of tocopheryl quinones and tocotrienyl quinones with the same substitution pattern on the chromanol ring. Therefore, it may be possible that the differences observed in biological assays between the tocopherols, such as the ones seen earlier in **Figure 9**

and **Figure 10**, are a function of the rate of reactivity of the respective quinones with thiols. This data may also present an evolutionary reason for the preferential retention of α-tocopherol but a significant difference between the tocotrienols is still not established. To investigate further into this matter, we sought to investigate the redox properties of the tocols and their respective quinones using cyclic voltammetry (CV).

Table 8: The extracted rate constants of the reactions of tocol quinones with NAC fit to a one-phase association curve at three different pHs. The trials were done in triplicates. Four equivalents of NAC were used.

	pH 8.5 (100 mM Tris/HCl)			pH 7.5 (100 mM Tris/HCl)			pH 6.5 (100 mM bis-Tris/HCl)		
Compound	k (min^{-1})	Std. Err.	R^2	k (min^{-1})	Std. Err.	R^2	k (min^{-1})	Std. Err.	R^2
α-TQ	-	-	-	-	-	-	-	-	-
α-T3Q	-	-	-	-	-	-	-	-	-
γ-TQ	0.160	0.003	0.981	$0.083^{\dagger}$	0.002	0.958	0.00684	0.00002	0.9921
γ-T3Q	0.134	0.001	0.995	$0.0861^{\dagger}$	0.0002	0.9992	0.00595	0.00002	0.9926
δ-TQ	$5.81^{\ddagger}$	0.32	0.98	$0.63^{'}$	0.01	0.99	0.0621	0.0007	0.9066
δ-T3Q	$4.84^{\ddagger}$	0.26	0.96	$0.63^{'}$	0.02	0.96	0.0775	0.0005	0.9883

Note: $^{\dagger\ddagger'}$ symbols designate rate constants that are not significantly different at the 95 % confidence interval

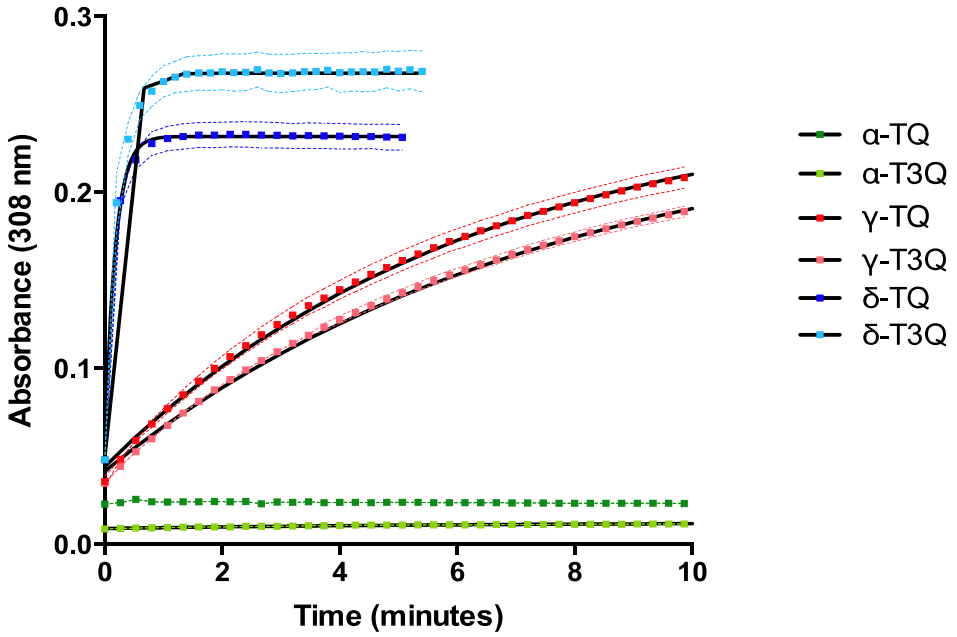

Figure 20: The rate of reactivity of tocol quinones (74 µM) with four equivalents of NAC in a solvent system of 67% MeOH/ 33% Tris/HCl buffer at pH 8.5

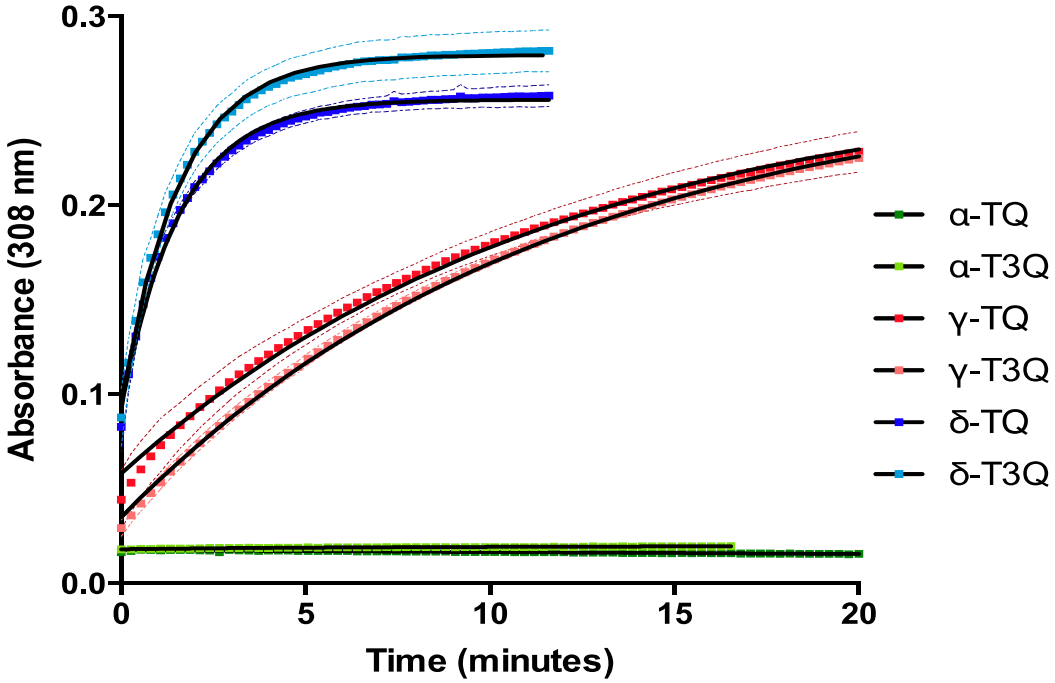

Figure 21: The rate of reactivity of tocol quinones (74 µM) with four equivalents of NAC in a solvent system of 67% MeOH/ 33% Tris/HCl buffer at pH 7.5

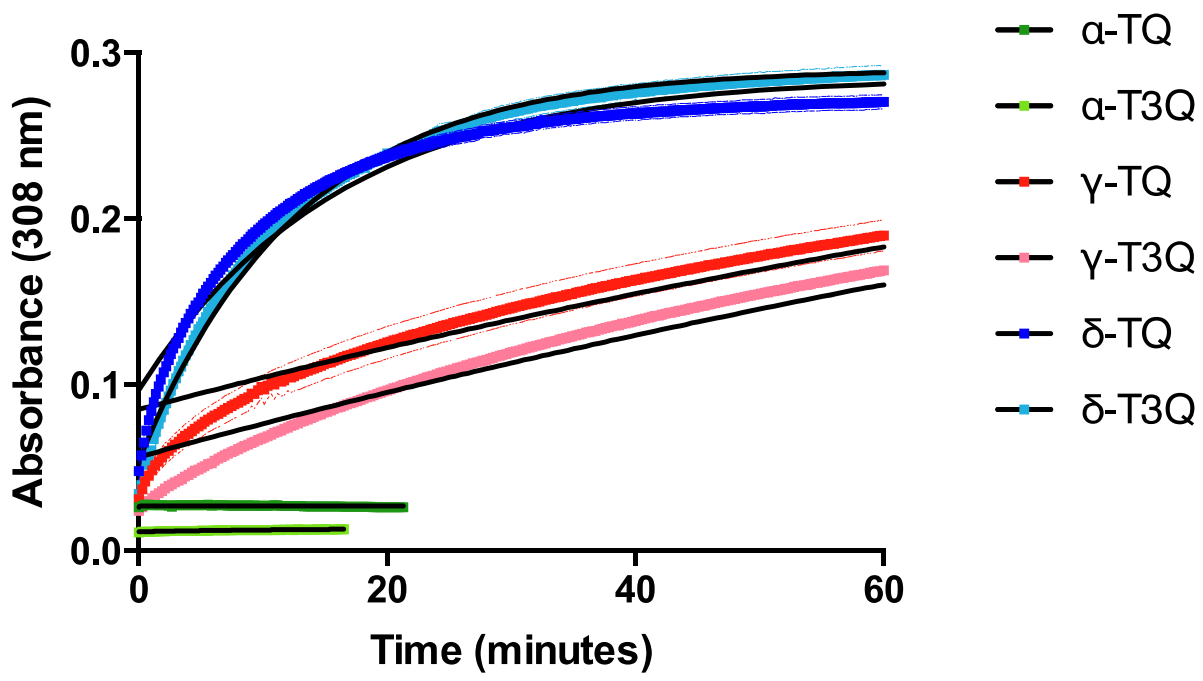

Figure 22: The rate of reactivity of tocol quinones (74 µM) with four equivalents of NAC in a solvent system of 67% MeOH/ 33% bis-Tris/HCl buffer at pH 6.5

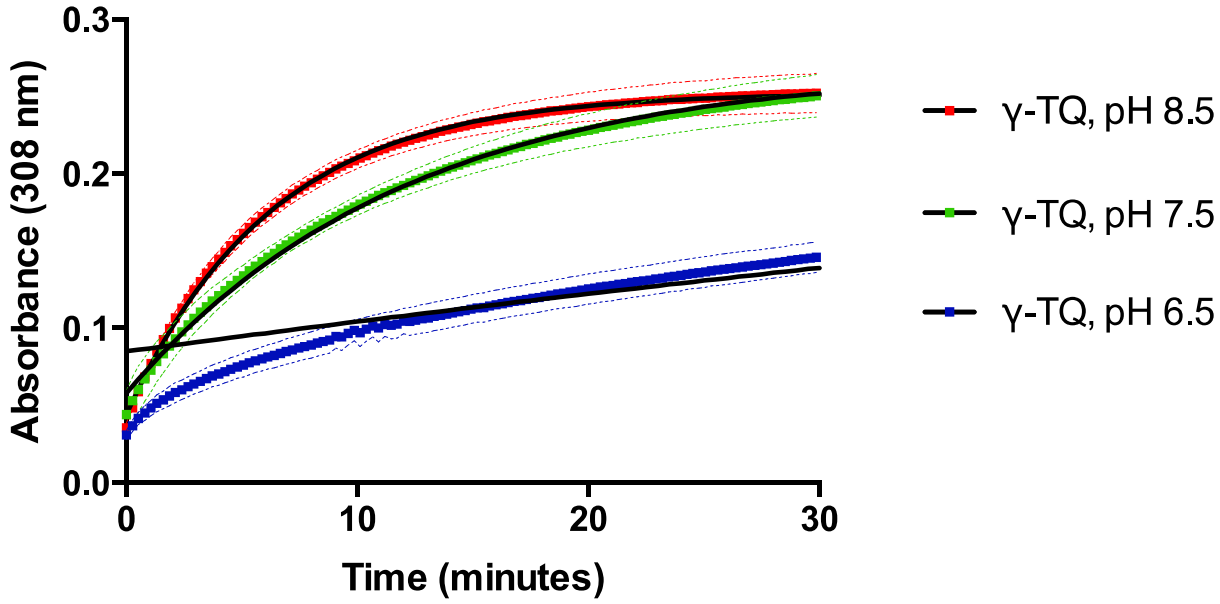

Figure 23: The effect of pH on the rate of reactivity of γ-tocopherol quinone (74µM) with four equivalents of NAC in a 67% MeOH/ 33% aqueous buffer solvent system. Similar effects are observed for all non α-tocol quinones.

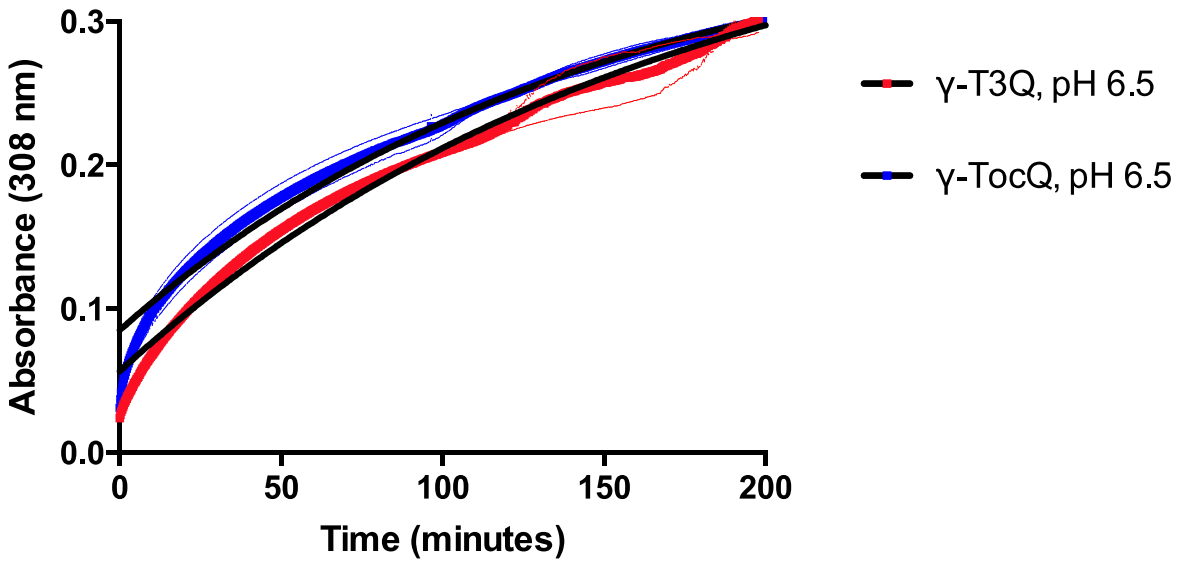

Figure 24: The the rate of reactivity of γ-tocopheryl quinone (74 μM) and γ-tocotrienyl quinone (74 μM) with four equivalents of NAC in a 67% MeOH/ 33% aqueous buffer solvent system.

2.3 Tocol and Tocol Quinone Redox Activity

In this study, we have demonstrated the rate of reactivity of the tocol quinones with a model thiol at various pHs. It was observed that the δ-tocol quinone isoforms react much quicker than the γ-tocol quinones whereas no reactivity was observed with the α-isoforms. In contrast to our hypothesis, there was no significant difference in reactivity observed between the tocopherols and tocotrienols with the same chromanol methylation pattern. We suggest that this may explain the differences observed between the tocols with different methylation patterns in biological assays, however, it does not explain the differences observed between tocopherols and tocotrienols. Furthermore, in most cell culture assays and *in vivo* assays, the cells and animals are supplemented with the tocols and not the quinones, which complicates the issue, as any oxidation of the tocols to their respective quinones may occur at substantially different rates.

As mentioned previously, Christen *et al.* studied the inhibition of peroxynitrite and SIN-1 induced PC liposome hydroperoxide formation by α- and γ-tocopherol.[49] In these experiments, it

was found that α-tocopherol was oxidized almost quantitatively to α-tocopherol quinone (90%) and γ-tocopherol formed an oxidized *ortho*-γ-tocopherol quinone product called tocored (~25%), 5-nitro- γ-tocopherol derivative (50%) and 25% remained unreacted.[49] Although these studies suggest the formation of quinones in biological assays, it is rather concerning that much of the literature on tocols in cell culture assays do not look for the formation of quinones after the assay. For instance, in the experiments mentioned earlier by McCormick and Parker, cell lines were incubated with various tocopherols for up to 48 hours.[51] The general trend observed was that δ-tocopherol was more cytotoxic than γ-tocopherol whereas α-tocopherol was not cytotoxic. However, the cytotoxic effects were not observed in two out of the six cell lines tested and the authors attributed this to a lower accumulation of the tocopherols in these two cell lines. Based on their ability to metabolize tocopherols and their reduced cellular uptake of tocopherols, the authors chose to examine the resistant hepatocyte cell line HepG2 for water-soluble tocopherol metabolites.[51] It was observed that greater than 90% of the tocopherols were recovered in the combined medium and cell extracts, thus, the difference in cellular uptake of tocopherols could not be explained by increased metabolism. Still, the authors did mention that no cytotoxic effects were observed despite forcing the cellular concentration in the "resistant" cell lines to be as high as in the other cell lines. Therefore, this suggested that another mechanism other than the cellular accumulation must be taking place, although the mechanism is unclear. It is plausible that the cytotoxicity is a function of the oxidative status in the different cell lines which may form quinones in the non-resistant cells and remain as tocopherols in the resistant cell lines. The studies mentioned earlier by Elisia and Kitts, which demonstrated the difference in the ability for different tocopherol isoforms to modulate the Nrf-2 and Nf-κB pathways, also refrained from identifying the quinones even after incubating in IFNγ/PMA induced pro-inflammatory oxidative

conditions of Caco-2 cells for 24 hours.[52] Given the highly oxidative conditions of these cells, it would not be surprising that the effects observed in these experiments are a result of the formation of the quinones. The studies mentioned earlier performed by Yu *et al.* showed the tocotrienols to be more effective at inducing apoptotic properties in two human breast cancer cell lines after incubation for 3 days. The authors did not mention any recovery of the tocols and made no attempt at identifying any quinones. Therefore, it is possible that the tocols in the cells were oxidized to the quinones and the effects observed are a property of the quinone products. There are various reports of cell culture assays supplemented with the various tocols in the literature that fail to make any attempts at identifying the quinones or even recovering the tocols after long incubation periods in the cells. Furthermore, the effects seem to be cell specific which may be a result of the concentration of quinones governed by the oxidative status of the cell.

Thus, we are suggesting that the different effects observed with the tocols is the result of the formation of the quinones and different reactivities between these quinone products, and not the antioxidant ability of the tocols themselves. Since there is no significant difference in reactivity with thiols between the tocotrienol quinones and the tocopherol quinones with the same methylation pattern, it is plausible that there are differences in other properties of tocols and their quinones. These properties may include: the ease of forming the quinones in the first place, a difference in the redox properties of the quinones, or the biological behavior of the tocols in membranes (depth, mobility or intermembrane-transfer rates).[34,43,47] It has been demonstrated that α-tocotrienol was more readily transferred between membranes than α-tocopherol and that α-tocopherol increased the rigidity of the membrane compared to α-tocotrienol.[47] Therefore, our attention was turned towards identifying differences in the first two properties across the tocol family and their quinones.

Cyclic voltammetry (CV) is a technique that has been applied by organic chemists for more than five decades for various purposes such as studying reaction pathways or electrochemically generated free radicals.[86] Briefly, CV measures the current generated in a working electrode immersed in a solution of the analyte by applying a ramping potential up to a predetermined potential where the applied potential is then reversed to the starting potential.[86,87] The current is measured using three electrodes: a working electrode, a reference electrode and an auxiliary electrode.[87] The working electrode is used to remove electrons from the analyte if a positive potential is applied resulting in an oxidation, or provide electrons to the analyte if a negative potential is applied resulting in a reduction. The electrons provided to or removed from the analyte generates a current through the working electrode. The reference electrode maintains a constant potential, therefore the current passing through the working electrode can be compared to the reference electrode. The auxiliary electrode is required to complete the circuit for the electrons. In theory, the reference electrode could also be used as an auxiliary electrode, however this would require a current to pass through it which would disturb the constant potential required the reference electrode.[87] The current generated through the working electrode is plotted against the applied potential to generate a cyclic voltammogram seen in **Figure 24**. The cyclic voltammogram in **Figure 24** demonstrates the oxidation potential of ferrocene in dry DCM at a scan rate of 100 mV per second, which is generated from applying a positive potential at the working electrode to promote the oxidation of ferrocene to the ferricenium ion. The current is reversed at the switching potential of 1200 mV where the ferricenium ion begins to be reduced back to ferrocene in a reversible process. It is common practice to report the average potential of the forward and reverse peaks as a formal reduction potential ($E^{o'}$) for the redox couple in reversible processes.[86] A peak with a positive current is called the cathodic peak (E_{pc}) whereas a

peak with negative current is termed the anodic peak (E_{pa}).[87] The formal reduction potential can be applied to determine the potential necessary to oxidize or reduce an analyte. A reversible electrochemical process is generally defined as an electron transfer reaction so fast that the oxidized and reduced species maintain an equilibrium at the electrode surface. In other words, the electrochemistry at the electrode surface is happening before any appreciable homogeneous reactions in solution can occur.[86] If the relationship is completely reversible, the difference between peaks (ΔE_p) is around 58 mV per electron, however, this has been shown to vary significantly depending on the electron transfer rate between the analyte and the electrode, and on the scan rate.[86] A cyclic voltammogram with larger peak separation is commonly referred to as quasi-reversible processes.[86] The voltammogram of ferrocene shown in **Figure 24** has a peak separation of about 280 mV which is significantly greater than the 58 mV separation of reversible processes. However, it is well known that ferrocene is oxidized to the ferricenium ion in a completely reversible one electron process, therefore ferrocene is generally used as an internal standard to compensate for the variance in peak separation.[88,89] The formal reduction potential obtained from the cyclic voltammogram of ferrocene seen in **Figure 24** is about 0.57 V Vs. Ag wire.

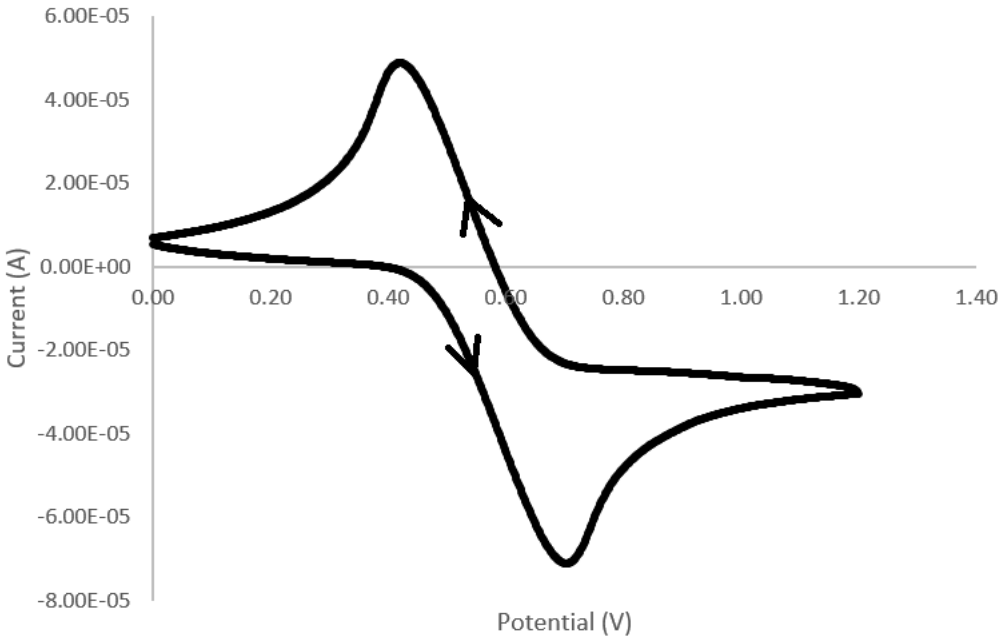

Figure 25: The cyclic voltammogram of ferrocene (2.3 mM) at a scan rate of 100 mV/s in the direction of the arrows with a switching potential of 1200 mV in dry DCM vs Ag wire with 77 mM tetrabutylammonium hexafluorophosphate as the electrolyte. The arrows indicate the direction of the sweeping potential. The current generated in the forward direction is from the oxidation of ferrocene to the ferrocenium cation and the negative current in the reverse direction is from reduction of the ferrocenium cation to ferrocene. The process is described as reversible with a peak separation of ~0.28 V and oxidation potential of around 0.57 V vs Ag wire.

Since the formation of the quinone from the parent tocol is an oxidative process, the use of cyclic voltammetry should provide insights into the ease of forming the quinones. Furthermore, the reduction of the quinones can also be investigated as they are redox active. The use of cyclic voltammetry will provide insight into the redox behavior of the quinones. The electrochemistry of the tocopherols has been described in various experiments using cyclic voltammetry and digital simulations.[90–93]

The electrochemical behaviors of the tocopherols are relatively complex due to heterogeneous electron transfer at the electrode surface followed by homogeneous chemical and electron transfer reactions in solution. Even more complex behavior is observed when water is

present as seen in **Figure 26**.[91] In general, the tocopherols can undergo two one-electron oxidations to form a phenoxonium cation. The first oxidation is a one-electron transfer which generates a tocopheroxyl radical cation.[90–93] The subsequent loss of a proton generates a resonance stabilized tocopheroxyl radical which can be further oxidized to a phenoxonium cation. The phenoxonium quickly reacts with water to form the corresponding quinone.[91] Overall, the oxidation of the tocopherol to the quinone is the loss of two electrons and two protons ($-2e^-/-2H^+$) with the addition of water. The formal oxidation potential of the first electron for the tocopherols is ~500 mV *vs* ferrocene, but increases progressively as the degree of methylation on the chroman ring decreases.[90,93] This is demonstrated in **Table 9** where the α-tocopherol analogue with a only a methyl group at C-2 instead of the phytyl chain (CH_3)α-TOH, had the lowest formal redox potential at +0.50 ± 0.05V which progressively increases to 0.65 ± 0.05 V with (CH_3)δ-TOH.[93] The methyl group derivative was used instead of the natural tocopherols with the phytyl chain because the side chain was previously shown to not significantly impact the electrochemical behavior of the tocopherols.[93] This would suggest that the α-tocopherol is the easiest to oxidize forming the phenoxonium cation. However, another major difference between the tocopherols lies in the stability of the phenoxonium cation, where α- is stable for hours, β- for minutes and γ- and δ- for less than 1s.[94] The rate constants of the reaction of the phenoxonium with water to form the hemiketal have been calculated using digital simulations of CV data and have shown a slight increase in the rate when decreasing the methylation pattern in the order of (CH_3)α- < (CH_3)γ- ≈ (CH_3)δ-TOH.[90] The rate constant for the ring opening isomerization of the hemiketal was similar across all tocopherol derivatives.[90] Together this data would suggest that although, α-tocopherol may undergo a reversible two-

electron oxidation more easily than the other isoforms, the phenoxonium cation generated is more stable to hydrolysis than the other isoforms.[90]

Table 9: The formal reduction potential of the tocopherols obtained by digital simulation of CV data[a] for the two one-electron oxidation processes of tocopherols to the phenoxonium cation.[90]

compound	solvent	$E^0_{f(1)}$[b]/V	$E^0_{f(2)}$[b]/V
$(CH_3)\alpha$-TOH	CH_3CN	$+0.50 \pm 0.05$	$+0.15 \pm 0.05$
$(CH_3)\alpha$-TOH	CH_2Cl_2	$+0.50 \pm 0.05$	$+0.15 \pm 0.05$
$(CH_3)\gamma$-TOH	CH_3CN	$+0.55 \pm 0.05$	$+0.25 \pm 0.05$
$(CH_3)\delta$-TOH	CH_3CN	$+0.65 \pm 0.05$	$+0.30 \pm 0.05$
$(CH_3)H_3$-TOH	CH_3CN	$+0.75 \pm 0.05$	$+0.40 \pm 0.05$

[a] CV data recorded with 0.5 M n-Bu_4NPF_6 as the supporting electrolyte with 20 μm, 50 μm, 0.1 mm, and 1 mm diameter Pt electrodes, at scan rates between 0.1 and 500 V s^{-1} and at temperatures from 313 to 253 K. [b] Formal potential vs Fc/Fc^+. Heterogeneous rate constants were estimated to be between 0.1 and 0.3 cm s^{-1}. Diffusion coefficient values (2.5×10^{-5} cm^2 s^{-1} at 313 K to 0.3×10^{-5} cm^2 s^{-1} at 253 K) for the starting materials were estimated by simulation techniques (the same values were used for all oxidized forms of the same compound).

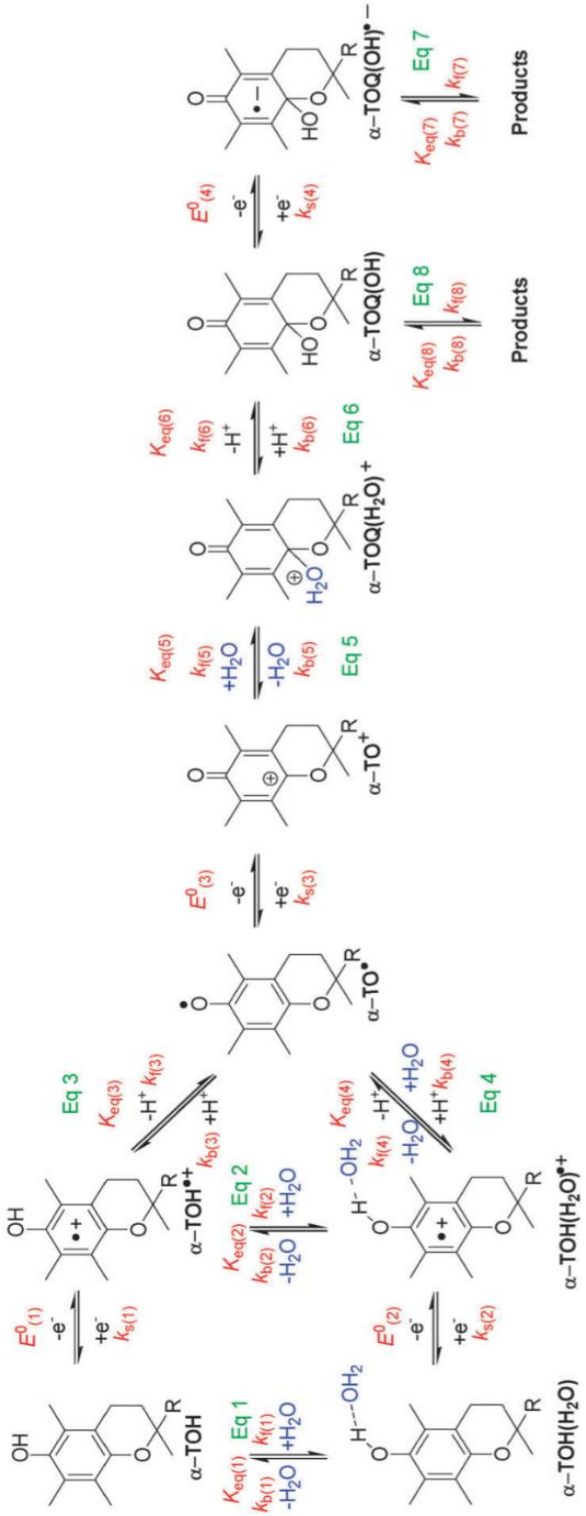

Figure 26: Electrochemical oxidation mechanism of α-tocopherol in acetonitrile determined over a range of scan rates and water concentrations. Figure adapted from Tan *et al*.[91]

To the best of our knowledge the electrochemical behavior of the tocotrienols has not been established using cyclic voltammetry. This may have been influenced by the earlier observation that no significant differences in the electrochemical behavior were observed when the phytyl chain of tocopherol was replaced by a methyl group.[90] It was concluded that the tail was not important in the electrochemistry, however, it may be possible that the unsaturated chain of tocotrienols imparts different electrochemical behavior than the tocopherols. We report here the cyclic voltammograms of the tocopherols and tocotrienols under the same conditions to make a comparison between the tocopherols and tocotrienols. The cyclic voltammograms of the tocols are shown in **Figures 26-28** and the extracted data is compiled in **Table 10**.

The behavior is similar for all compounds showing what appears to be two one-electron oxidation processes which would suggest the presence of a phenoxonium species. It appears that the first oxidation is quasi-reversible whereas the second oxidation is irreversible. More experiments at different scan rates, concentrations and concentrations of water may provide kinetic parameters that confirm the data presented here such as identifying the lifetime of the phenoxyl radical and phenoxonium cation.[93] However, we decided that there was no compelling need to devote further effort on this topic. We observed the same trend of decreased redox potential with an increasing degree of chroman methylation as seen in the literature, where α-tocols had the lowest oxidation potential (~ +0.3 V *vs* Fc/Fc^+) and was progressively increased going from γ-tocol (~ +0.5 V *vs* Fc/Fc^+) to δ-tocol (~ +0.6 V *vs* Fc/Fc^+). Although, the curves do not appear exactly similar presumably because of different scan rates and switching potentials, there is little or no difference between the tocopherols and tocotrienols having the same methylation pattern as seen by the location of the anodic peak in **Figure 27-29**. Therefore, we conclude that the electrochemical behavior of the tocopherols and tocotrienols is not a factor in

the biological differences observed between the two groups. On the other hand, the fact that the phenoxonium ion is accessible at physiological oxidation potentials (up to ~2.2 V *vs* standard hydrogen electrode (S.H.E) by hydroxyl radicals)[35] with the presence of water *in vivo* suggests that the biological activity of the quinones should not be ignored.

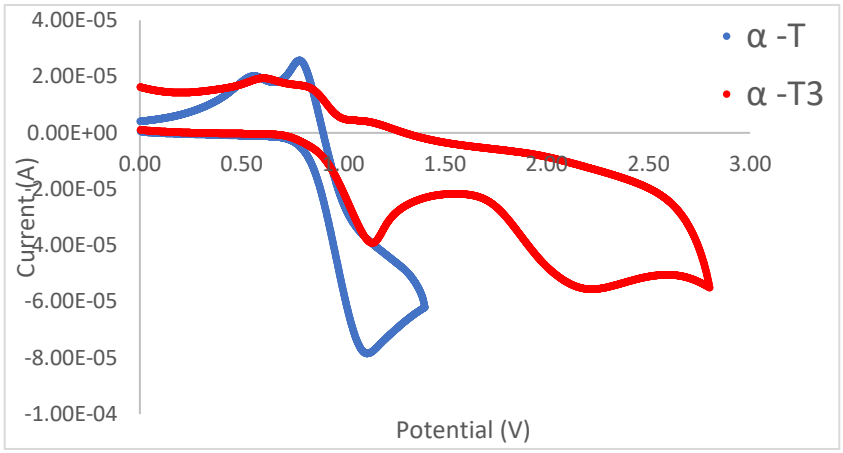

Figure 27: Bioanalytical Systems Inc. (BASI) Epsilon cyclic voltammetry at 100 mV/s of α-tocopherol in dry CH_2Cl_2 with 77 mM tetrabutylammonium hexafluorophosphate *vs.* Ag wire and 300 mV/s of α-tocotrienol (2.4 mM) in dry CH_2Cl_2 with 77 mM tetrabutylammonium hexafluorophosphate *vs*. Ag wire. The scan of α-tocopherol was performed by Mikel Ghelfi using an unknown concentration.

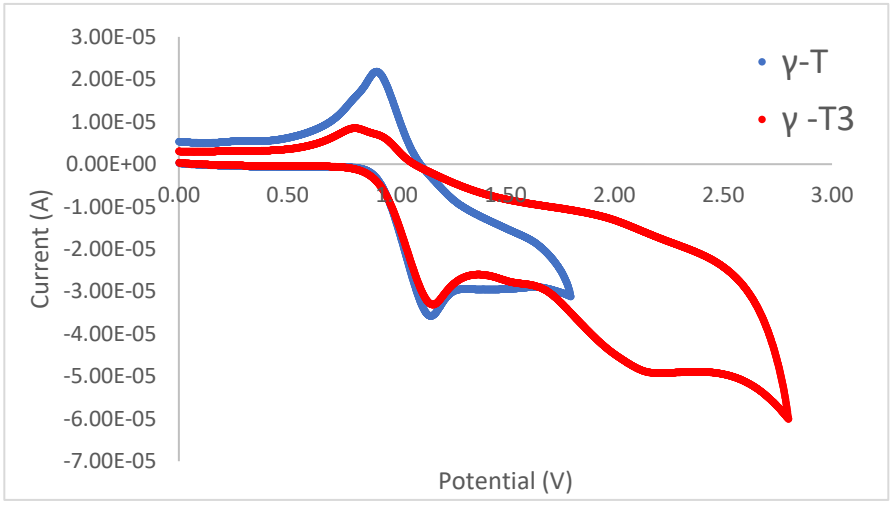

Figure 28: BASI Epsilon cyclic voltammetry at 500 mV/s of γ-tocopherol (2.4 mM) in dry CH_2Cl_2 with 77 mM tetrabutylammonium hexafluorophosphate *vs.* Ag wire and 300 mV/s of γ-tocotrienol (2.4 mM) in dry CH_2Cl_2 with 77 mM tetrabutylammonium hexafluorophosphate *vs.* Ag wire.

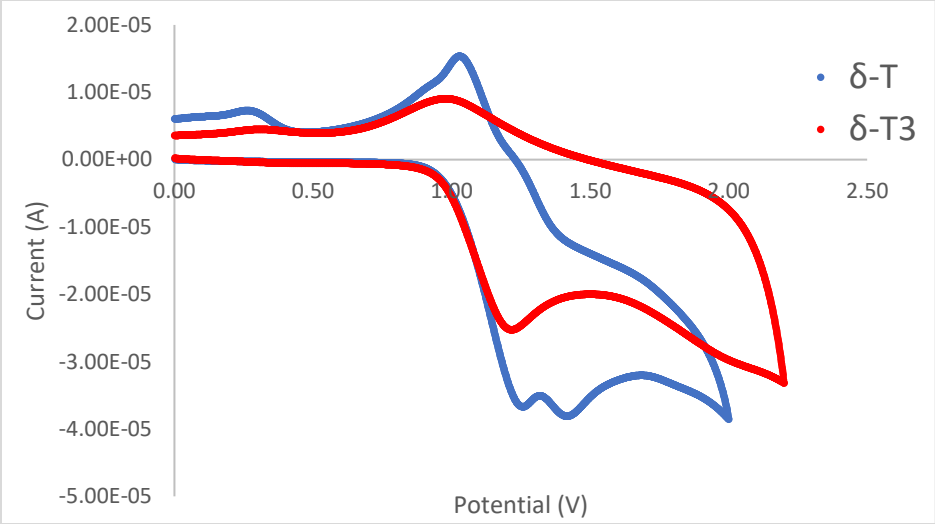

Figure 29: BASI Epsilon cyclic voltammetry at 300 mV/s of δ-tocopherol (2.4 mM) in dry CH_2Cl_2 with 77 mM tetrabutylammonium hexafluorophosphate *vs.* Ag wire and 500 mV/s of δ-tocotrienol (2.4 mM) in dry CH_2Cl_2 with 77 mM tetrabutylammonium hexafluorophosphate *vs.* Ag wire.

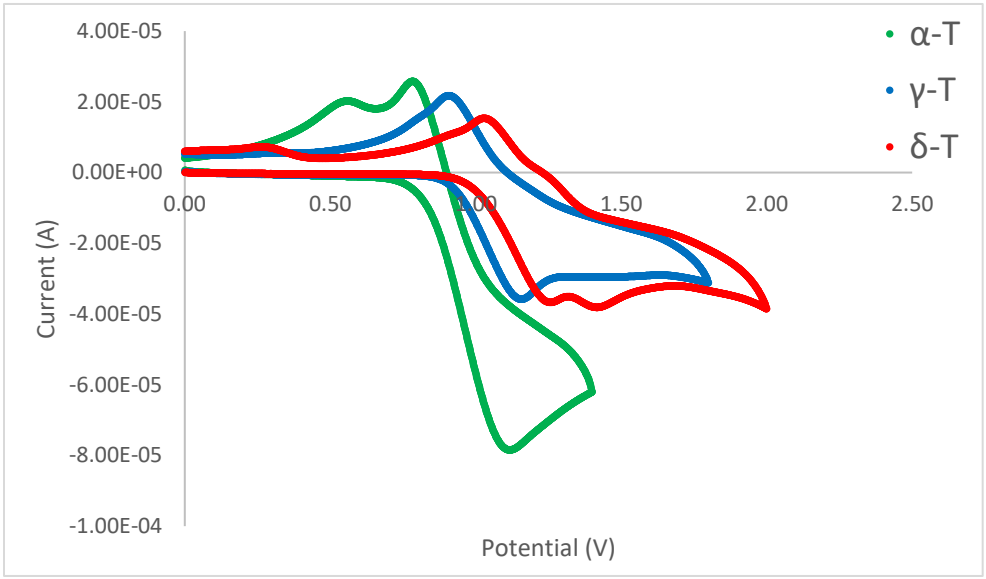

Figure 30: BASI Epsilon cyclic voltammetry at 100 mV/s of α-tocopherol (2.4 mM) in dry CH_2Cl_2 with 77 mM tetrabutylammonium hexafluorophosphate *vs.* Ag wire, 500 mV/s of γ-tocopherol (2.4 mM) in dry CH_2Cl_2 with 77 mM tetrabutylammonium hexafluorophosphate *vs.* Ag wire, and 300 mV/s of δ-tocopherol (2.4 mM) in dry CH_2Cl_2 with 77 mM tetrabutylammonium hexafluorophosphate *vs.* Ag wire.

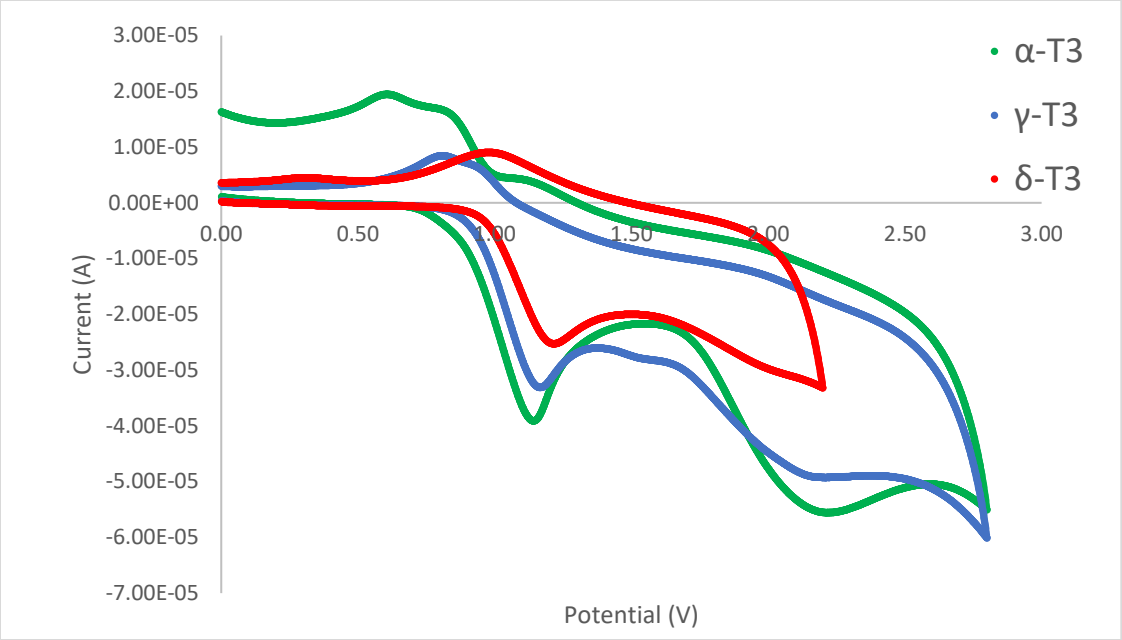

Figure 31: BASI Epsilon cyclic voltammetry at 300 mV/s of α-tocotrienol (2.4 mM) in dry CH_2Cl_2 with 77 mM tetrabutylammonium hexafluorophosphate *vs.* Ag wire, 300 mV/s of γ-tocotrienol (2.4 mM) in dry CH_2Cl_2 with 77 mM tetrabutylammonium hexafluorophosphate *vs.* Ag wire, and 500 mV/s of δ-tocotrienol (2.4 mM) in dry CH_2Cl_2 with 77 mM tetrabutylammonium hexafluorophosphate *vs.* Ag wire.

Table 10: The extracted data from the experimental CV of the tocols. Ferrocene was used as an external standard.

Compound	Cathodic peaks (E_{pc}) V	Anodic peaks (E_{pa}) V	Formal oxidation potential (E_0) *vs* Ag wire $\frac{E_{pc} + E_{pa}}{2}$ V	Formal reduction potential for 1st electron oxidation *vs* Fc/Fc^+ V	Reversibility	Scan speed mV/s
Ferrocene	0.431	0.711	0.571	-	Reversible	100
α-T[a]	0.557 0.798	1.130	0.844	+ 0.27	Quasi	100
α-T3	0.599 0.807	1.150 2.171	0.875 1.489	+ 0.30	Quasi	300
γ-T	0.925	1.16	1.043	+ 0.47	Quasi	500
γ-T3	0.807 0.940	1.181 2.150	0.994 1.545	+ 0.42	Quasi	300
δ-T	1.041 1.242	1.260 1.453	1.151 1.348	+ 0.58	Quasi	300
δ-T3	1.232 1.970	1.010	1.121	+ 0.66	Quasi	500

[a] Data obtained from Mikel Ghelfi

The fact that the quinones could be reduced by sodium borohydride and be oxidized back to the quinones in the presence of air as seen in the UV/vis experiments suggests that, in addition to being able to form cysteine adducts, the quinones are redox active *in vitro* and may exhibit similar activity *in vivo*. Therefore, differences in the redox activity of the quinones may also provide chemical evidence explaining the differences observed in biological samples. In this case, once the tocols are oxidized to the quinones, the quinones can be reduced by one-electron to the semiquinone radical or by two electrons to the neutral hydroquinone. It has been shown that the reduction of estrogen quinones to the estrogen hydroquinone is accomplished by NADPH-dependent cytochrome P450 reductase enzyme or NADPH: quinone oxidoreductase.[95] It is possible that similar enzymes can reduce the vitamin E quinones to the hydroquinones. Once the hydroquinone is formed, it can be oxidized back to the quinone by diatomic oxygen forming

two equivalents of superoxide anion ($O_2^{\bullet-}$) or one equivalent of hydrogen peroxide. The resulting superoxide anion or hydrogen peroxide are reactive oxygen species leading to a pro-oxidant activity generated by the redox cycling of quinones as seen in **Scheme 4**.[95] The redox potential of the quinone is crucial for the ability of the hydroquinone to reduce diatomic oxygen.[84] The more positive the redox potential of the quinone, the less likely the hydroquinone is to reduce molecular oxygen.[84] Therefore, it is possible that differences in the redox potential of the vitamin E quinones can lead to differences in pro-oxidant activity and consequently, different cytotoxicities observed in cell culture assays supplemented with the tocols. Several studies have demonstrated the potential for pro-oxidant activity of vitamin E in cell culture assays and in humans.[96–98] In a randomized control trial with 72 human patients 18-60 years old with a current diagnosis of asthma and taking regular corticosteroids, the supplementation of two capsules of vitamin E (250 mg vitamin E [*d*-α-tocopherol]) per day for six weeks was found to increase the levels of lipid peroxidation by 27% compared to the group receiving two identical placebo capsules.[98]

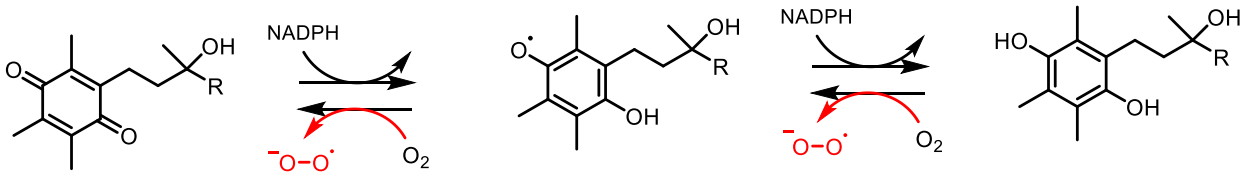

Scheme 4: The proposed redox cycling of vitamin E quinones generating ROS superoxide ($O_2^{\bullet-}$) by the reduction of molecular oxygen. Figure adapted from Liehr and Roy (1990).[95]

The redox potential of the vitamin E quinones observed by CV are shown in **Figures 32-34**. The reduction appears to go through two one-electron reduction processes. The first electron reduction is the reduction of the quinone to the semi-quinone radical anion which is then protonated. This reduction process appears to be quasi-reversible. The second electron reduction

is the reduction of the semi-quinone radical to the hydroquinone anion which is then protonated to form the neutral hydroquinone. This process appears to be less reversible. The lack of reversibility is likely a product of the homogeneous electron transfer and chemical proton transfers in solution.[91] There does not appear to be significant difference in redox potential of the tocopheryl and tocotrienyl quinones having the same methylation pattern. However, the first electron redox potential decreases from δ- (~ -1.1 V *vs* Fc/Fc^+) > γ- (~ -1.2 V *vs* Fc/Fc^+) > α- (~ -1.3 V *vs* Fc/Fc^+) (**Figures 35-36** & **Table 11**). This would suggest that the δ- and γ- tocol quinones are easier to reduce than α-tocol quinones, which may make them less susceptible to redox activity by the reduction of diatomic molecular oxygen. This pro-oxidant activity may be required under certain conditions in the cell. The apparent increased redox potential of α-tocopheryl quinone compared to the other isoforms may also provide a reason for the preferential retention of α-tocopherol, though the differences are rather minor compared to the drastic differences in the rates of reactivity of the vitamin E quinones with thiols. The CV scan of α-tocopheryl quinone only shows one reduction in the forward direction because it was not scanned to a far enough negative potential. The CV scan of α-tocotrienyl quinone was scanned at a rate much too quick (600 mV/s) and not far enough in the negative potential (only -1.0 V) for reliable results. Therefore, the redox potential of α-tocotrienyl quinone was omitted for the comparison towards the other isoforms. The limitations of this data include only one scan rate and only one concentration.

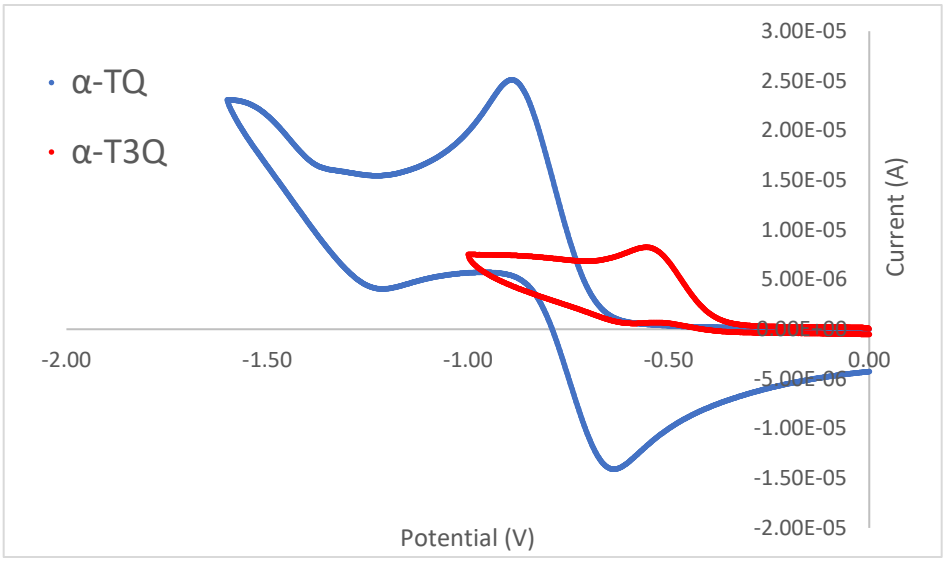

Figure 32: BASI Epsilon cyclic voltammetry at 300 mV/s of α-tocopheryl quinone (2.4 mM) in dry CH_2Cl_2 with 77 mM tetrabutylammonium hexafluorophosphate *vs*. Ag wire, and 600 mV/s of α-tocotrienyl quinone (2.4 mM) in dry CH_2Cl_2 with 77 mM tetrabutylammonium hexafluorophosphate *vs*. Ag wire.

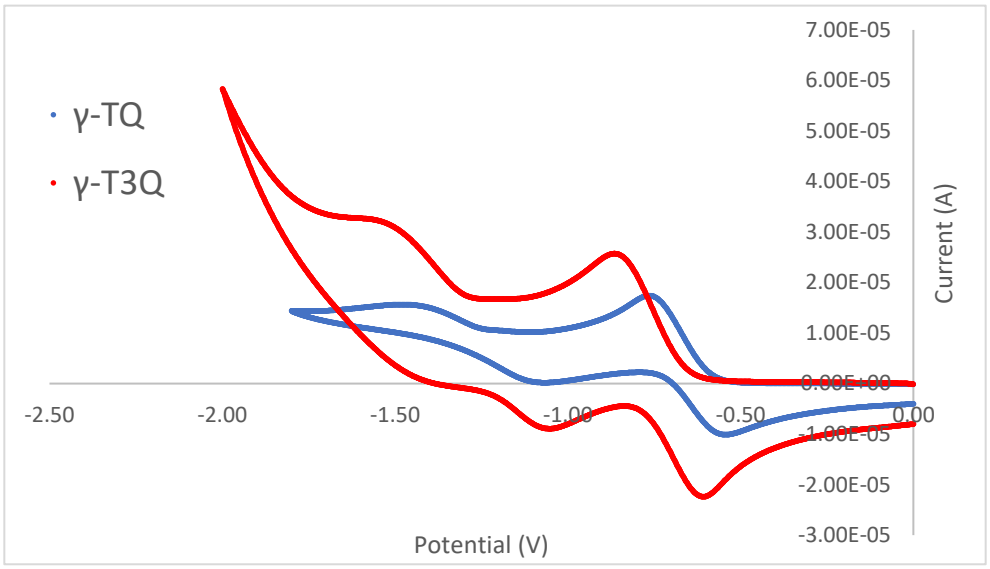

Figure 33: BASI Epsilon cyclic voltammetry at 300 mV/s of γ-tocopheryl quinone (2.4 mM) in dry CH_2Cl_2 with 77 mM tetrabutylammonium hexafluorophosphate *vs*. Ag wire, and 500 mV/s of γ-tocotrienol (2.4 mM) in dry CH_2Cl_2 with 77 mM tetrabutylammonium hexafluorophosphate *vs*. Ag wire.

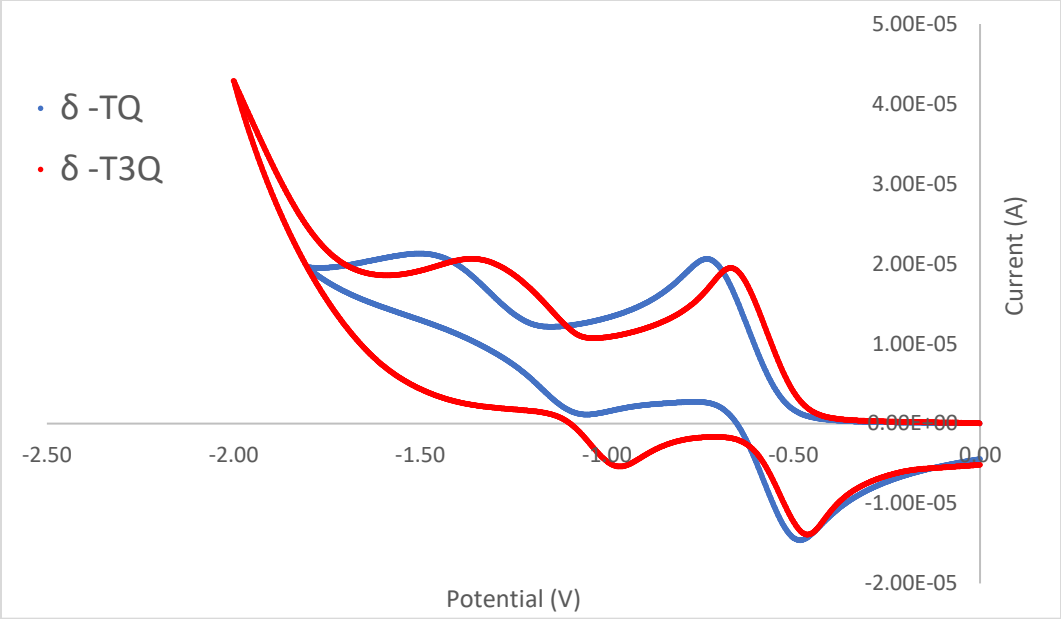

Figure 34: BASI Epsilon cyclic voltammetry at 300 mV/s of δ-tocopheryl quinone (2.4 mM) in dry CH_2Cl_2 with 77 mM tetrabutylammonium hexafluorophosphate *vs.* Ag wire, and 300 mV/s of δ-tocotrienyl quinone (2.4 mM) in dry CH_2Cl_2 with 77 mM tetrabutylammonium hexafluorophosphate *vs*. Ag wire.

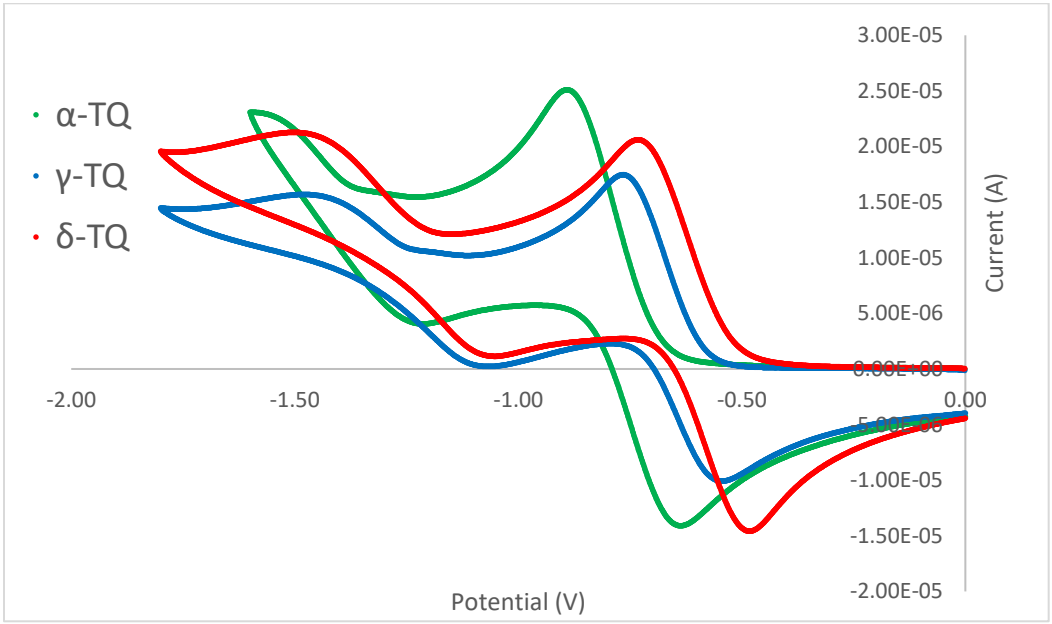

Figure 35: BASI Epsilon cyclic voltammetry at 300 mV/s of α-tocopheryl quinone (2.4 mM) in dry CH_2Cl_2 with 77 mM tetrabutylammonium hexafluorophosphate *vs*. Ag wire, 300 mV/s of γ-tocopheryl quinone (2.4 mM) in dry CH_2Cl_2 with 77 mM tetrabutylammonium hexafluorophosphate *vs*. Ag wire, and 300 mV/s of δ-tocopheryl quinone (2.4 mM) in dry CH_2Cl_2 with 77 mM tetrabutylammonium hexafluorophosphate *vs*. Ag wire.

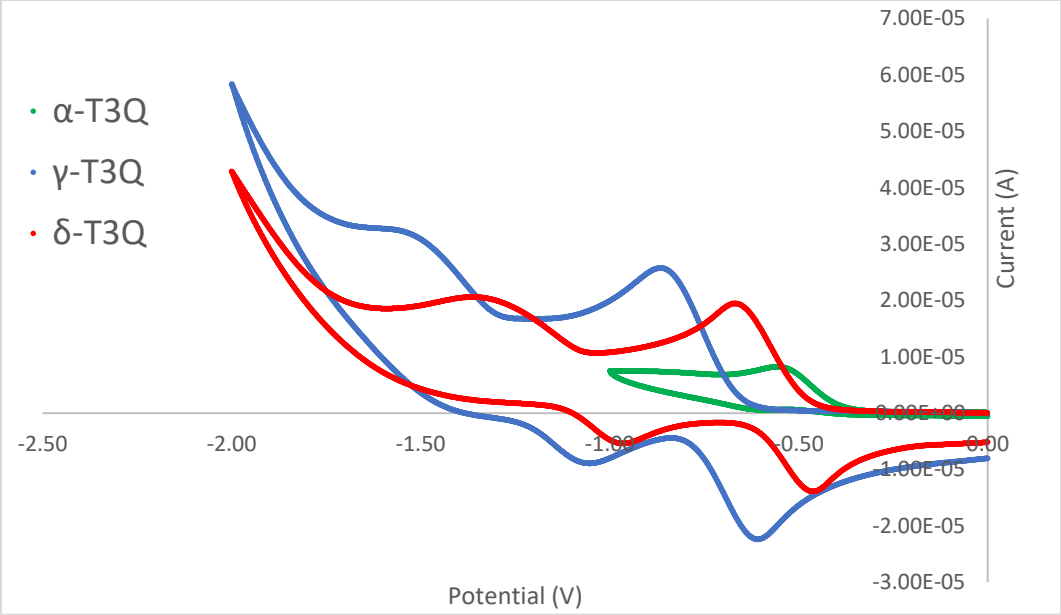

Figure 36: BASI Epsilon cyclic voltammetry at 600 mV/s of α-tocotrienyl quinone (2.4 mM) in dry CH_2Cl_2 with 77 mM tetrabutylammonium hexafluorophosphate *vs*. Ag wire, 500 mV/s of γ-tocotrienyl quinone (2.4 mM) in dry CH_2Cl_2 with 77 mM tetrabutylammonium hexafluorophosphate *vs*. Ag wire, and 300 mV/s of δ-tocotrienyl quinone (2.4 mM) in dry CH_2Cl_2 with 77 mM tetrabutylammonium hexafluorophosphate *vs*. Ag wire.

Table 11: The extracted data obtained from the cyclic voltammetry of the vitamin E quinones.

Compound	Cathodic peaks (E_{pc}) V	Anodic peaks (E_{pa}) V	Formal reduction potential (E_0) vs Ag wire $\frac{E_{pc} + E_{pa}}{2}$ V	Formal reduction potential for 1st reduction vs Fc/Fc^+ V	Reversibility	Scan speed mV/s
Ferrocene	0.431	0.711	0.571	-	Reversible	100
α-TQ[a]	-0.875	-0.643	-0.759	-1.33	Quasi	300
α-T3Q[b]	-0.547	-0.602	-0.575	-1.15	Quasi	600
γ-TQ	-0.759 -1.440	-0.540 -1.060	-0.650 -1.250	-1.22	Quasi	300
γ-T3Q	-0.837 -1.540	-0.609 -1.112	-0.723 -1.326	-1.29	Quasi	500
δ-TQ	-0.712 -1.480	-0.487 -1.071	-0.600 -1.276	-1.17	Quasi	300
δ-T3Q	-0.638 -1.300	-0.452 -0.990	-0.545 -1.145	-1.12	Quasi	300

[a]The potential was not scanned far enough in the negative to catch the reduction of the second electron. [b]The scan rate was too fast and not far enough for reliable results.

3. SUMMARY AND FUTURE PERSPECTIVES

There is plenty of evidence in the literature describing how vitamin E is a fat-soluble antioxidant that inhibits lipid peroxidation. The antioxidant ability of the tocopherols and tocotrienols have been established in various solvents.[34,45] The antioxidant ability decreases slightly in the order of α > γ ≈ β > δ-tocopherol (see **Table 2**) while there is no significant differences between the tocopherols and tocotrienols with the same methylation pattern.[34,45] That said, the differences in antioxidant ability are rather minor compared to the significant biological differences observed between the isoforms of vitamin E demonstrated in a fetal resorption assay in rats.[34] The differences observed in the rat fetal resorption assay can be attributed to the preferential tissue and plasma retention of α-tocopherol by α-TTP and increased metabolism of the other isoforms by CYP4F2.[34] Nonetheless, the evolutionary advantage for the retention of α-tocopherol is not known. Various studies using cultured cells incubated with the vitamin E isoforms have demonstrated the increased cytotoxicity of the non-α-tocols. The general trend observed is that δ-tocopherol is more cytotoxic than γ-tocopherol whereas cytotoxicity is generally not observed in the same cells supplemented with α-tocopherol. This may explain the preferential retention of α-tocopherol in animal tissues, that is, the α-tocopheroxyl quinone is far less toxic than the other tocol quinones. In some cases, the tocotrienols have been shown to exhibit different biological effects from their tocopherol counterpart. To date, there has been no clear mechanism describing the different effects observed in cell culture supplemented with tocols. It is possible that the tocols are oxidized to the corresponding quinones depending on the oxidative status of the cell culture conditions, and the different effects observed are manifested by different reactivities between the tocol quinones. Cornwell's group has demonstrated the ability for the non-α-tocopherol quinones to form thiol

adducts by a Michael-addition reaction.[64,66] The quinone may form adducts with protein thiols which can induce different cell signalling cascades. The rate of reactivity of the quinones with thiols may correlate to the different activities observed in cell cultures. We have demonstrated that the rate of the reactivity with thiols is significantly greater with the δ-tocol quinones compared to the γ-tocol quinones whereas no reactivity is observed with the α-tocol quinones. These findings on the rate of reactivity are observed to follow roughly the degree of cytotoxicity observed in cell culture assays supplemented with the tocopherols and tocotrienols. On the other hand, there is no significant differences observed between the rate of reactivity of the tocopheryl and tocotrienyl quinones having the same methylation pattern. Therefore, the rates of reactivity of the quinones can not explain some of the different effects observed *in vivo* between the tocopherols and tocotrienols.[34,51,52,58]

Our attention was then shifted towards the possibility of identifying differences in the ease of formation of the quinone using cyclic voltammetry. It was determined that the electrochemical behavior of the tocols are similar, however, a slight increase in redox potential (rightward shift, more positive) is observed when decreasing the extent of methylation on the chromanol ring. There does not seem to be significantly different behavior observed between the similarly methylated tocopherols and tocotrienols. This would suggest that rate of formation of the quinones is similar between the similarly methylated tocopherols and tocotrienols. Therefore, the electrochemical behavior of the tocols can not explain the differences observed in cell cultures supplemented with the tocotrienols. We also used cyclic voltammetry to identify differences in the redox activity of the quinones. The reduction potential of the quinones with respect to methylation pattern on the quinone ring showed that as methylation increases the reduction potential increases, reflecting the greater difficulty of adding an electron to quinones

bearing more electron donating methyl groups (*i.e.*, α-tocopheryl quinone has a more negative reduction potential than γ-tocopheryl quinone). There does not seem to be significantly different behavior exhibited between the tocopheryl quinones and tocotrienyl quinones with the same methylation pattern. Therefore, we may conclude that the different cytotoxic activities observed between the tocols having different methylation patterns correlates with the rate of reactivity of their quinones with thiols. The difference in the biological activity of the tocopherols and tocotrienols is most likely a function of the way they sit in the membrane, inter-membrane transfer rates or possibly interfering with cholesterol biosynthesis by inhibiting HMG-CoA reductase.

From our results, we would emphasize the necessity of quantifying the presence of tocol quinone concentration of any cell culture assay supplemented with the tocols. Future studies should be aimed towards identifying which protein thiols the non-α-tocol quinones may form an adduct with. These proteins may be involved in redox sensitive cell signalling cascades like apoptosis or cellular antioxidant enzyme production. The cell signalling cascades leading to apoptosis are poorly understood and identifying these reactive protein thiols with vitamin E quinones may improve our understanding of apoptosis and redox sensitive cell signalling cascades. This may be achieved using a similar methodology developed by the Weerapana group for identifying reactive cysteines in the mitochondria proteome which utilizes reactive probes and mass spectrometry.[71] In our case, the reactive probes would be an isotopically labelled non-α-tocol quinone.

4. EXPERIMENTAL

4.1 General Methods

4.1.1 Materials and Reagents

All reagents were purchased from Sigma-Aldrich Co., in Oakville, Ontario. All glassware was dried in an oven at 90°C overnight. The vitamin E rich vegetable oil suspension was graciously donated by Archer Daniels Midland Co. (ADM) and the TOCOMIN® palm kernel oil suspension was graciously donated by Carotech Sdn Bhd.

4.1.2 Chromatography

Column chromatography was performed on either silica gel (SiliCycle® SiliaFlash P60, particle size: 40-63μm, pore size: 60 Å) or neutral alumina gel (Sigma-Aldrich, pore size: 150 Å) with the solvent system stated. Thin layer chromatography (TLC) was performed on silica gel plates (Merck, TLC Silica gel 60 F_{254}) or alumina plates (EM Science, Aluminiumoxid 60 F_{254} neutral).

4.1.2 Spectroscopy

Spectroscopic analysis of compounds was performed using ^{1}H and ^{13}C NMR acquired using a Bruker Avance DPX-400 Digital FT-NMR spectrometer at 400 MHz and 100 MHz respectively. The solvent used for analysis was deuterated chloroform (Cambridge Isotope Laboratories, Inc. deuterated chloroform, 99.8% pure). This solvent has a residual solvent peak corresponding to (^{1}H=7.26 ppm, ^{13}C=77.0 ppm). Chemical shifts are reported in ppm (δ) relative to tetramethyl silane (δ 0.00 ppm), multiplicity, number of protons and assignment. Multiplicity is described using the following abbreviations: s (singlet), d (doublet), t (triplet), q (quartet), m (multiplet). Low resolution mass spectra (MS) were recorded with a Carlo Erba/ Kratos GC/MS Concept 1S

double focusing mass spectrometer using electron impact (EI) or electrospray ionization (ESI) ionization methods. The molecular ions and major fragments are reported as *m/z* values. Absorption spectroscopy was performed using a Genesis 10X UV/Vis spectrophotometer with ScanLite software. Quartz cuvettes (3 mL, 1 cm path length) were used when recording absorbance values.

4.2 Preparation of Starting Materials

4.2.1 Synthesis of α-Tocopherol

α-Tocopherol acetate (5.49 g, 11.6 mmol) was dissolved in ethanol (100 mL). KOH pellets (2.44 g, 43.5 mmol) were added to the solution and left to stir for 30 minutes at 10 °C. The reaction mixture was golden yellow. The solvent was partially evaporated *in vacuo* and 6 M HCl was added until the solution turned pink. The solution was extracted with diethyl ether. The organic layer was retained and dried with magnesium sulfate. The solvent was removed *in vacuo* and subjected to silica column chromatography with a hexane and dichloromethane (DCM) solvent gradient system starting with 20% DCM and finishing with 50% DCM. The solvent was removed from eluted materials to afford α-tocopherol (4.33 g, 10.1 mmol, 87.1%).

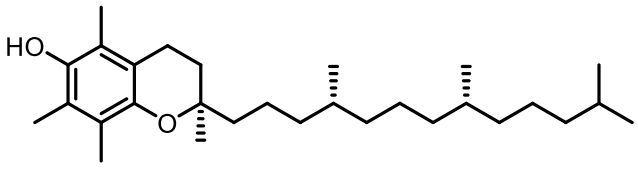

Chemical Formula: $C_{29}H_{50}O_2$
Molecular Weight: 430.7170

Pale yellow oil, R_f = (0.35, hexanes/DCM 1:1, visualized by iodine and Hanessian's stain). ^{1}H NMR (400 MHz, $CDCl_3$) δ 4.20 (s, 1H, OH), 2.63 (t, 2H, CH_2, *J* = 6.8 Hz), 2.19 (s, 3H, CH_3), 2.14 (s, 6H, 2 CH_3), 1.80 (m, 2H, CH_2), 1.60 (m, 5H, CH_2, 3 CH), 1.5 (s, 3H, CH_3), 1.23 (m, 16H, 8 CH_2), 0.91 (m, 12H, 4 CH_3).

^{13}C NMR (100 MHz, $CDCl_3$) δ 145.56, 144.53, 122.63, 120.99, 118.46, 117.37, 74.54, 39.82, 39.39, 37.48, 37.46, 37.44, 37.30, 32.81, 32.72, 31.56, 27.99, 24.81, 24.46, 23.81, 22.73, 22.64, 21.05, 20.77, 19.76, 19.67, 12.22, 11.78, 11.29.

4.2.2 Isolation of γ-Tocopherol

A purchased vitamin E oil suspension from Archer Daniels Midland (ADM) (5.93 g) was subjected to silica column chromatography with a hexane and ethyl acetate solvent gradient system, usually starting with 1% ethyl acetate and finishing with 25% ethyl acetate. The solvent was removed from eluted materials *in vacuo* to afford γ-tocopherol (2.60 g, 6.24 mmol, 43.8% (w/w)).

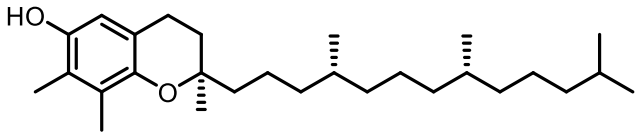

Chemical Formula: $C_{28}H_{48}O_2$
Molecular Weight: 416.6900

Clear oil, R_f = (0.51, hexanes/ethyl acetate 6:1, visualized by iodine stain).

^{1}H NMR (400 MHz, $CDCl_3$) δ 6.40 (s, 1H, Ar-H), 4.22 (s, 1H, OH), 2.69 (m, 2H, CH_2), 2.16 (s, 3H, CH_3), 2.13 (s, 3H, CH_3), 1.75 (m, 3H, CH_3), 1.56 (m, 5H, CH_2, 3 CH), 1.26 (m, 18H, 9 CH_2), 0.90 (m, 12H, 4 CH_3).

^{13}C NMR (100 MHz, $CDCl_3$) δ 146.20, 145.77, 125.81, 121.58, 118.33, 112.13, 75.48, 40.05, 39.39, 37.48, 37.46, 37.43, 37.29, 32.81, 32.70, 31.40, 27.99, 24.81, 24.46, 24.10, 22.73, 22.64, 22.33, 21.02, 19.76, 19.67, 11.91, 11.87.

MS (+EI) *m/z* 416 (M+, 100.0%), 191 (10.5 %), 151 (53.6%).

4.2.3 Isolation of δ-Tocopherol

A purchased vitamin E oil suspension from ADM (5.93 g) was subjected to multiple silica chromatography columns with a hexane and ethyl acetate solvent gradient system, usually starting with 1% ethyl acetate and finishing with 25% ethyl acetate. The solvent was removed from eluted materials *in vacuo* to afford δ-tocopherol (0.80 g, 1.99 mmol, 13.5% (w/w)).

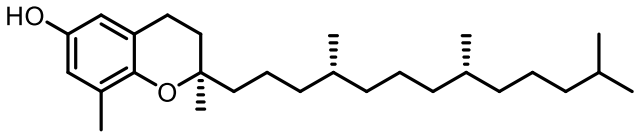

Chemical Formula: $C_{27}H_{46}O_2$
Molecular Weight: 402.6630

Clear oil, R_f = (0.53, hexanes/ethyl acetate 17:3, visualized by iodine stain).

^{1}H NMR (400 MHz, $CDCl_3$) δ 6.50 (d, 1H, Ar-H, *J* = 3.2 Hz), 6.41 (d, 1H, Ar-H, *J* = 3.2 Hz), 4.22 (s, 1H, OH), 2.71 (m, 2H, CH_2), 2.14 (s, 3H, CH_3), 1.75 (m, 3H, CH_3), 1.55 (m, 5H, CH_2, 3 CH), 1.26 (m, 18H, 9 CH_2), 0.88 (m, 12H, 4 CH_3).

^{13}C NMR (100 MHz, $CDCl_3$) δ 147.65, 146.09, 127.37, 121.32, 115.60, 112.56, 75.58, 39.96, 39.96, 39.39, 37.48, 37.43, 37.29, 32.81, 32.70, 31.34, 27.99, 24.81, 24.46, 24.12, 22.73, 22.64, 22.53, 20.99, 19.76, 19.66, 16.07.

MS (+EI) *m/z* 402 (M+, 100.0%), 177 (38.6%), 137 (72.9%).

4.2.4 Isolation of α-Tocotrienol

A commercial palm oil suspension, TOCOMIN® (25.0 g) was subjected to multiple silica columns with a hexane and ethyl acetate solvent gradient system starting with 1 % ethyl acetate and ending with 10 % ethyl acetate. Samples containing α-tocotrienol from previous years were also added to the column. The solvent was removed from eluted materials *in vacuo* to afford α-Tocotrienol (1.50 g, 3.53 mmol, 6% (w/w)).

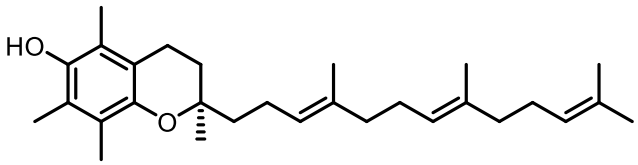

Chemical Formula: $C_{29}H_{44}O_2$
Molecular Weight: 424.6690

Orangey-yellow oil, R_f = (0.45, hexanes/ethyl acetate 9:1, visualized by iodine stain).

^{1}H NMR (400 MHz, $CDCl_3$) δ 5.15 (t, 3H, CH), 4.20 (s, 1H, OH), 2.63 (t, 2H, CH_2, J = 6.8 Hz), 2.18 (s, 3H, CH_3), 2.14 (s, 3H, CH_3), 2.13 (s, 3H, CH_3), 2.07 (m, 6H, 3 CH_2), 1.97 (m, 4H, 2 CH_2), 1.80 (m, 2H, CH_2), 1.62 (m, 12H, 4 CH_3), 1.55 (m, 2H, CH_2), 1.26 (s, 3H, CH_3).

^{13}C NMR (100 MHz, $CDCl_3$) δ 145.50, 144.58, 135.06, 134.97, 131.27, 124.44, 124.41, 124.21, 122.65, 121.01, 118.47, 117.31, 74.30, 39.72, 39.70, 39.54, 31.58, 26.77, 26.61, 25.71, 23.73, 22.23, 20.75, 17.70, 16.01, 15.90, 12.22, 11.79, 11.28.

MS (+EI) *m/z* 424 (M+, 96.3%), 205 (23.1%), 165 (100.0%), 149 (71.1%), 69 (79.4%).

4.2.5 Isolation of γ-Tocotrienol

A commercial palm oil suspension, TOCOMIN® (25.0 g) was subjected to multiple silica columns with a hexane and ethyl acetate solvent gradient system starting with 1 % ethyl acetate and ending with 10 % ethyl acetate. The solvent was removed from eluted materials *in vacuo* to afford γ-Tocotrienol (2.90 g, 7.06 mmol, 11.6% (w/w)).

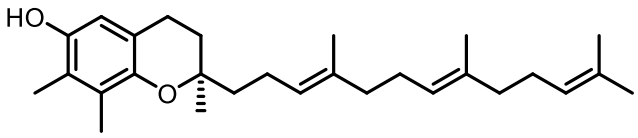

Chemical Formula: $C_{28}H_{42}O_2$
Molecular Weight: 410.6420

Orangey-yellow oil, R_f = (0.41, hexanes/ethyl acetate 6:1, visualized by iodine stain).

^{1}H NMR (400 MHz, $CDCl_3$) δ 6.40 (s, 1H, Ar-H), 5.13 (m, 3H, 3 CH), 4.27 (s, 1H, OH), 2.71 (t, 2H, CH_2, *J* = 6.8 Hz), 2.16 (s, 3H, CH_3), 2.15 (s, 3H, CH_3), 2.10 (m, 6H, 3 CH_2), 2.00 (m, 4H, 2 CH_2), 1.65 (m, 12H, 4 CH_3), 1.29 (s, 3H, CH_3).

^{13}C NMR (100 MHz, $CDCl_3$) δ 146.26, 145.71, 135.11, 134.98, 131.27, 125.83, 124.42, 124.35, 124.21, 121.63, 118.25, 112.15, 75.24, 39.79, 39.73, 39.70, 31.42, 26.77, 26.61, 25.71, 24.01, 22.30, 22.22, 17.70, 16.01, 15.90, 11.92, 11.87.

MS (+EI) *m/z* 410 (M+, 89.4%), 151 (100.0%), 69 (60.0%).

4.2.6 Isolation of δ-Tocotrienol

A commercial palm oil suspension, TOCOMIN® (25.0 g) was subjected to multiple silica columns with a hexane and ethyl acetate solvent gradient system starting. The solvent was removed from eluted materials *in vacuo* to afford δ-Tocotrienol (1.96 g, 4.94 mmol, 7.8% (w/w)).

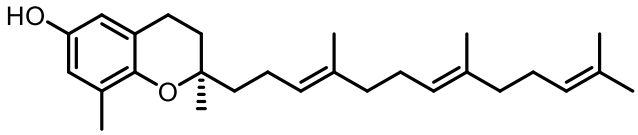

Chemical Formula: $C_{27}H_{40}O_2$
Molecular Weight: 396.6150

Golden yellow oil, R_f = (0.33, hexanes/ethyl acetate 17:3, visualized by iodine stain).

^{1}H NMR (400 MHz, $CDCl_3$) δ 6.50 (d, 1H, Ar-H, *J* = 3.2 Hz), 6.40 (d, 1H, Ar-H, *J* = 3.2 Hz), 5.13 (m, 3H, 3 CH), 4.28 (s, 1H, OH), 2.71 (t, 2H, CH_2, *J* = 6.8 Hz), 2.15 (s, 3H, CH_3), 2.12 (m, 2H, CH_2), 2.00 (m, 8H, 4 CH_2), 1.77 (m, 2H, CH_2), 1.65 (m, 14H, 4 CH_3, CH_2), 1.28 (s, 3H, CH_3).

^{13}C NMR (100 MHz, $CDCl_3$) δ 147.72, 146.01, 135.15, 134.98, 131.27, 127.83, 124.41, 124.29, 124.19, 121.24, 115.62, 112.57, 75.33, 39.73, 39.71, 39.69, 31.36, 26.76, 26.60, 25.71, 24.04, 22.49, 22.17, 17.69, 16.06, 16.01, 15.88.

MS (+ESI) *m/z* 419 (M+ 23 (Na), 100.0%).

4.3 General Procedure for Synthesis of Quinones

A 100-mL round bottom flask was charged with 6 g of flash chromatographic grade silica gel, a magnetic stirring bar and fitted with a rubber septum. Ceric ammonium nitrate (CAN, $(NH_4)_2Ce(NO_3)_6$) (1.65 g, 3.0 mmol, 2.1 eq.) was dissolved in 2.0 mL of water. This solution was added drop wise by syringe to the silica under continuous stirring which remained dry. The silica was left to stir for 5 minutes which produced a free-flowing yellow sand-like solid. 25 mL of DCM was added to the silica. For the oxidation, 0.50 g of pure previously isolated tocols (~1.2 mmol) was dissolved in 2 mL of DCM and added to the round bottom flask. The yellow solution turned dark orange immediately after the addition. The reaction was left to stir and monitored by TLC which determined the reaction to be complete after 30 minutes. The solid waste was filtered and washed with DCM. The solvent was removed *in vacuo* and the oil was subjected to silica column chromatography with a hexane and 10% ethyl acetate mixture. The solvent was removed from eluted materials to afford isolated products.

4.3.1 Synthesis of α-Tocopheryl Quinone

Pure α-tocopherol, 0.5020 g (1.16 mmol), and 1.3360 g (2.43 mmol) of CAN were used as starting materials. The reaction was monitored by TLC and showed one spot after 30 minutes with no starting material observable. The product was isolated by column chromatography to afford α-tocopheryl quinone (0.4245 g, 0.95 mmol, 81.9%).

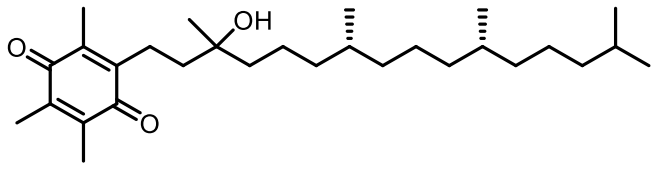

Chemical Formula: $C_{29}H_{50}O_3$
Molecular Weight: 446.7160

Bright yellow oil, R_f = (0.24, hexane/ethyl acetate 4:1, visualized by UV and iodine stain).

^{1}H NMR (400 MHz, $CDCl_3$) δ 2.58 (s, 2H, CH_2), 2.06 (s, 3H, CH_3), 2.03 (s, 6H, 2 CH_3), 1.62 (m, 23H, 10 CH_2, 3 CH), 1.25 (s, 3H, CH_3), 0.91 (m, 12H, 4 CH_3).

^{13}C NMR (100 MHz, $CDCl_3$) δ 187.70, 187.24, 144.45, 140.54, 140.48, 140.18, 72.68, 42.30, 40.27, 39.38, 37.61, 37.44, 37.29, 32.81, 32.78, 31.60, 27.98, 26.59, 24.81, 24.50, 22.73, 22.63, 21.42, 21.32, 19.76, 19.71, 14.13, 12.38, 12.11.

MS (+EI) *m/z* 446 (M+, 74.0%), 428 (100.0%), 378 (42.5%).

4.3.2 Synthesis of γ-Tocopheryl Quinone

Pure γ-tocopherol, 0.8983 g (2.15 mmol), and 2.4872 g (4.53 mmol) of CAN were used as starting materials. The reaction was monitored by TLC which showed two spots after 30 minutes, neither of which was starting material. The products were isolated by column chromatography to afford *para*-γ-tocopheryl quinone (0.4106 g, 0.95 mmol, 44.2%) and *ortho*-γ-tocopheryl quinone (0.2502 g, 0.58 mmol, 27.0%).

***Para*-γ-tocopheryl quinone**:

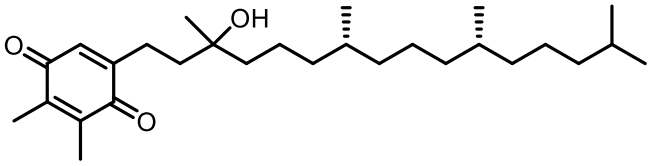

Chemical Formula: $C_{28}H_{48}O_3$
Molecular Weight: 432.6890

Bright yellow oil, R_f = (0.18, hexane/ethyl acetate 6:1, visualized by UV and iodine stain).

^{1}H NMR (400 MHz, $CDCl_3$) δ 6.55 (s, 1H, Ar-H), 2.50 (m, 2H, CH_2), 2.05 (s, 3H, CH_3), 2.03 (s, 3H, CH_3), 1.32 (m, 23H, 10 CH_2, 3 CH), 1.24 (s, 3H, CH_3), 0.91 (m, 12H, 4 CH_3).

^{13}C NMR (100 MHz, $CDCl_3$) δ 187.64, 187.57, 149.38, 141.08, 140.67, 132.14, 72.53, 42.42, 39.91, 39.37, 37.57, 37.44, 37.29, 32.81, 32.77, 27.98, 26.74, 24.80, 24.50, 23.97, 22.73, 22.63, 21.39, 19.75, 19.69, 12.40, 12.06.

MS (+EI) *m/z* 432 (M+, 84.0%), 414 (100.0%), 399 (15.0%).

***Ortho*-γ-tocopheryl quinone**:

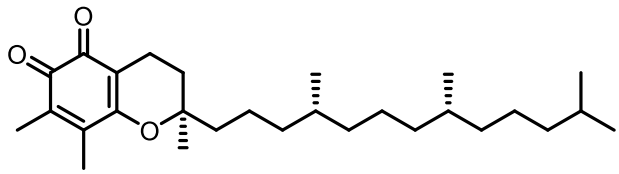

Chemical Formula: $C_{28}H_{46}O_3$
Molecular Weight: 430.6730

Bright red oil, R_f = (0.23 hexane/ethyl acetate 6:1, visualized by UV and iodine stain).

^{1}H NMR (400 MHz, $CDCl_3$) δ 2.45 (m, 2H, CH_2), 2.05 (s, 3H, CH_3), 1.97 (s, 3H, CH_3), 1.74 (m, 2 H, CH_2), 1.59 (m, 21 H, 9 CH_2, 3 CH), 1.34 (s, 3H, CH_3), 0.88 (m, 12H, 4 CH_3).

^{13}C NMR (100 MHz, $CDCl_3$) δ 180.85, 177.87, 163.31, 143.67, 134.18, 110.28, 81.38, 39.94, 39.37, 37.44, 37.37, 37.28, 37.24, 32.80, 32.62, 31.60, 29.71, 27.99, 24.80, 24.44, 23.89, 22.72, 22.63, 20.90, 19.75, 19.62, 15.37, 14.12, 13.73, 11.57.

MS (+ESI) *m/z* 431 (M+, 100.0%), 360 (17.0%).

4.3.3 Synthesis of δ-Tocopheryl Quinone

Pure δ-tocopherol, 0.1021 g (0.25 mmol), and 0.2865 g (0.52 mmol) of CAN were used as starting materials. The reaction was monitored by TLC which showed two spots after 30 minutes, neither of which was starting material. The products were isolated by column chromatography to afford *p*-δ-tocopheryl quinone (0.0311 g, 0.07 mmol, 29.7%) and *o*-δ-tocopheryl quinone (δ-tocored) (0.0232 g, 0.06 mmol, 22.2%).

***Para*-δ-tocopheryl quinone**:

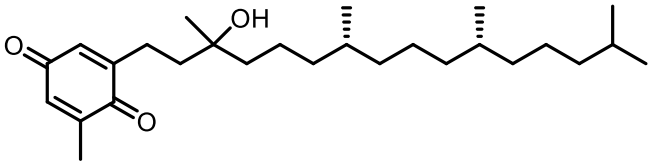

Chemical Formula: $C_{27}H_{46}O_3$
Molecular Weight: 418.6620

Bright yellow oil, R_f = (0.33, hexane/ethyl acetate 4:1, visualized by UV and iodine stain).

^{1}H NMR (400 MHz, $CDCl_3$) δ 6.57 (m, 1H, Ar-H), 6.55 (m, 1H, Ar-H), 2.53 (m, 2H, CH_2), 2.08 (s, 3H, CH_3), 1.62 (m, 2H, CH_2), 1.28 (m, 24H, CH_3, 9 CH_2, 3 CH), 0.89 (m, 12H, 4 CH_3).

^{13}C NMR (100 MHz, $CDCl_3$) δ 187.92, 187.79, 149.89, 145.99, 133.17, 132.38, 72.51, 42.44, 39.89, 39.38, 37.56, 37.44, 37.29, 32.81, 32.78, 29.71, 27.98, 26.76, 24.80, 24.50, 24.09, 22.73, 22.63, 21.40, 19.75, 19.69, 16.05.

MS (+ESI) *m/z* 441 (M+ 23 (Na), 100.0%), 401 (90.0%).

***Ortho*-δ-tocopheryl quinone**:

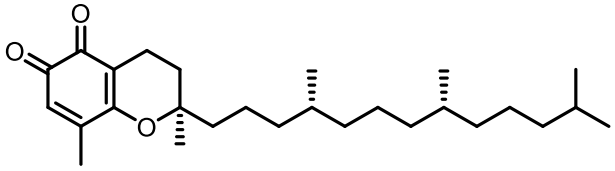

Chemical Formula: $C_{27}H_{44}O_3$
Molecular Weight: 416.6460

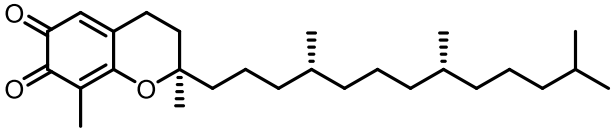

Chemical Formula: $C_{27}H_{44}O_3$
Molecular Weight: 416.6460

Bright red oil, R_f = (0.42, hexane/ethyl acetate 4:1, visualized by UV and iodine stain).

^{1}H NMR (400 MHz, $CDCl_3$) δ 6.17 (s, 1H, Ar-H), 2.46 (m, 2H, CH_2), 2.10 (s, 3H, CH_3), 1.76 (m, 2H, CH_2), 1.62 (m, 5H, CH_2, 3 CH), 1.34 (s, 3H, CH_3), 1.28 (m, 16H, 8 CH_2), 0.89 (m, 12H, 4 CH_3).

^{13}C NMR (100 MHz, $CDCl_3$) δ 180.77, 177.94, 162.12, 150.27, 126.63, 112.20, 81.40, 39.88, 39.37, 37.43, 37.37, 37.28, 37.23, 32.80, 32.63, 29.62, 27.99, 24.80, 24.44, 23.85, 22.72, 22.63, 20.88, 19.75, 19.61, 17.87, 15.57.

MS (+ESI) *m/z* 432 (M+1, 84.0%), 414 (100.0%).

4.3.4 Synthesis of α-Tocotrienyl Quinone

Pure α-tocotrienol, 0.2064 g (0.49 mmol), and 0.5647 g (1.03 mmol) of CAN were used as starting materials. The reaction was monitored by TLC which showed one spot after 30 minutes with no starting material observable. The products were isolated by column chromatography to afford α-tocotrienyl quinone (0.1703 g, 0.39 mmol, 79.6%).

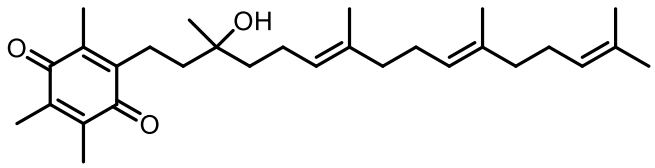

Chemical Formula: $C_{29}H_{44}O_3$
Molecular Weight: 440.6680

Bright yellow oil, R_f = (0.22, hexane/ethyl acetate 6:1, visualized by UV and iodine stain).

^{1}H NMR (400 MHz, $CDCl_3$) δ 5.12 (m, 3H, 3 CH), 2.57 (m, 2H, CH_2), 2.01 (m, 19H, 3 CH_3, 5 CH_2), 1.59 (m, 16H, 4 CH_3, 2 CH_2), 1.27 (s, 3H, CH_3).

^{13}C NMR (100 MHz, $CDCl_3$) δ 187.70, 187.23, 144.41, 140.54, 140.44, 140.19, 135.60, 135.07, 131.27, 124.39, 124.14, 124.11, 72.68, 41.61, 40.30, 39.72, 26.77, 26.59, 26.51, 25.71, 22.67, 21.35, 17.70, 16.03, 12.38, 12.30, 11.98.

MS (+EI) *m/z* 440 (M+, 3.9%), 422 (3.9%), 69 (100.0%).

4.3.5 Synthesis of γ-Tocotrienyl Quinone

Pure γ-tocotrienol, 0.4206 g (1.02 mmol), and 1.1743 g (2.14 mmol) of CAN were used as starting materials. The reaction was monitored by TLC which showed two spots after 30 minutes, neither of which was starting material. The products were isolated by column chromatography to afford *para*-γ-tocotrienyl quinone (0.1841 g, 0.43 mmol, 42.3%) and *ortho*-γ-tocotrienyl quinone, analogous to tocored (0.1536 g, 0.36 mmol, 35.3%).

***Para*-γ-tocotrienyl quinone**:

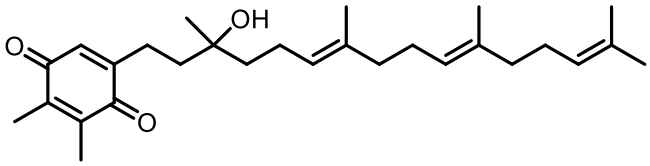

Chemical Formula: $C_{28}H_{42}O_3$
Molecular Weight: 426.6410

Bright yellow oil, R_f = (0.17, hexanes/ethyl acetate 6:1, visualized by iodine stain).

^{1}H NMR (400 MHz, $CDCl_3$) δ 6.55 (s, 1H, Ar-H), 5.14 (m, 3H, 3 CH), 2.52 (m, 2H, CH_2), 2.08 (m, 16H, 5 CH_2, 2 CH_3), 1.64 (m, 10H, 2 CH_3, 2 CH_2), 1.26 (s, 3H, CH_3).

^{13}C NMR (100 MHz, $CDCl_3$) δ 187.64, 187.55, 149.35, 141.08, 140.64, 135.72, 135.10, 132.15, 131.28, 124.39, 124.09, 124.00, 72.55, 41.72, 40.00, 39.72, 26.77, 26.67, 26.58, 25.71, 24.01, 23.44, 22.61, 17.70, 16.06, 12.40, 12.06.

MS (+EI) *m/z* 426 (M+, 2.07%), 295 (5.26%), 149 (21.81%), 69 (100.0%).

***Ortho*-γ-tocotrienyl quinone**:

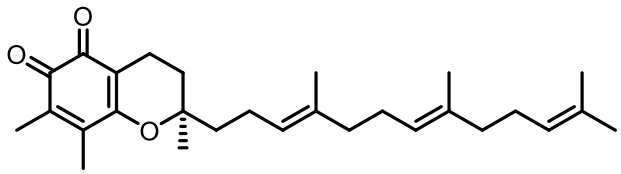

Chemical Formula: $C_{28}H_{40}O_3$
Molecular Weight: 424.6250

Bright red oil, R_f = (0.22, hexanes/ethyl acetate 6:1, visualized by iodine stain).

^{1}H NMR (400 MHz, $CDCl_3$) δ 5.14 (m, 3H, 3 CH), 2.46 (m, 2H, CH_2), 2.05 (m, 16H, 5 CH_2, CH_3), 1.70 (m, 16H, 4 CH_3, 2 CH_2), 1.36 (s, 3H, CH_3).

^{13}C NMR (100 MHz, $CDCl_3$) δ 180.76, 177.84, 163.19, 143.60, 136.15, 134.18, 124.33, 124.23, 124.06, 124.00, 123.86, 123.19, 81.14, 40.04, 39.71, 32.18, 31.98, 29.70, 26.75, 26.62, 26.51, 25.69, 23.79, 23.72, 23.39, 17.68, 16.00, 11.55.

MS (+ESI) *m/z* 447 (M+23 (Na), 30.0%), 425 (M+1, 50.0%).

4.3.6 Synthesis of δ-Tocotrienyl Quinone

Pure δ-tocotrienol, 0.4206 g (1.02 mmol), and 0.5411 g (0.99 mmol) of CAN were used as starting materials. The reaction was monitored by TLC which showed two spots after 30 minutes, neither of which was starting material. The products were isolated by column chromatography to afford *para*-δ-tocotrienyl quinone (0.0842 g, 0.20 mmol, 43.4%) and *ortho*-δ-tocotrienyl quinone (0.0398 g, 0.10 mmol, 20.6%).

***Para*-δ-tocotrienyl quinone**:

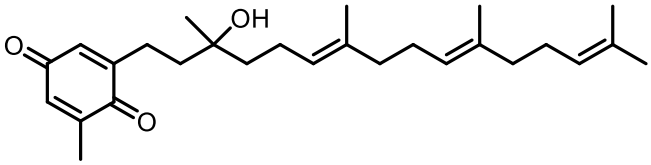

Chemical Formula: $C_{27}H_{40}O_3$
Molecular Weight: 412.6140

Bright yellow oil, R_f = (0.30, hexanes/ethyl acetate 4:1, visualized by UV and iodine stain).

^{1}H NMR (400 MHz, $CDCl_3$) δ 6.57 (m, 1H, Ar-H), 6.54 (m, 1H, Ar-H), 5.15 (m, 3H, 3CH), 2.52 (m, 2H, CH_2), 2.08 (m, 13H, 5 CH_2, 1 CH_3), 1.65 (m, 16H, 4 CH_3, 2 CH_2), 1.26 (s, 3H, CH_3).

^{13}C NMR (100 MHz, $CDCl_3$) δ 187.90, 187.78, 149.87, 145.99, 135.74, 135.10, 133.17, 132.38, 131.27, 124.39, 124.07, 123.97, 72.51, 41.73, 39.97, 39.72, 39.70, 26.76, 26.67, 26.57, 25.70, 24.13, 22.61, 17.69, 16.05, 16.03.

MS (+ESI) *m/z* 435 (M+23 (+Na), 100.0%), 413 (M+1, (25.0%), 395 (70.0%).

***Ortho*-δ-tocotrienyl quinone**:

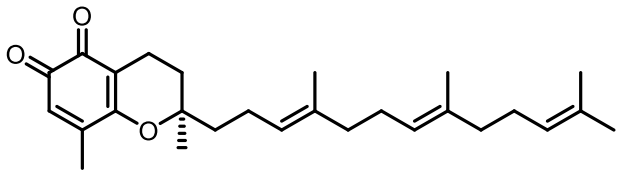

Chemical Formula: $C_{27}H_{38}O_3$
Molecular Weight: 410.5980

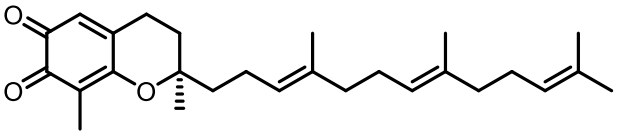

Chemical Formula: $C_{27}H_{38}O_3$
Molecular Weight: 410.5980

Bright red oil, R_f = (0.40, hexanes/ethyl acetate 4:1, visualized by iodine stain).

^{1}H NMR (400 MHz, $CDCl_3$) δ 6.18 (s, 1H, Ar-H), 5.11 (m, 3H, 3 CH), 2.48 (m, 2H, CH_2), 2.10 (m, 13H, 5 CH_2, 1 CH_3), 1.69 (m, 16H, 4 CH_3, 2 CH_2), 1.36 (s, 3H, CH_3).

^{13}C NMR (100 MHz, $CDCl_3$) δ 180.72, 177.92, 162.05, 150.24, 136.07, 135.15, 131.31, 126.64, 124.34, 123.98, 123.12, 112.20, 81.14, 39.72, 39.64, 29.62, 26.75, 26.51, 25.70, 23.77, 22.04, 17.87, 17.69, 16.02, 15.97, 15.56.

MS (+ESI) *m/z* 411 (M+1, 100.0%), 193 (15.0%).

4.3.7 Synthesis of p-Benzoquinone

Purchased *p*-hydroxyquinone, 1.0026 g (9.11 mmol), and 10.4887 g (19.13 mmol) of CAN were used as starting materials. The reaction was monitored by TLC which showed one spot after 15 minutes with no starting material observable. The yellow product crystallized upon solvent removal *in vacuo* to afford p-benzoquinone (0.9382 g, 8.68 mmol, 95.3%).

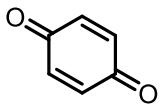

Chemical Formula: $C_6H_4O_2$
Molecular Weight: 108.0960

^{1}H NMR (400 MHz, $CDCl_3$) δ 6.81 (s, 4H, Ar-H).

4.3.8 Synthesis of 1,3,5-Trimethyl Quinone

Purchased 1,3,5-trimethyl hydroquinone, 1.0000 g (6.57 mmol), and 7.5643 g (13.80 mmol) of CAN were used as starting materials. The reaction was monitored by TLC which showed one spot after 15 minutes with no starting material observable. The yellow product crystallized upon solvent removal *in vacuo* to afford 1,3,5-trimethyl quinone (0.8032 g, 5.35 mmol, 81.4%).

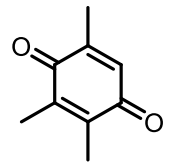

Chemical Formula: $C_9H_{10}O_2$
Molecular Weight: 150.1770

^{1}H NMR (400 MHz, $CDCl_3$) δ 6.57 (q, 1H, Ar-H, J = 1.6 Hz), 2.05 (m, 9H, CH_3).

4.4 General Procedure for Synthesis of Quinone Thiol Conjugates

The synthesized *p*-benzoquinone, 0.0500 g (0.46 mmol), was dissolved in 2 mL of ethanol in a 5-mL vial. In a separate vial, 0.0802 g (0.51 mmol, 1.1 eq.) of *N*-acetyl cysteine was dissolved in 2 mL of 0.1 mM Tris/HCl buffer at pH 8.5. The two vials were combined in a round bottom flask equipped with a magnetic stir bar and left to stir for 1 hour. The reaction was monitored by TLC in a solvent system of acetonitrile/methanol/acetic acid (9:1:0.1). To the reaction mixture, 10 mL of DCM was added followed by 3 mL of 6 M HCl and 10 mL of brine solution. The aqueous layer was washed with 3 portions of 5 mL of DCM. The combined organic layers were dried with Na_2SO_4. The product was isolated by column chromatography using the TLC solvent conditions. The solvent was removed *in vacuo* to afford an *N*-acetyl cysteine benzoquinone adduct (0.0912 g ,0.34 mmol, 73.9%).

4.4.1 Synthesis of N-acetyl Cysteine p-Benzoquinone Conjugate

p-benzoquinone, 0.0500 g (0.46 mmol), and 0.0802 g (0.51 mmol, 1.1 eq.) of *N*-acetyl cysteine were used as a starting material. TLC showed the presence of one spot after 1 hour. The product was isolated by column chromatography to afford *N*-acetyl cysteine *p*-benzoquinone conjugate (0.0912 g, 0.34 mmol, 73.9%).

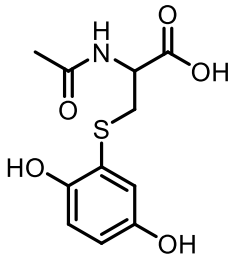

Chemical Formula: $C_{11}H_{13}NO_5S$
Molecular Weight: 271.2870

R_f = (0.10, ACN/MeOH/HOAc 9:1:0.1, visualized by Hannessian's stain)

^{1}H NMR (400 MHz, MeOD) δ 6.87 (d, 1H, Ar-H, *J* = 2.7 Hz), 6.70 (d, 1H, Ar-H, *J* = 8.7 Hz), 6.68 (dd, 1H, Ar-H, *J* = 2.7 Hz *J* = 8.7 Hz), 4.40 (q, 1H, CH), 3.32 (m, 2H, CH_2), 1.96 (s, 3H, CH_3).

MS (+EI) *m/z* 271 (M+, 12.0%), 142 (100.0%).

4.4.2 Synthesis of N-acetyl Cysteine 2,3,5-Trimethylbenzoquinone Conjugate

2,3,5-trimethylbenzoquinone, 0.1000 g (0.66 mmol), and 0.1196 g (0.73 mmol, 1.1 eq.) of *N*-acetyl cysteine were used as a starting material. TLC showed the presence of one spot after 1 hour. The product was isolated by column chromatography to afford *N*-acetyl cysteine 2,3,5-trimethylbenzoquinone conjugate (0.1512 g, 0.48 mmol, 72.7%).

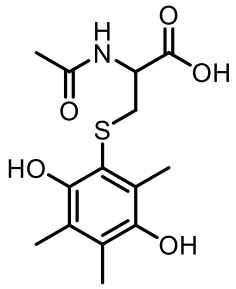

Chemical Formula: $C_{14}H_{19}NO_5S$
Molecular Weight: 313.3680

R_f = (0.43, ACN/MeOH/HOAc 9:1:0.1, visualized by Hannessian's stain)

^{1}H NMR (400 MHz, D_2O) δ 4.18 (dd, 1H, CH, *J* = 4.0 Hz, *J* =8.8 Hz), 3.15 (dd, 1H, CH_2, *J* = 4.0 Hz *J* = 14.0 HZ), 2.89 (dd, 1H, CH_2, *J* = 8.8 Hz *J* = 14.0 Hz), 2.28 (s, 3H, CH_3), 2.06 (s, 3H, CH_3), 2.04 (s, 3H, CH_3), 1.79 (s, 3H, CH_3).

MS (-ESI) *m/z* 312 (M-1, 100.0%), 142 (100.0%).

4.4.3 Synthesis of N-acetyl Cysteine γ-Tocopheryl Quinone Conjugate

γ-tocopherol quinone, 0.0689 g (0.16 mmol), and 0.0294 g (0.18 mmol, 1.1 eq.) of *N*-acetyl cysteine were used as a starting material. TLC showed the presence of one spot after 1 hour. The product was isolated by column chromatography to afford *N*-acetyl cysteine of γ-tocopheryl quinone conjugate (0.0713 g, 0.12 mmol, 75.0 %).

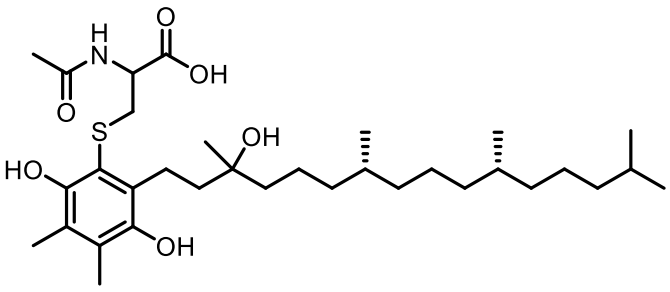

Chemical Formula: $C_{33}H_{57}NO_6S$
Molecular Weight: 595.8800

Orange oil, R_f = (0.23, ACN/MeOH/HOAc 9:1:0.1, visualized by Hannessian's stain)

λ_{max} = 265 nm, ε = ~ 3,300 M^{-1}•cm^{-1}, λ_{max} = 307 nm, ε = ~ 2,700 M^{-1}•cm^{-1}

^{1}H NMR (400 MHz, MeOH) δ 4.18 (dd, 1H, CH, *J* = 4.0 Hz *J* =7.6 Hz), 3.65 (dd, 1H, CH_2, *J* = 4.0 Hz *J* = 14.0 HZ), 3.35 (dd, 1H, CH_2, *J* = 8.8 Hz *J* = 14.0 Hz), 2.77 (m, 2H, CH_2), 2.10 (s, 3H, CH_3), 2.09 (s, 3H, CH_3), 1.95 (s, 3H, CH_3), 1.40 (m, 23H, 10 CH_2, 3 CH), 1.23 (s, 3H, CH_3), 0.91 (m, 12H, 4 CH_3).

^{13}C NMR (100 MHz, $CDCl_3$) δ 184.12, 182.97, 174.01, 171.44, 149.74, 142.24, 141.94, 140.62, 72.17, 54.21, 41.21, 39.80, 39.15, 37.48, 37.14, 37.09, 37.01, 35.03, 32.60, 32.55, 27.74, 25.46, 24.50, 24.16, 23.83, 21.70, 21.61, 21.28, 20.97, 18.90, 18.81, 11.49, 11.03. MS (+ESI) *m/z* 600 (M+5 (-H_2O + Na), 46.0%), 578 (100.0%), 532 (80.0%).

4.4.4 Synthesis of N-acetyl Cysteine δ-Tocopheryl Quinone Conjugate

δ-tocopheryl quinone, 0.0447 g (0.11 mmol), and 0.0366 g (0.22 mmol, 2.1 eq.) of *N*-acetyl cysteine were used as a starting material. TLC showed the presence of one spot after 1 hour. The product was isolated by column chromatography to afford *N*-acetyl cysteine of δ-tocopheryl quinone conjugate (0.0358 g, 0.06 mmol, 56.1 %).

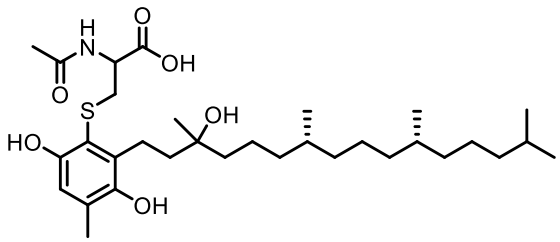

Chemical Formula: $C_{32}H_{55}NO_6S$
Molecular Weight: 581.8530

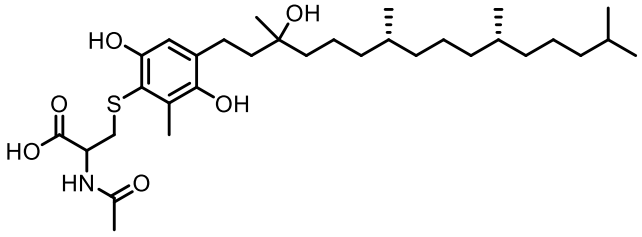

Chemical Formula: $C_{32}H_{55}NO_6S$
Molecular Weight: 581.8530

Orange oil, R_f = (0.18, ACN/MeOH/HOAc 9:1:0.1, visualized by Hannessian's stain)

λ_{max} = 257 nm, ε = ~ 1,600 M^{-1}•cm^{-1}, λ_{max} = 303 nm, ε = ~ 3,300 M^{-1}•cm^{-1}

^{1}H NMR (400 MHz, $CDCl_3$) δ 6.92-7.05 (dd, 1H, NH), 6.66 (s, 1H, Ar-H)^a, 6.62 (s, 1H, Ar-H)^b 4.64 (m, 1H, CH), 3.19 (m, 2H, CH_2)^a, 2.95 (m, 2H, CH_2)^b, 2.64 (m, 2H, CH_2), 2.39 (s, 3H, CH_3)^a, 2.19 (s, 3H, CH_3)^b, 1.94 (s, 3H, CH_3)^a, 1.89 (s, 3H, CH_3)^b, 1.70 (m, 2H, CH_2), 1.53 (m, 3H, 3 CH), 1.23 (m, 24H, 9 CH_2, 2 CH_3^{a,b}), 0.87 (m, 12H, 4 CH_3).

^{13}C NMR (100 MHz, $CDCl_3$) δ 173.04, 171.86, 171.79, 150.87, 146.20, 145.99, 133.39, 133.03, 129.92, 129.19, 115.73, 114.80, 114.69, 113.22, 74.32, 74.09, 53.08, 42.61, 42.46,

41.13, 39.38, 37.62, 37.53, 37.48, 37.30, 32.82, 32.78, 27.98, 26.31, 26.10, 24.81, 24.52, 22.93, 22.74, 22.64, 21.57, 20.58, 19.75, 19.63, 16.68, 14.60.

MS (+ESI) *m/z* 647 (10.0 %), 604 (M+23 (Na), 100.0%), 564 ((-H_2O), 10.0%)

Note: This reaction produced a mixture of regio-isomers that were not separated. The 1H NMR spectra showed two distinct signals for the regio-isomers designated as [a] and [b]. The ratio is approximately $1.2^a : 1^b$.

4.4.5 Synthesis of N-acetyl Cysteine γ-Tocotrienyl Quinone Conjugate

γ-tocotrienyl quinone, 0.0189 g (0.04 mmol), and 0.0149 g (0.09 mmol, 2.2 eq.) of *N*-acetyl cysteine were used as a starting material. TLC showed the presence of one spot after 1 hour. The product was isolated by column chromatography to afford *N*-acetyl cysteine of γ-tocotrienyl quinone conjugate (0.0081 g, 0.01_3 mmol, 34.7 %).

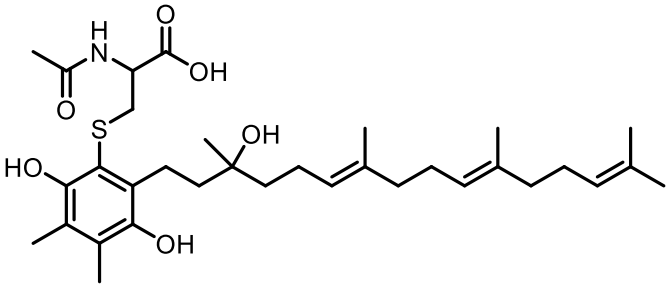

Chemical Formula: $C_{33}H_{51}NO_6S$
Molecular Weight: 589.8320

Orange oil, R_f = (0.22, ACN/MeOH/HOAc 9:1:0.1, visualized by Hannessian's stain)

λ_{max} = 265 nm, ε = ~ 3,300 M^{-1}•cm^{-1}, λ_{max} = 307 nm, ε = ~ 2,700 M^{-1}•cm^{-1}

^{1}H NMR (400 MHz, $CDCl_3$) δ 7.12 (d, 1H, NH, *J* = 6.8 Hz), 5.12 (m, 3H, 3 CH), 4.79 (m, 1H, CH), 3.14 (m, 2H, CH_2), 2.82 (m, 2H, CH_2), 2.20 (d, 3H, CH_3), 2.10 (m, 16H, 2 CH_3, 5 CH_2), 1.65 (m, 16H, 4 CH_3, 2 CH_2), 1.28 (s, 3H, CH_3).

^{13}C NMR (100 MHz, $CDCl_3$) δ 177.09, 148.99, 136.07, 135.19, 131.30, 124.38, 124.11, 124.03, 123.93, 123.85, 74.30, 39.72, 29.71, 26.76, 26.63, 26.58, 26.26, 26.15, 25.70, 22.83, 22.68, 20.74, 17.69, 16.07, 16.02, 12.91, 12.83, 12.63, 12.49.

MS (+ESI) *m/z* 659 (M+70, 25.0%), 628 (M+ 39 (K), 42.0 %), 626 (30.0%), 612 (M+23 (Na), 100.0 %), 610 (70.0%), 381 (20.0%).

4.4.6 Synthesis of N-acetyl Cysteine δ-Tocotrienyl Quinone Conjugate

δ-tocotrienyl quinone, 0.0633 g (0.16 mmol), and 0.0522 g (0.32 mmol, 2.1 eq.) of *N*-acetyl cysteine were used as a starting material. TLC showed the presence of one spot after 1 hour. The product was isolated by column chromatography to afford *N*-acetyl cysteine of δ-tocotrienyl quinone conjugate (0.0492 g, 0.08 mmol, 53.4 %).

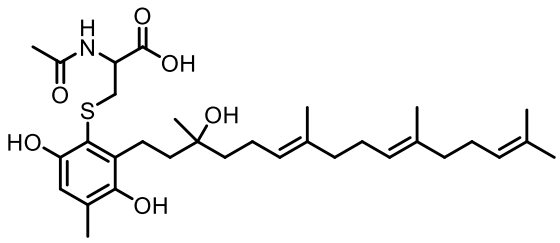

Chemical Formula: $C_{32}H_{49}NO_6S$
Molecular Weight: 575.8050

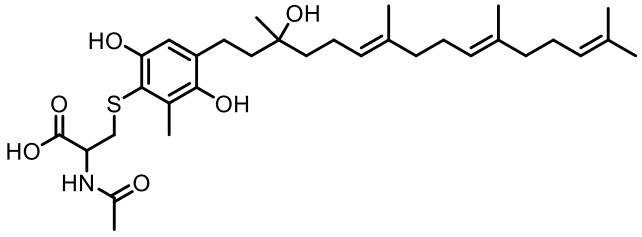

Chemical Formula: $C_{32}H_{49}NO_6S$
Molecular Weight: 575.8050

Orange oil, R_f = (0.17, ACN/MeOH/HOAc 9:1:0.1, visualized by Hannessian's stain)

λ_{max} = 257 nm, ε = ~ 1,600 M^{-1}•cm^{-1}, λ_{max} = 303 nm, ε = ~ 3,300 M^{-1}•cm^{-1}

^{1}H NMR (400 MHz, $CDCl_3$) δ 6.71-6.79 (dd, 1H, NH), 6.68 (s, 1H, Ar-H)^a, 6.64 (s, 1H, Ar-H)^b, 5.12 (m, 3H, 3 CH), 4.72 (m, 1H, CH), 3.13 (m, 2H, CH_2)^a, 3.01 (m, 2H, CH_2)^b, 2.65 (m, 2H, CH_2), 2.41 (s, 3H, CH_3)^a, 2.21 (s, 3H, CH_3)^b, 1.89-2.12 (m, 13H, CH_3, 5 CH_2), 1.69 (m, 4H, 2 CH_2), 1.61 (m, 12H, 4 CH_3), 1.28 (s, 3H, CH_3)^a, 1.26 (s, 3H, CH_3)^b.

^{13}C NMR (100 MHz, $CDCl_3$) δ 176.57, 173.41, 171.66, 150.74, 150.70, 146.32, 146.11, 136.00, 135.93, 135.16, 135.15, 133.11, 132.87, 131.30, 129.73, 129.19, 124.38, 124.05,

123.87, 123.82, 115.77, 114.67, 113.17, 74.39, 74.11, 53.73, 53.02, 41.66, 41.20, 41.08, 39.72, 37.75, 26.77, 26.61, 26.34, 26.16, 25.71, 24.79, 22.97, 22.81, 22.67, 22.62, 20.71, 17.70, 16.68, 16.08, 16.06, 16.03, 14.56.

MS (+ESI) *m/z* 598 (M+23 (Na), 100.0%), 558 (5.0%), 437 (5.0%), 185 (10.0%).

Note: This reaction produced a mixture of regio-isomers that were not separated. The ^{1}H NMR spectra showed two distinct signals for the regio-isomers designated as ^{a} and ^{b}. The ratio is approximately 1.2^{a} : 1^{b}.

4.5 Monitoring Reactivity of Quinones with Model Thiol

Stock solutions of quinones (0.096 mg/mL) were prepared by dissolving 0.0096 g of quinone in 100 mL of methanol and stored in a freezer at -20 ℃. One millilitre of the quinone stock solution was added to a 3-mL quartz cuvette and left to dry under nitrogen for about 1 hour. The cuvette containing dry quinone and a dry blank cuvette were placed in the respective cell holders of the spectrophotometer. The spectrophotometer was set up in a large two hand zipper lock Aldrich® Atmosbag with a nitrogen inlet and vacuum outlet to remove air and minimize the oxygen present. A solution of methanol was degassed by bubbling nitrogen through the solution while sonicating overnight. Stock solutions of *N*-acetyl cysteine (0.145 mg/mL) were prepared by dissolving 0.0145g of *N*-acetyl cysteine in 100 mL of the desired buffer: 100 mM Tris/HCl pH 8.5, 100mM Tris/HCl pH 7.5 or 100 mM bis-Tris/HCl pH 6.5. The stock solutions of *N*-acetyl cysteine were degassed by bubbling nitrogen through the solution while sonicating for 3 hours. The degassed methanol and the stock solutions of *N*-acetyl cysteine were placed inside the bag. The bag was purged with nitrogen five times to remove most of the oxygen. Two millilitres of methanol was added to the blank cuvette and the reaction cuvette. The cuvettes were shaken lightly by hand. One millilitre of the *N*-acetyl cysteine stock solution (4 eq.) was added to the

blank cuvette and the reaction cuvette. The increase in absorbance at 308 nm was recorded on Genesis 10x spectrophotometer every nine seconds using Vision Lite software. The reactions took between 5 minutes and 4 hours depending on conditions.

4.5.1 Identification of Stoichiometry: Titration of Quinone with N-acetyl cysteine

One millilitre of the γ-tocopherol quinone stock solution (0.096 mg/mL) was added to a 3-mL quartz cuvette and left to dry under nitrogen for about 1 hour. The cuvette containing dry quinone and a dry blank cuvette were placed in the respective cell holders of the spectrophotometer. The spectrophotometer was set up in a large two hand zipper lock Aldrich® Atmosbag with a nitrogen inlet and vacuum outlet to minimize the oxygen present. The bag was purged with nitrogen five times to remove most of the oxygen. A stock solution of *N*-acetyl cysteine (0.361 mg/mL) was prepared fresh inside the bag by dissolving 0.0361 g in 100 mL of degassed 100 mM Tris/HCl buffer (pH 8.5). Two millilitres of the degassed methanol and 0.8 mL of degassed 100 mM Tris/HCl buffer (pH 8.5) was added to both cuvettes. A 10 µL aliquot of the *N*-acetyl cysteine stock solution (0.1 eq.) was added to the cuvettes and the absorbance at 308 nm was recorded every nine seconds for about 30 minutes until no increase in absorbance was observed. After this time, an additional 10 µL aliquot was added and the absorbance was measured every nine seconds. A total of 20 aliquots were added and the maximum absorbance after each addition was recorded.

4.5.2 Identification of Suitable Solvent Systems

One millilitre of the γ-tocopherol quinone stock solution was added to a 3-mL quartz cuvette and left to dry under nitrogen for about 1 hour. The cuvette containing dry quinone and a dry blank cuvette were placed in the respective cell holders of the spectrophotometer. The

spectrophotometer was set up in a large two hand zipper lock Aldrich® Atmosbag with a nitrogen inlet and vacuum outlet to minimize the oxygen present. A solution of methanol and isopropyl alcohol were degassed by bubbling nitrogen through the solution while sonicating overnight. A stock solution of *N*-acetyl cysteine (0.074 mg/mL) was prepared fresh inside the bag by dissolving 0.0074 g in 100 mL of degassed 100 mM Tris/HCl buffer (pH 8.5). The solvent systems studied were: 67% methanol (2mL), 58% methanol (1.75 mL), 50% methanol (1.5 mL), 10% methanol (0.3 mL) and 67% isopropyl alcohol (2 mL). The appropriate amount of methanol or isopropyl alcohol was added to the sample cuvette and the blank cuvette. The sample cuvette was shaken lightly by hand to dissolve the quinone. One millilitre of the *N*-acetyl cysteine stock solution (2 eq.) was added to the blank cuvette and the reaction cuvette. The increase in absorbance at 308 nm was recorded on a Genesis 10x spectrophotometer every nine seconds using Vision Lite software. The reactions were monitored for about an hour.

4.6 General procedure for Cyclic Voltammetry

Cyclic voltammetry (CV) experiments were performed with a Bioanalytical Systems Inc. (BASI) Epsilon electrochemical workstation. All applicable compounds were dissolved with anhydrous DCM and deaerated by sparging N_2 gas for 10 minutes. Solution concentrations were approximately 2.4 mM in analyte containing 77 mM supporting electrolyte tetrabutylammonium hexafluorophosphate (NBu_4PF_6). A typical three electrode setup was used including a platinum working electrode, Ag wire reference electrode and a platinum wire auxiliary electrode. Scan speeds are noted in the results.

5. REFERENCES

1. Evans, H. & Bishop, K. S. On the Existence of a Hitherto Unrecognized Dietary Factor Essential for Reproduction: On the Existence of a Hitherto Unrecognized Dietary Factor Essential for Reproduction. *Science (80-.).* **56,** 650–651 (1922).
2. Sure, B. Dietary Requirements for Reproduction II. The Existence of a Specific Vitamin for Reproduction. *J. Biol. Chem.* **58,** 693–709 (1923).
3. Evans, H. M. & Burr, G. O. The destructive effect of certain fats and fractions thereof on the antisterility vitamin in wheat germ and in wheat germ oil. *J. Am. Med. Assoc.* **89,** 1587–1590 (1927).
4. Cummings, M. J. & Mattill, H. A. The Auto-Oxidation of Fats with Reference to Their Destructive Effect on Vitamin E. *J. Nutr.* **3,** 421–432 (1931).
5. Wolf, G. The discovery of the antioxidant function of vitamin E: the contribution of Henry A. Mattill. *J. Nutr.* **135,** 363–366 (2005).
6. Evans, H. M., Emerson, O. H. & Emerson, G. A. The isolation from wheat germ oil of an alcohol, α-tocopherol, having the properties of vitamin E. *J. Biol. Chem.* **113,** 319–332 (1935).
7. Emerson, O. H., Emerson, G. A., Mohammad, A. & Evans, H. M. The chemisty of vitamin E: Tocopherols from various sources. *J. Biol. Chem.* **122,** 99–107 (1937).
8. Fernholz, E. On the Constitution of α-Tocopherol. *J. Am. Chem. Soc.* **60,** 700–705 (1938).
9. Pennock, J. F., Hemming, F. W. & Kerr, J. D. A reassessment of tocopherol chemistry. *Biochem. Biophys. Res. Commun.* **17,** 542–548 (1964).
10. Kelly, J. W. The effect of vitamin E-deficient diets on the growth of the chick. (Iowa State University, 1942).

11. Adamstone, F. B. A lymphoblastoma occurring in young chicks reared on a diet treated with ferric chloride to destroy vitamin e. *Cancer Res.* **28,** 540–549 (1936).

12. Goettsch, M. & Pappenheimer, A. M. Nutritional muscular dystrophy in the guinea pig and rabbit. *J. Exp. Med.* **54,** 145–165 (1931).

13. Meier, R., Tomizaki, T., Schulze-Briese, C., Baumann, U. & Stocker, A. The molecular basis of vitamin E retention: Structure of human α-tocopherol transfer protein. *J. Mol. Biol.* **331,** 725–734 (2003).

14. Euch-Fayache, G. El, Bouhlal, Y., Amouri, R., Feki, M. & Hentati, F. Molecular, clinical and peripheral neuropathy study of Tunisian patients with ataxia with vitamin E deficiency. *Brain* **137,** 402–410 (2014).

15. Gabsi, S., Gouider-Khouja, N., Belal, S., Fki, M., Kefi, M., Turki, I., Ben Hamida, M., Kayden, H., Mebazaa, R. & Hentati, F. Effect of vitamin E supplementation in patients with ataxia with vitamin E deficiency. *Eur. J. Neurol.* **8,** 477–81 (2001).

16. Rizvi, S., Raza, S. T., Ahmed, F., Ahmad, A., Abbas, S. & Mahdi, F. The role of Vitamin E in human health and some diseases. *Sultan Qaboos Univ. Med. J.* **14,** 157–165 (2014).

17. Traber, G. & Sies, H. Vitamin E in humans: Demand and delivery. *Annu. Rev. Nutr.* **16,** 321–347 (1996).

18. Kamal-Eldin, A. & Andersson, R. A multivariate study of the correlation between tocopherol content and fatty acid composition in vegetable oils. *J. Am. Oil Chem. Soc.* **74,** 375–380 (1997).

19. Yang, W., Cahoon, R. E., Hunter, S. C., Zhang, C., Han, J., Borgschulte, T. & Cahoon, E. B. Vitamin e biosynthesis: Functional characterization of the monocot homogentisate geranylgeranyl transferase. *Plant J.* **65,** 206–217 (2011).

20. DellaPenna, D. A decade of progress in understanding vitamin E synthesis in plants. *J. Plant Physiol.* **162,** 729–737 (2005).

21. Lemaire-Ewing, S., Desrumaux, C., Néel, D. & Lagrost, L. Vitamin E transport, membrane incorporation and cell metabolism: Is α-Tocopherol in lipid rafts an oar in the lifeboat? *Mol. Nutr. Food Res.* **54,** 631–640 (2010).

22. Reboul, E., Klein, A., Bietrix, F., Gleize, B., Malezet-Desmoulins, C., Schneider, M., Margotat, A., Lagrost, L., Collet, X. & Borel, P. Scavenger receptor class B type I (SR-BI) is involved in vitamin E transport across the enterocyte. *J. Biol. Chem.* **281,** 4739–4745 (2006).

23. Anwar, K., Iqbal, J. & Hussain, M. M. Mechanisms involved in vitamin E transport by primary enterocytes and in vivo absorption. *J. Lipid Res.* **48,** 2028–2038 (2007).

24. Anwar, K., Kayden, H. J. & Hussain, M. M. Transport of vitamin E by differentiated Caco-2 cells. *J. Lipid Res.* **47,** 1261–73 (2006).

25. Podda, M., Weber, C., Traber, M. G. & Packer, L. Simultaneous determination of tissue tocopherols, tocotrienols, ubiquinols, and ubiquinones. *J. Lipid Res.* **37,** 893–901 (1996).

26. Hosomi, A., Arita, M., Sato, Y., Kiyose, C., Ueda, T., Igarashi, O., Arai, H. & Inoue, K. Affinity for α-tocopherol transfer protein as a determinant of the biological activities of vitamin E analogs. *FEBS Lett.* **409,** 105–108 (1997).

27. Panagabko, C., Morley, S., Hernandez, M., Cassolato, P., Gordon, H., Parsons, R., Manor, D. & Atkinson, J. Ligand specificity in the CRAL-TRIO protein family. *Biochemistry* **42,** 6467–6474 (2003).

28. Mangialasche, F., Xu, W., Kivipelto, M., Costanzi, E., Ercolani, S., Pigliautile, M., Cecchetti, R., Baglioni, M., Simmons, A., Soininen, H., Tsolaki, M., Kloszewska, I.,

Vellas, B., Lovestone, S. & Mecocci, P. Tocopherols and tocotrienols plasma levels are associated with cognitive impairment. *Neurobiol. Aging* **33,** 2282–2290 (2012).

29. Jiang, X. C., Tall, A. R., Qin, S., Lin, M., Schneider, M., Lalanne, F., Deckert, V., Desrumaux, C., Athias, A., Witztum, J. L. & Lagrost, L. Phospholipid transfer protein deficiency protects circulating lipoproteins from oxidation due to the enhanced accumulation of vitamin E. *J. Biol. Chem.* **277,** 31850–31856 (2002).
30. Atkinson, J., Epand, R. F. & Epand, R. M. Tocopherols and tocotrienols in membranes: A critical review. *Free Radic. Biol. Med.* **44,** 739–764 (2008).
31. Sontag, T. J. & Parker, R. S. Cytochrome P450 ω-hydroxylase pathway of tocopherol catabolism: Novel mechanism of regulation of vitamin E status. *J. Biol. Chem.* **277,** 25290–25296 (2002).
32. Mustachich, D. J., Leonard, S. W., Patel, N. K. & Traber, M. G. α-Tocopherol β-oxidation localized to rat liver mitochondria. *Free Radic. Biol. Med.* **48,** 73–94 (2010).
33. Wolf, R., Wolf, D. & Ruocco, V. Vitamin E: The radical protector. *J. Eur. Acad. Dermatology Venereol.* **10,** 103–117 (1998).
34. Traber, M. G. & Atkinson, J. Vitamin E, antioxidant and nothing more. *Free Radic. Biol. Med.* **43,** 4–15 (2007).
35. Buettner, G. R. The Pecking Order of Free Radicals and Antioxidants: Lipid Peroxidation, α-Tocopherol, and Ascorbate. *Arch. Biochem. Biophys.* **300,** 535–543 (1993).
36. Cordeiro, R. M. Reactive oxygen species at phospholipid bilayers : Distribution , mobility and permeation. *Biochim. Biophys. Acta* **1838,** 438–444 (2014).
37. Lubos, E., Loscalzo, J. & Handy, D. E. Glutathione Peroxidase-1 in Health and Disease : *Antioxidants redox Signal.* **15,** 1957–1997 (2011).

38. Marquardt, D., Williams, J. A., Kucerka, N., Atkinson, J., Wassall, S. R., Katsaras, J. & Harroun, T. A. New Perspective on the Antioxidant Vitamin E. *J. Am. Chem. Soc.* **135,** 7523–7533 (2013).

39. Niki, E. Interaction of Ascorbate and α-Tocopherol. *Ann. N.Y. Acad. Sci.* **498,** 186–199 (1987).

40. Azzi, A. & Stocker, A. Vitamin E: Non-antioxidant roles. *Prog. Lipid Res.* **39,** 231–255 (2000).

41. Chakraborti, T., Das, S. & Chakraborti, S. Proteolytic Activation of Protein Kinase Cα by Peroxynitrite in Stimulating Cytosolic Phospholipase A2 in Pulmonary Endothelium: Involvement of a Pertussis Toxin Sensitive Protein. *Biochemistry* **44,** 5246–5257 (2005).

42. Suzuki, Y. J., Tsuchiya, M., Wassall, S. R., Choo, Y. M., Govil, G., Kagan, V. E. & Packer, L. Structural and Dynamic Membrane Properties. *Biochemistry* **32,** 10692–10699 (1993).

43. Grau, A. & Ortiz, A. Dissimilar protection of tocopherol isomers against membrane hydrolysis by phospholipase A2. *Chem. Phys. Lipids* **91,** 109–118 (1998).

44. Peh, H. Y., Tan, W. S. D., Liao, W. & Wong, W. S. F. Vitamin E therapy beyond cancer: Tocopherol versus tocotrienol. *Pharmacol. Ther.* **162,** 152–169 (2016).

45. Yoshida, Y., Saito, Y., Jones, L. S. & Shigeri, Y. Chemical reactivities and physical effects in comparison between tocopherols and tocotrienols: physiological significance and prospects as antioxidants. *J. Biosci. Bioeng.* **104,** 439–45 (2007).

46. Müller, L., Theile, K. & Böhm, V. In vitro antioxidant activity of tocopherols and tocotrienols and comparison of vitamin E concentration and lipophilic antioxidant capacity in human plasma. *Mol. Nutr. Food Res.* **54,** 731–742 (2010).

47. Yoshida, Y., Niki, E. & Noguchi, N. Comparative study on the action of tocopherols and tocotrienols as antioxidant: Chemical and physical effects. *Chem. Phys. Lipids* **123,** 63–75 (2003).

48. Kushi, L. H., Folsom, A. R., Prineas, R. J., Mink, P. J., Wu, Y. & Bostick, R. M. Dietary Antioxidant vitamins and death from coronary heart disease in postmenopausal women. *N. Engl. J. Med.* **334,** 1156–1162 (1996).

49. Christen, S., Woodall, A. A., Shigenaga, M. K., Southwell-Keely, P. T., Duncan, M. W. & Ames, B. N. γ-Tocopherol traps mutagenic electrophiles such as NO x and complements α-tocopherol: Physiological implications. *Med. Sci.* **94,** 3217–3222 (1997).

50. Heinonen, O. & Albanes, D. The effect of Vitamin E and Beta Carotene on the incidence of lung cancer in male smokers. *N. Engl. J. Med.* **330,** 1029–1035 (1994).

51. McCormick, C. C. & Parker, R. S. The cytotoxicity of vitamin E is both vitamer- and cell-specific and involves a selectable trait. *J. Nutr.* **134,** 3335–3342 (2004).

52. Elisia, I. & Kitts, D. D. Tocopherol isoforms (α-, γ-, and δ-) show distinct capacities to control Nrf-2 and NfκB signaling pathways that modulate inflammatory response in Caco-2 intestinal cells. *Mol. Cell. Biochem.* **404,** 123–131 (2015).

53. Qureshi, A. A., Burger, W. C., Peterson, D. M. & Elson, C. E. The Structure of an Inhibitor of Cholesterol Biosynthesis Isolated from Barley. *J. Biol. Chem.* 10544–10550 (1986).

54. Zielinski, H., Ciska, E. & Kozlowska, H. The Cereal Grains : Focus on Vitamin E. *Czech J. Food Sci.* **19,** 182–188 (2001).

55. Pearce, B. C., Parker, R. A., Demon, M. E., Qureshi, A. A. & Wright, J. J. K. Hypocholesterolemic Activity of Synthetic and Natural Tocotrienols. *J. Med. Chem.* **35,**

3595–3606 (1992).

56. Parker, R. A., Pearceq, B. C., Clark, R. W., Gordon, D. A. & Wright, J. J. K. Tocotrienols Regulate Cholesterol Production in Mammalian Cells bv Post-transcriptional Suppression of 3-Hydroxy-3-methylglutaryl- Coenzyme A Reductase *. *J. Biol. Chem.* **268,** 11230–11238 (1993).

57. Fu, J. Y., Blatchford, D. R., Tetley, L. & Dufès, C. Tumor regression after systemic administration of tocotrienol entrapped in tumor-targeted vesicles. *J. Control. Release* **140,** 95–99 (2009).

58. Karim, R., Somani, S., Al Robaian, M., Mullin, M., Amor, R., McConnell, G. & Dufès, C. Tumor regression after intravenous administration of targeted vesicles entrapping the vitamin E α-tocotrienol. *J. Control. Release* **246,** 79–87 (2017).

59. Meyenberg, A., Goldblum, D., Zingg, J.-M., Azzi, A., Nesaretnam, K., Kilchenmann, M. & Frueh, B. E. Tocotrienol inhibits proliferation of human Tenon's fibroblasts in vitro: a comparative study with vitamin E forms and mitomycin C. *Graefes Arch. Clin. Exp. Ophthalmol.* **243,** 1263–71 (2005).

60. Yu, W., Simmons-Menchaca, M., Gapor, A., Sanders, B. G. & Kline, K. Induction of apoptosis in human breast cancer cells by tocopherols and tocotrienols. *Nutr. Cancer* **33,** 26–32 (1999).

61. Yu, W., Heim, K., Qian, M., Simmons-menchaca, M., Sanders, B. G. & Kline, K. Evidence for Role of Transforming Growth Factor-β in RRR-a-Tocopheryl Succinate-Induced Apoptosis of Human MDA-MB-435 Breast Cancer Cells. **27,** 267–278 (1997).

62. He, L., Mo, H., Hadisusilo, S., Qureshi, a a & Elson, C. E. Isoprenoids suppress the growth of murine B16 melanomas in vitro and in vivo. *J. Nutr.* **127,** 668–674 (1997).

63. Cornwell, D. G., Kim, S., Mazzer, P. A., Jones, K. H. & Hatcher, P. G. Electrophile tocopheryl quinones in apoptosis and mutagenesis: Thermochemolysis of thiol adducts with proteins and in cells. *Lipids* **38,** 973–979 (2003).

64. Sachdeva, R., Thomas, B., Wang, X., Ma, J., Jones, K. H., Hatcher, P. G. & Cornwell, D. G. Tocopherol metabolism using thermochemolysis: chemical and biological properties of gamma-tocopherol, gamma-carboxyethyl-hydroxychroman, and their quinones. *Chem. Res. Toxicol.* **18,** 1018–25 (2005).

65. Wang, X., Thomas, B., Sachdeva, R., Arterburn, L., Frye, L., Hatcher, P. G., Cornwell, D. G. & Ma, J. Mechanism of arylating quinone toxicity involving Michael adduct formation and induction of endoplasmic reticulum stress. *Proc. Natl. Acad. Sci. U. S. A.* **103,** 3604–9 (2006).

66. Thornton, D. E., Jones, K. H., Jiang, Z., Zhang, H., Liu, G. & Cornwell, D. G. Antioxidant and cytotoxic tocopheryl quinones in normal and cancer cells. *Free Radic. Biol. Med.* **18,** 963–976 (1995).

67. Lane, N. Mitonuclear match: Optimizing fitness and fertility over generations drives ageing within generations. *Bioessays* **33,** 860–869 (2011).

68. Schultz, B. E. & Chan, S. I. Structures and proton-pumping strategies of mitochondrial respiratory enzymes. *Annu. Rev. Biophys. Biomo. Struct.* **30,** 23–65 (2001).

69. Jastroch, M., Divakaruni, A. S., Mookerjee, S., Treberg, J. R. & Brand, M. D. Mitochondrial proton and electron leaks. *Essays Biochem.* **47,** 53–67 (2010).

70. Chouchani, E. T., Kazak, L., Jedrychowski, M., Lu, G. Z., Erickson, B. K., Szpyt, J., Pierce, K. A., Laznik-Bogoslavski, D., Vetrivelan, R., Clish, C. B., Robinson, A. J., Gygi, S. P. & Spiegelman, B. M. Mitochondrial ROS regulate thermogenic energy expenditure

and sulfenylation of UCP1. *Nature* **532,** 112–116 (2016).

71. Bak, D. W., Pizzagalli, M. D. & Weerapana, E. Identifying Functional Cysteine Residues in the Mitochondria. *ACS Chem. Biol.* **12,** 947–957 (2017).

72. Kaspar, J. W., Niture, S. K. & Jaiswal, A. K. Nrf2:INrf2 (Keap1) signaling in oxidative stress. *Free Radic. Biol. Med.* **47,** 1304–1309 (2009).

73. Uruno, A. & Motohashi, H. The Keap1-Nrf2 system as an in vivo sensor for electrophiles. *Nitric Oxide* **25,** 153–160 (2011).

74. Kansanen, E., Kuosmanen, S. M., Leinonen, H. & Levonenn, A. L. The Keap1-Nrf2 pathway: Mechanisms of activation and dysregulation in cancer. *Redox Biol.* **1,** 45–49 (2013).

75. Schwarz, D. S. & Blower, M. D. The endoplasmic reticulum : structure , function and response to cellular signaling. *Cell. Mol. Life Sci.* **73,** 79–94 (2016).

76. van Galen, P., Kreso, A., Mbong, N., Kent, D. G., Fitzmaurice, T., Chambers, J. E., Xie, S., Laurenti, E., Hermans, K., Eppert, K., Marciniak, S. J., Goodall, J. C., Green, A. R., Wouters, B. G., Wienholds, E. & Dick, J. E. The unfolded protein response governs integrity of the haematopoietic stem-cell pool during stress. *Nature* **510,** 268–72 (2014).

77. Khurana, J. M., Chauhan, S. & Bansal, G. Facile Hydrolysis of Esters with KOH-Methanol at Ambient Temperature. *Monatshefte fur Chemie* **87,** 83–87 (2004).

78. Ali, M. H., Niedbalski, M., Bohnert, G. & Bryant, D. Silica-Gel-Supported Ceric Ammonium Nitrate (CAN): A Simple and Efficient Solid-Supported Reagent for Oxidation of Oxygenated Aromatic Compounds to Quinones. *Synth. Commun.* **36,** 1751–1759 (2006).

79. Sridharan, V. & Menendez, J. C. Cerium (IV) Ammonium Nitrate as a Catalyst in

Organic Synthesis. *Am. Chem. Soc. Chem. Rev.* 3805–3849 (2010).

80. Saladino, R., Neri, V., Farina, A., Crestini, C., Nencioni, L. & Palamara, A. T. A novel and efficient synthesis of tocopheryl quinones by homogeneous and heterogeneous methyltrioxorhenium/hydrogen peroxide catalytic systems. *Adv. Synth. Catal.* **350,** 321–331 (2008).

81. Lide, D. Dissociation constants of organic acids and bases. *CRC Handb. Chem. physics, Internet …* 42–51 (2005). doi:10.1351/pac196920020133

82. Khalife, K. H. & Lupidi, G. Nonenzymatic reduction of thymoquinone in physiological conditions. *Free Radic. Res.* **41,** 153–161 (2007).

83. Wilson, I., Wardman, P., Lin, T.-S. & Sartorelli, A. C. Reactivity of thiols towards derivatives of 2- and 6-methyl-1,4-napthoquinone bioreductive alkylating agents. *Chem.-Biol., Interact.* **61,** 229–240 (1987).

84. Song, Y. & Buettner, G. Thermodynamic and kinetic considerations for the reaction of semiquinone radicals to form superoxide and hydrogen peroxide. *Free Radic. Biol. Med.* **49,** 919–962 (2010).

85. Roginsky, V. A., Pisarenko, L. M., Bors, W. & Michel, C. The kinetics and thermodynamics of quinone – semiquinone – hydroquinone systems under physiological conditions. *J. Chem. Soc., Perkin Trans 2* 871–876 (1999).

86. Mabbott, G. A. An introduction to cyclic voltammetry. *J. Chem. Educ.* **60,** 697–702 (1983).

87. Kissinger, P. T. & Heinemen, W. R. Cyclic Voltammetry. *J. Chem. Educ.* **60,** 702–706 (1983).

88. Neghmouche, N. S., Khelef, A. & Lanez, T. Electrochemistry characterization of

ferrocene / ferricenium redox couple at glassycarbon electrode. *Rev. sci. fond. app.* **1,** 23–30 (2009).

89. Gagne, R. R., Koval, C. A. & Lisensky, G. C. Ferrocene as an Internal Standard for Electrochemical Measurements. *Inorg. Chem.* **19,** 2854–2855 (1980).

90. Yao, W. W., Peng, H. M., Webster, R. D. & Gill, P. M. W. Variable Scan Rate Cyclic Voltammetry and Theoretical Studies on Tocopherol (Vitamin E) Model Compounds. *J . Phys. Chem* **112,** 6847–6855 (2008).

91. Tan, Y. S., Chen, S., Hong, W. M., Kan, J. M., Swee, E., Kwek, H., Lim, S. Y., Lim, Z. H., Tessensohn, M. E., Zhang, Y. & Webster, R. D. The role of low levels of water in the electrochemical oxidation of a -tocopherol (vitamin E) and other phenols in acetonitrile. *Phys. Chem. Chem. Phys.* **13,** 12745–12754 (2011).

92. Williams, L. L. & Webster, R. D. Electrochemically Controlled Chemically Reversible Transformation of α-Tocopherol (Vitamin E) into Its Phenoxonium Cation. *J. Am. Med. Assoc.* **126,** 12441–12450 (2004).

93. Wilson, G. J., Lin, C. Y. & Webster, R. D. Significant Differences in the Electrochemical Behavior of the α- , β- , γ- , and δ -Tocopherols (Vitamin E). *J . Phys. Chem* **110,** 11540–11548 (2006).

94. Webster, R. D. New Insights into the Oxidative Electrochemistry of Vitamin E. *Acc. Chem. Res.* **40,** 251–257 (2007).

95. Liehr, J. & Roy, D. Free radical generation by redox cycling of estrogens. *Free Radic. Biol. Med.* **8,** 415–423 (1990).

96. Tafazoli, S., Wright, J. S. & O'Brien, P. J. Prooxidant and Antioxidant Activity of Vitamin E Analogues and Troglitazone. *Chem. Res. Toxicol.* **18,** 1567–1574 (2005).

97. Kontush, A., Finckh, B., Karten, B., Kohlschutter, A. & Beisiegel, U. Antioxidant and prooxidant activity of a-tocopherol in human plasma and low density lipoprotein. *J. Lipid Res.* **37,** 1436–1448 (1996).

98. Pearson, P., Lewis, S. A., Britton, J., Young, I. S. & Fogarty, A. The Pro-Oxidant Activity of High-Dose Vitamin E Supplements in Vivo. *Biodrugs* **20,** 271–273 (2006).